ANALYSIS OF FACTORS THAT AFFECT ION BEAM CURRENTS FOR COSMOGENIC ^{10}Be AND ^{26}Al ANALYSIS BY ACCELERATOR MASS SPECTROMETRY (AMS)

A Dissertation Presented

by

Adam Lewis Hunt

to

The Faculty of the Graduate College

of

The University of Vermont

In Partial Fulfillment of the Requirements
for the Degree of Doctor of Philosophy
Specializing in Chemistry

February, 2008

Accepted by the Faculty of the Graduate College, The University of Vermont, in partial fulfillment of the requirements for the degree of Doctor of Philosophy specializing in Chemistry.

Thesis Examination Committee:

_____ Advisor
Giuseppe A. Petrucci, Ph.D.

_____
William Geiger, Ph. D.

_____
Christopher Allen, Ph.D.

_____ Chairperson
Paul R. Bierman, Ph.D.

_____ Vice President for Research
Frances E. Carr, Ph. D   and Dean of Graduate Studies

Date: November 12, 2007

ABSTRACT

The experiments described herein are designed to improve accelerator mass spectrometry (AMS) of ^{10}Be and ^{26}Al for a wide range of geological applications. In many cases, the precision of the AMS isotope ratio measurement is restricted by counting statistics for the cosmogenic isotope, which are in turn limited by the intensity of AMS stable ion beam currents. We present data indicating that AMS ion beam currents are impacted by certain elemental impurities. For ^{10}Be analysis, the AMS ion beam current is most adversely affected by the presence of Ti (which can be challenging to separate chemically during sample preparation because of its tendency toward stable refractory forms) and Al (which can co-elute with Be during cation exchange chromatography). In order to minimize impurities that suppress AMS ion beam currents, we recommend a chemical separation protocol involving a multi-acid digestion scheme, pre-separation elemental analysis, anion exchange chromatography, ad hoc selective precipitation, cation exchange chromatography, and post-separation elemental analysis.

Herein also is shown that ion beam currents depend strongly on the metal matrix in which BeO is dispersed, on the matrix:BeO ratio, and for some metals, such as Ag, on the depth to which the sample is packed in the AMS cathode. Typical instantaneous Be^{+3} currents (μA) produced by the LLNL CAMS Cs sputter ion source and measured in a Faraday cup after the accelerator are 7.6 for samples in Ag, 19.9 in Ta, 20.9 in Mo, 21.1 in W, 25.5 in Nb, and 27.5 in V. The AMS counting efficiency (ions detected per Be atom loaded) for a routine analysis time (300 s) for equimolar mixtures of BeO and matrix is in the range $2x10^{-4}$ to $6x10^{-4}$ in the order V>Ta>Mo>W>Nb>Ag. Additionally, an inverse linear correlation between electron affinity of the matrix and beam current is observed, suggesting that the propensity of the metal matrix to attach electrons impacts the ion signal.

Herein also is shown, that ion beam currents are affected by the metal matrix in which Al_2O_3 is dispersed, by the matrix-to-Al_2O_3 mixing ratio, and for at least some matrices, such as Ag, by the depth to which the sample is packed in the AMS cathode. Typical instantaneous Al^{+7} currents (μA) produced by the LLNL CAMS Cs sputter ion source and measured in a Faraday cup after the accelerator are 2.26 for samples in Ag, 2.17 in Re, 2.00 in Nb, 1.92 in V, and 1.73 in Mo. The AMS counting efficiency (Al^- ions detected per Al atom loaded in the target) for a constant analysis time (900 s) and for equimolar mixtures of Al_2O_3 and matrix is in the range $6x10^{-5}$ to $9x10^{-5}$ in the order Ag>Re>Nb>V>Mo. Additionally, we observed a correlation between the ion detection efficiency (Al ions detected per Al atoms loaded) and the matrix work function and inverse vaporization enthalpy of the matrix and beam current. Typical currents (μA) obtained with elemental Al are 13.3 for samples in no matrix, 3.23 in V, 3.14 in Nb, 3.07 in Re, 2.85 in Mo, 1.46 in Ag. The ion detection efficiency for elemental Al correlates strongly with matrix electron affinity. Thus, our data indicate that the current practice of mixing Al_2O_3 with Ag is reasonable until a means is found to produce cathodes of elemental Al.

CITATIONS

Material from this dissertation has been published in the following form:

Hunt, A.L.; Petrucci, G.A.; Bierman, P.R.; Finkel, R.C. "Metal matrices to optimize ion beam currents for accelerator mass spectrometry" *Nuclear Instruments and Methods in Physics Research Section B: Beam Interactions with Materials and Atoms* **2006**, 243, 216-222.

Hunt, A.L.; Petrucci, G.A.; Bierman, P.R.; Finkel, R.C. "Investigation of metal matrix systems for cosmogenic ^{26}Al analysis by accelerator mass spectrometry" *Nuclear Instruments and Methods in Physics Research Section B: Beam Interactions with Materials and Atoms* **2007**, 260, 633-636.

Material from this dissertation had been submitted for publication to *Analytical Chemistry* on August 10, 2007 in the following form:

Hunt, A.L.; Larsen, J.; Bierman, P.R.; Petrucci, G.A. "Investigation of factors which affect the sensitivity of accelerator mass spectrometry (AMS) for cosmogenic ^{10}Be and ^{26}Al isotope analysis."

> **What are you doing, young man?**
> **Are you so earnest—so given up to literature, science, art, amours?**
> **These ostensible realities, politics, points?**
> **Your ambition or business, whatever it may be?**
> **It is well—Against such I say not a word—I am their poet also…**
>
> -Walt Whitman in *Leaves of Grass* (1855)

TABLE OF CONTENTS

LIST OF FIGURES

CHAPTER 1: INTRODUCTION

1.1. Cosmogenic production of in situ ^{10}Be and ^{26}Al in quartz

Galactic cosmic rays are comprised of a plethora of atomic and sub-atomic components with a wide range of energies. Typical populations include interstellar protons (~90%), α particles (10%), and electrons and heavier nuclides (~1%). On Earth, the incidence of cosmic rays provides a rich medium for ambient nuclear reactivity. The vast majority of these reactions are nuclear transformations occurring in atmosphere; however, cosmic ray-induced nuclear reactions also occur at or near Earth's surface, albeit with far less frequency. Such nuclear reactions in the terrestrial crust are of tremendous interest to geologist on account of their potential for forming exceptionally rare nuclides in situ in surficial rocks. Of particular interest to this dissertation are the rare terrestrial nuclides, ^{10}Be and ^{26}Al, produced by cosmic rays in situ in surficial quartz.[1-3]

From a geological perspective, quartz serves as an excellent primary source material because of its near-ubiquitous distribution in rocks and soils over Earth's surface. In addition, quartz is naturally resistant to chemical weathering processes; therefore, it survives as a dosimeter and tracer of erosion. From an analytical perspective, quartz is a good material for ^{10}Be and ^{26}Al analysis because the common nuclides, ^{9}Be and ^{27}Al, are natively present in negligible or trace concentrations. Low abundances of the stable analyte nuclides in the quartz phase greatly facilitate low level isotope ratio analysis. Finally, quartz is relatively easy to chemically process in the laboratory, as it is

readily isolated from other minerals with liquid density separation methods and acid etching.[4]

The major in situ source of ^{10}Be and ^{26}Al in terrestrial quartz is nuclear reactions that occur when cosmic particles interact with silicon and oxygen atoms within the mineral lattice.[5-7] Even though the energetic distribution of particles comprising the cosmic ray flux is broad, the cosmogenic production of ^{10}Be and ^{26}Al can only be orchestrated by a specific class of particles with the proper kinetic energy. This class of cosmic particles is populated by secondary neutrons, which are a common product of cascade reactions of primary cosmic rays with ambient atmospheric or subsurface atoms.[7] Despite the relatively low abundance of secondary neutrons in the global cosmic ray flux, the population of secondary neutrons is actually relatively dense near Earth's surface compared to other cosmic ray components. The high terrestrial concentration of secondary neutrons is attributed to their inherent electrical neutrality, which negates deceleration effects as a function of ionization energy losses to ambient species in their trajectory.

In quartz, the in situ production of cosmogenic ^{10}Be and ^{26}Al by secondary neutrons proceeds through a spallation mechanism (Figure 1-1). The predominant reaction pathways are (a) ^{16}O(n,4p3n)^{10}Be; and (b) ^{28}Si(n,6p3n)2^{10}Be. The dominant pathway for ^{26}Al production in quartz is ^{28}Si(n,p2n)^{26}Al. All of these prevalent cosmogenic spallation mechanisms occur at shallow (<2 m) subterranean depths. At greater subterranean depths, due to attenuation of the secondary neutron flux, cosmogenic production of ^{10}Be and ^{26}Al by this mechanism is not as significant.[8, 9, 2]
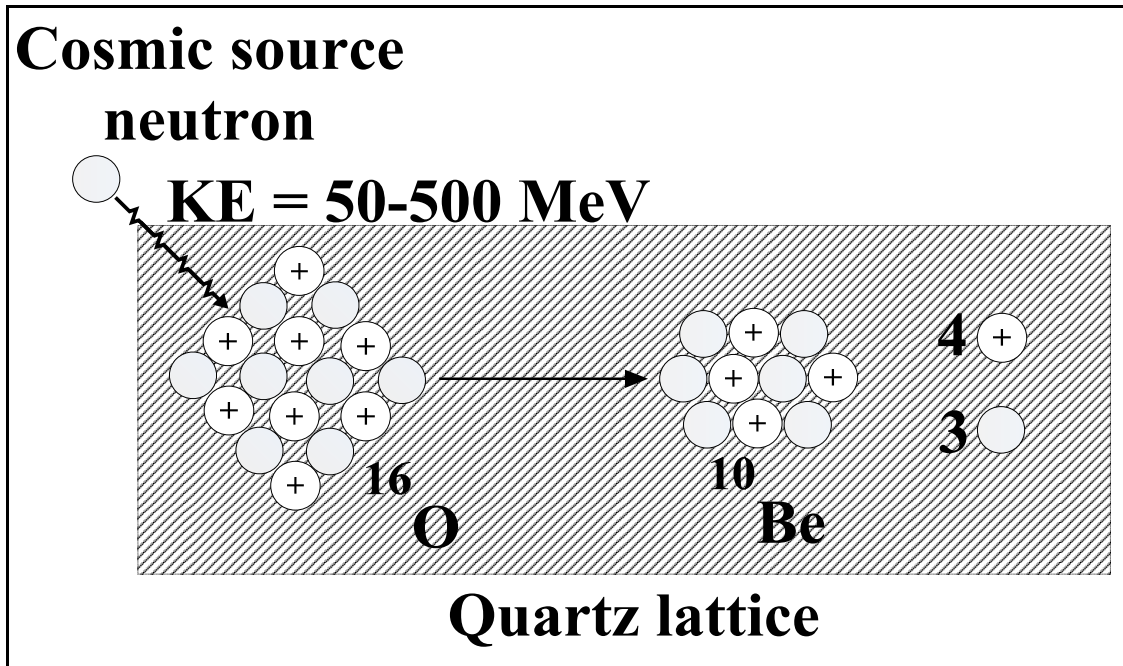
Figure 1-1: In situ cosmogenic production of [10]Be in quartz by spallation of a lattice-bound oxygen atom. This reaction occurs at a rate of 5.2 [10]Be atoms per gram per annum at sea level and high altitude.

One of the key assumptions commonly incorporated into simple geomorphologic interpretive models based upon experimental quantification of [10]Be and [26]Al abundances is that the rare nuclides are exclusively of in situ spallogenic origin. In actuality, experimentally measured rare nuclide abundances in quartz probably include at least some level of contribution from other sources. In particular, when considering [10]Be and [26]Al production, other potential in situ production sources include formation by interstellar protons, muons, and radiogenic precursors. Furthermore, non in situ contaminations accumulate from precipitation of cosmogenic nuclides produced in the atmosphere. In most geomorphologic interpretive models, the discrimination of in situ [10]Be and [26]Al from other background production sources is paramount for meaningful

AMS data analysis. For a thorough discussion of cosmogenic nuclide production rates, the interested reader is referred to the pioneering theoretical and experimental research of D. Lal.[5, 1, 2, 7] The ensuing section is a brief summary of production mechanisms, derived from the aforementioned references, relative to geomorphologic applications involving ^{10}Be and ^{26}Al analysis.

1.2 Other mechanisms of ^{10}Be and ^{26}Al production

In general, spallogenic production of ^{10}Be and ^{26}Al by interstellar proton sources is insignificant compared to production by secondary neutrons. In addition, the extent by which these other reactions occur is commonly invariant (and therefore predictable) as a function of the latitude and altitude of the quartz substrate.

Much more significant to the overall ^{10}Be and ^{26}Al production budget is the contribution due to the phenomenon of negative muon capture. In quartz, muon capture mechanisms produce ^{10}Be and ^{26}Al by the reaction pathways ^{16}O(μ^-,3p3n)^{10}Be and ^{28}Si(μ^-,2n)^{26}Al respectively. Due to the great penetrating power of subatomic particles in terrestrial surfaces, muon capture reaction cross sections decrease more gradually as a function of subterranean depth than other cosmogenic production pathways. Fortunately, in most applications the muon capture production rates of ^{10}Be and ^{26}Al can be predicted with good confidence.

Finally, non-cosmogenic rare nuclides can accumulate in quartz as a consequence of radiogenic reactions, in which the nuclide is a direct daughter of radioactive decay; or from nucleogenic interactions, whereby nucleons produced from local radioactive sources

interact with target atoms. Both of these production mechanisms can be considered special cases that occur only in the presence of certain radioactive species. In most applications, radiogenic production of ^{10}Be, for example via ^{7}Li$(\alpha,p)^{10}$Be, is negligible in surficial quartz; however, the production of ^{26}Al via ^{23}Na$(\alpha,n)^{26}$Al can be significant in some cases. The difference between radiogenic ^{10}Be and ^{26}Al production rates is attributed to difference in precursor concentrations. For example, the ^{10}Be precursor, lithium, is present at only trace levels; while the ^{26}Al precursor, sodium, is more common in quartz.[10]

Upon penetrating the atmosphere, galactic cosmic rays collide with ambient stratospheric gas phase molecules or noble species, producing an air shower (a cascading meteoric reaction series resulting in a series of lower mass products). Among these products are meteoric (also called "garden variety" in older literature) ^{10}Be and ^{26}Al, which can be scavenged in the troposphere by atmospheric aerosols, transported great distances, and precipitated with particulate matter into rocks and sediment. In many cases, meteoric cosmogenic nuclides are a significant contamination of the in situ cosmogenic component; for example, meteoric ^{10}Be is produced at a tenfold production rate compared to in situ ^{10}Be in quartz.[11]

The primary mechanism of meteoric ^{10}Be formation is by spallation of atmospheric nitrogen nuclei with medium energy (50-500 MeV) neutrons. Furthermore, because the nitrogen precursor has high (78%) atmospheric concentration, this reaction is relatively common; thus, meteoric production rates of ^{10}Be are often a significant source of contamination to cosmogenic ^{10}Be produced in situ in quartz. Fortunately, sequential

acid etching of quartz in HF has been demonstrated to be effective for removing meteoric ^{10}Be contamination that adheres to quartz grains.[12] This etching procedure is effective because meteoric ^{10}Be usually enters the silicate lattice through topical fissures and therefore is confined to the surface of quartz grains (contaminating only ~20% of the total grain mass).

In contrast to meteoric ^{10}Be, the primary mechanism of meteoric ^{26}Al formation is by spallation of atmospheric argon nuclei. Because argon has low (~1%) atmospheric concentration, the meteoric production rates of ^{26}Al are relatively low. The difference is evident in the meteoric ^{26}Al to meteoric ^{10}Be production ratio, which is 4×10^{-3}.[13] As a result of this low production ratio, meteoric nuclide contaminations are not as ubiquitous in the quartz phase for ^{26}Al as for ^{10}Be.

1.3 Cosmogenic production rates of ^{10}Be and ^{26}Al in situ in quartz

A complete assessment of the nuclide inventory incorporates terms from all potential production sources; however, for practicality, it is usually convenient to focus analysis and interpretation toward a single source. Unfortunately, the production rates of ^{10}Be and ^{26}Al by a single source are obfuscated by the variety of formation mechanisms described in the previous section. Nevertheless, at or near Earth's surface, the major in situ production mechanism for ^{10}Be and ^{26}Al in quartz is spallation induced by secondary neutrons. Other mechanisms are either ignored (if, under certain sampling conditions, the mechanisms can be considered negligible contributors to the rare nuclide budget) or integrated into data interpretive models (if the mechanisms are known to be significant).

Upon impingement and penetration of Earth's surface, the cosmic ray flux decreases exponentially as the terrestrial matter (e.g. quartz) slows and absorbs the fast-moving particles. In the spallation-dominated production regime (Equation 1.1), the in situ cosmogenic nuclide production rate (P) at a given depth (x) is a function of the surface production rate (P_0) modified by the substrate density (ρ) and the characteristic attenuation depth (Λ):

$$(1.1)\ P_x = P_0\, e^{x\rho/\Lambda}$$

The attenuation parameter, defining the path length in quartz necessary to attenuate the cosmic ray flux by a factor of e^{-1} due to scattering and absorption is relatively constant with reported values of Λ ranging from 150 to 170 g cm^{-2};[8] also constant is the density of quartz at 2.7 g cm^{-3}; however, the surface production rate of cosmogenic nuclides is a variable affected by fluctuations in geomagnetic field strength and solar activity, which in turn are contingent upon sample altitude and latitude. Accurate determination of the rare nuclide production ratio is crucial to quality AMS data interpretation.[14-17]

Geomagnetic effects on cosmogenic nuclide production manifest due to localized deflections in the incident trajectory of primary cosmic rays at different global latitudes. In locations where the geomagnetic field strength is particularly strong (i.e. at latitudes <60°), the cosmic ray flux into the stratosphere is effectively modulated by the geomagnetic field. Modulation lowers the probability for formation of secondary neutrons with the requisite energy distribution, and thus decreases cosmogenic ^{10}Be and ^{26}Al production. In contrast, cosmic rays enter the stratosphere most readily at the

magnetic poles, where geomagnetic field lines are orthogonal to Earth's surface. In any case, only samples acquired at latitudes <35º require corrections of more than a few percent.[18] In contrast, in polar regions, the geomagnetic intensity is negligible.

Solar effects on cosmogenic nuclide production are dynamic and manifest due to the frequency of solar storms, which can also offset the incident trajectory of primary cosmic rays. Solar winds and solar flare particles create magnetic fields which can repulse or modulate galactic cosmic rays. For instance, during periods of high solar activity, solar storms produce localized magnetic fields which shield Earth from galactic cosmic rays. As a consequence of this shielding effect, cosmogenic nuclide production rates are inversely proportional to solar activity.[19] Note that the energetic conditions prerequisite for secondary neutron formation are not as available from the solar cosmic ray flux as from the galactic cosmic ray flux. In any case, ^{10}Be analysis in polar ice cores has been used to study variations in the solar cycle for time periods pre-dating historical records.[20]

On account of geomagnetic and solar related variations in cosmic ray flux, ^{10}Be and ^{26}Al production rates are highest in quartz surfaces exposed at elevated altitudes and high latitudes. Consequently, the classic reported activities of ^{10}Be and ^{26}Al were derived from analysis of quartz sampled from flat, glacially polished bedrock.[3] Analysis of this particular substrate, which guarantees negligible erosion since exposure 11 ka ago, determined that the cosmogenic ^{10}Be production rate in situ in quartz (scaled to sea level and high altitude) was 6.0 atoms $g^{-1}a^{-1}$. In addition, the cosmogenic ^{26}Al production rate in situ in quartz at the same site was 36.8 atoms $g^{-1}a^{-1}$. More recently, upon reevaluating

the contribution due to muon capture and the validity of the 11 ka estimation,[21, 22] the

production rates have been reevaluated at 5.2 and 30.1 atoms $g^{-1}a^{-1}$ for ^{10}Be and ^{26}Al

respectively. In any case, despite discrepancies in experimentally determined production

rates of the individual cosmogenic nuclides, there is good consensus that the ratio of the

^{26}Al production rate to the ^{10}Be production rate is 6.0 in quartz.[23]

Despite the better certainty in known cosmogenic ^{10}Be and ^{26}Al production rates

at high altitude and high latitude, it is generally impractical to restrain geological

applications to analyses of rocks and sediments from sites that typify this criterion. As a

result, there has been considerable effort to develop correction strategies for scaling

standard reference isotope production rates, allowing sample acquisition from diverse

latitudes, elevations, and surface geometries.[16, 2] For example, as described above, the

attenuation parameter (Λ) is typically treated as a constant; however, when an exposure

site is shielded by adjacent topographical features or by sloping landscape effects, the

attenuation parameter decreases as a function of surface dip.[24, 25] Other corrections are

necessary for samples affected by surface coverage such as snow.[26]

1.4 Special considerations for ^{10}Be and ^{26}Al analysis

^{10}Be and ^{26}Al are often measured in the same quartz sample because, under

certain conditions, dual analysis of cosmogenic nuclides by AMS permits mutual

quantification of the exposure age and erosion history of a single sample. Fortunately, on

account of the common chemical behavior of beryllium and aluminum (e.g. solubility in

a range of acids, amphoteric nature particularly with respect to the formation of hydrogel

precipitates in the presence of ammonium salts, retention behavior on ion exchange columns, etc.), the standard procedures for extracting both analytes from quartz are similar and readily performed concurrently. Consequently, it is of great importance that any changes in sample preparation and analysis methodologies that are uniformly applicable to both analytes.

In most quartz specimens, beryllium is non-existent as a native component. Therefore addition of an abundant beryllium isotope carrier (typically 250 μg of ^{9}Be) to the quartz digest is always necessary. The true abundance of the isotope carrier is pre-determined by AMS analysis of cathodes prepared from a sample of carrier minus quartz (i.e. a full process blank). Unfortunately, it is impossible to produce sufficient negative ion currents for the measurement of pure beryllium cathodes because Be⁻ is a low yield, or metastable, ion. Thus, the prevalent strategy for ^{10}Be analysis by AMS is to prepare BeO cathodes, enabling extraction of BeO⁻ from the ion source.[27] Using this method, AMS ion beam currents between 10-20 μA are now routinely obtainable. At present, these current levels are considered favorable by the AMS community in comparison to ion beam currents obtained with many other elements.

Because aluminum is almost always natively present in quartz in at least trace concentrations, the addition of an abundant isotope carrier is rarely a prerequisite for isotope ratio analysis. In any case, 20 g quartz samples generally should contain in excess of ~3 mg of aluminum (or <150 ppm Al in quartz). Higher concentrations of aluminum usually indicate the persistence of feldspar contaminants in the quartz bulk; meanwhile, lower concentrations require long AMS counting times. Note that as (a) an indirect

consequence of the aforementioned necessity of preparing beryllium samples as BeO cathodes; and (b) a direct consequence of the mutual chemical separation method used for the extraction of both analytes: aluminum samples must, like beryllium samples, be prepared as oxide cathodes. This conundrum is a major limitation in ^{26}Al analysis, as oxides of aluminum are impractical to analyze by AMS on account of the prevalence of molecular isobars, which are ion-optically degenerate (i.e. magnesium oxide impurities). Thus even though the atomic ion is formed in relatively low yield, Al$^-$ must be extracted from the ion source for acceleration because there are no major isobaric interferences for ^{26}Al (the atomic isobar ^{26}Mg does not form negative ions). Using this method, AMS ion beam currents of several μA are usually obtained for Al$_2$O$_3$ cathodes. These current levels are considered to be low by the AMS community and continue to present a major obstacle in expanding the utility of cosmogenic ^{26}Al analysis.

1.5 Determination of rare cosmogenic nuclide abundances

The first experiment demonstrating the power of using in situ terrestrial cosmogenic nuclides for geological applications was performed in 1955. The seminal report of this analysis describes quantification of rare ^{36}Cl nuclides, using a then state-of-the-art Geiger counter, in order to determine the exposure age of surface rocks.[28] Yet, even though this work established a scientific framework for interpreting cosmogenic nuclide abundances in terms of geological phenomenon, a strategy for measuring ^{10}Be and ^{26}Al by AMS was not formulated until 1986, when these analytes were measured in Libyan glass[29] and terrestrial quartz.[30] These and other early applications of AMS to

cosmogenic nuclide analysis[31] represented a monumental advantage over β-decay counting techniques, which suffer from notoriously time-consuming data acquisition and low efficiencies for isotopes with long half-lives. For example, a traditional analysis of ^{26}Al by counting methods requires $1x10^6$ kg of sample;[32] meanwhile, AMS analysis of the same substrate today might require at most ~ 30 g of sample.

Even though the exceptional sensitivity of AMS afforded by the capability to count single atoms represents a great advantage for the analysis of ^{10}Be and ^{26}Al, this method is not without limitations, primarily among which is the need for a dedicated particle accelerator. These instruments are prohibitively expensive to construct and maintain for all but the highest funded research facilities. A schematic of AMS instrumentation (Figure 1-2) neither adequately portrays the colossal size of its physical footprint nor the technical complexity of its principle components.[31, 33]
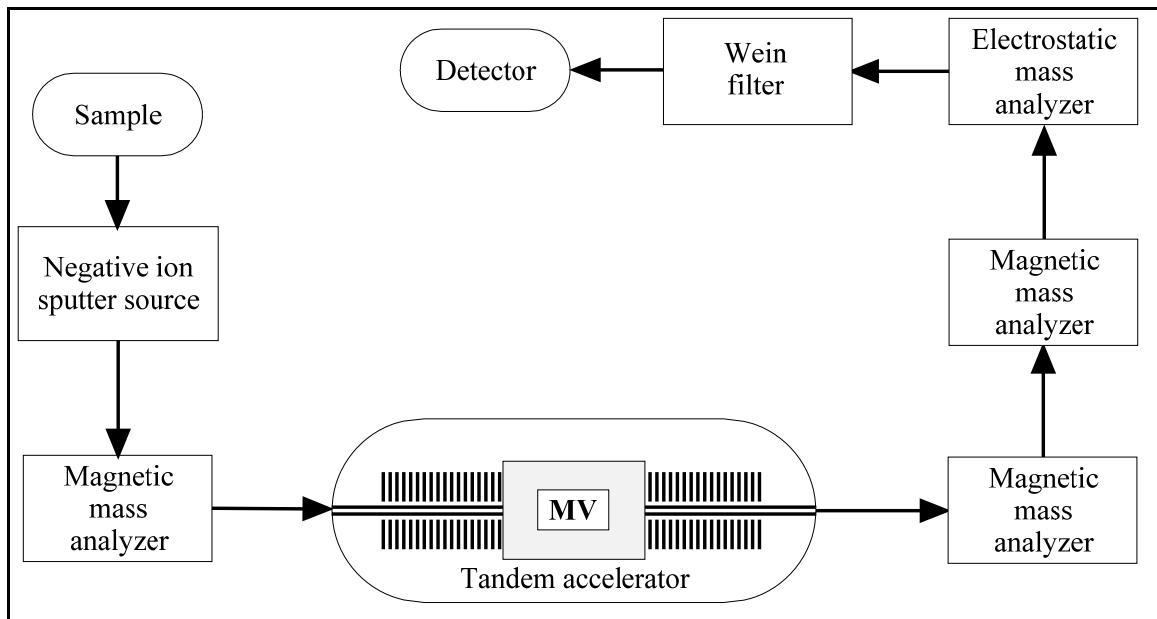
Figure 1-2: Schematic representation of the principle components of the CAMS instrument at LLNL.

All AMS analyses described in this dissertation were performed at the Center for Accelerator Mass Spectrometry (CAMS), which is a state-of-the-art facility operated at Lawrence Livermore National Laboratories (LLNL) in Livermore, CA.[34] Key features of the CAMS instrument include a Middleton-type cesium sputter source for the production of negative ions, a high voltage (10 MV) tandem van de Graaf accelerator, a battery of mass analyzers, and a gas ionization detector. The following section presents an overview of the AMS instrumentation, with special consideration to design elements that are pertinent and/or exclusive to ^{10}Be and ^{26}Al analyses.

1.6 Accelerator mass spectrometry (AMS)

A small mass (typically <2 mg) of BeO or Al_2O_3 sample material, pre-mixed with a metal matrix powder, is tamped into the recess of a custom stainless steel target receptacle. The loaded targets are mounted along the circumference of a sampling wheel, which supports a maximum of 64 samples, and inserted into the AMS ion source through a vacuum lock. A moveable rod transfers samples from the wheel to the focal point of the ion source; after analysis, the rod returns the spent samples to the wheel. Typically six batches (each batch is comprised of seven samples and a complete chemical process blank) are analyzed from a single sampling wheel; the remaining wheel positions are reserved for quality control purposes such as standardization and ion optics tuning.

Since its inauguration, the design of the CAMS high intensity ion source has been modified extensively as the art of "ion sourcery" has evolved through empirically driven improvements.[35, 36] The present incarnation is a high intensity source employing a

spherical ionizer. In terms of basic design, the AMS ion source is essentially a modification of the class of ion source conventionally used for secondary ion mass spectrometry (SIMS), with customization to facilitate the principle function of the AMS ion source: generation of a high current ($\sim\mu A$) of negative ions from the target cathode. The mechanism of ionization is by action of a primary electropositive ion beam on the cathode target surface, which sputters off a secondary electronegative ion beam, consisting in part of analyte ions (i.e. BeO^- or Al^-). The source of the primary ion beam is a reservoir of liquid (~120 °C) cesium that is jet sprayed onto a heated porous tungsten surface, producing Cs^+ by thermal ionization. The electropositive ($\sim mA$) cesium beam is accelerated with ion focusing optics to a fine (~1 mm) focal spot at the center of the sample cathode surface. In this manner, the surface of the sample is bombarded with energetic (~100 keV) positive ions continuously over the course of sample interrogation.

Upon impaction of the electropositive cesium beam onto the cathode surface, collisional energy is transferred to components of the sample subsurface, establishing a collision cascade as energetic recoil atoms collide with other atoms in the sample lattice structure. The collision cascade is violent, causing recoil particles (including atomic, molecular, charged, and neutral species) to eject through the sample surface as sputtered matter. For example, in the sputtering of cathodes prepared from BeO powder, the emitted ion population contains a distribution of BeO^- (10-20 μA); O^- (>100 μA); and Be^-, O_2^-, and BeO_2^- (all <1 μA).[37] An additional advantage of the sputter approach is that in a "knock-on" process, electropositive Cs ions can implant in the surface layer of the sample, reducing the effective work function of the solid, thereby enhancing negative ion

14

formation and increasing the sputter yields. In general, sputtered negative ion yields are a co-dependent function of (a) analyte electron affinity/work function (i.e. analytes with high electron affinity provide high negative ion yields and vice versa); and (b) the nature of the sample surface (i.e. ion beam currents are generally improved for chemically pure oxide samples and by inclusion of a metal matrix to the cathode).

After AMS analysis, examination of the spent target reveals that the sputter process etches a crater into the sample surface. Sometimes, spent samples are blackened, presumably the consequence of cesium deposition on the sample surface. Moreover, the geometric crater patterns can be remarkably anomalous on a sample-to-sample basis (Figure 1-3). The most common crater geometry evident in spent targets is a conical pit concentric with the orifice of the target recess; however, off-center pit alignments are not uncommon. Finally, in rare cases, craters can form exclusively along the target orifice perimeter, leaving a spike-shaped protrusion of sample that avoided sputtering, generally concentric with the target orifice. In any case, anomalous crater effects often correlate with significant deviation in the stability and magnitude of the negative ion beam current. The most likely sources of these anomalies are inaccuracies in electropositive cesium beam alignment and/or lattice defects in the packed sample.
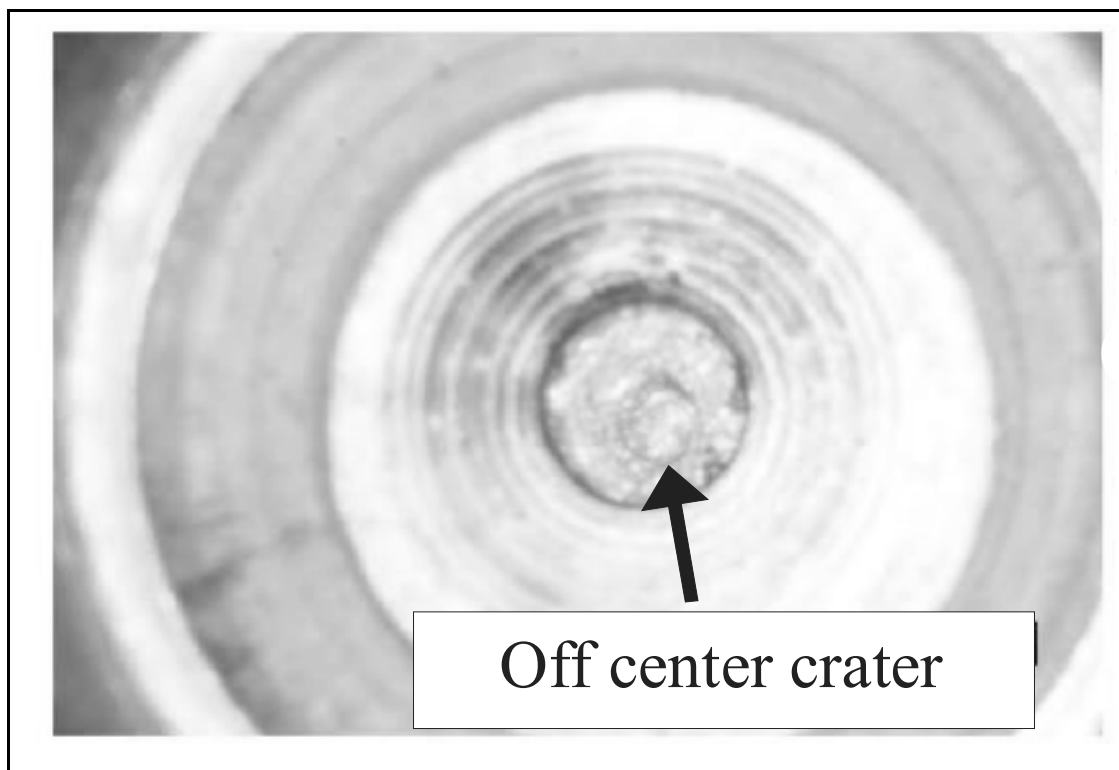
Figure 1-3: Anomalous crater formation, as in this example (a pit that is non-concentric with the cathode orifice) in target cathode during sputtering can result in deviations in ion beam currents.

The same electrode used to focus the primary ion beam doubles as the extraction electrode for focusing atomic or molecular ions (e.g. Al^- or BeO^-) into the AMS injection beam line, defined as the region between the ion sputter source and the tandem accelerator zone. Prior to acceleration, the trajectory of the injection ion beam is bent through a magnetic analyzer for low-resolution mass separation. The injector magnet is primarily useful as an early screen for separating analyte ions from non optimal masses; however, this stage also serves another function: the rapid pulsed injection of ions of the rare and abundant nuclides into the tandem accelerator (e.g. $^{10}BeO^-$ vs. $^9BeO^-$ or $^{26}Al^-$ vs. $^{27}Al^-$). Because the injector magnet only provides single Dalton mass resolution,

contaminations by ion-optically degenerate species (especially $^{10}BO^-$ for $^{10}BeO^-$ analysis) are typically in high population along with the analyte as the negative ion beam enters the tandem acceleration region.

The high energy tandem accelerator at CAMS, originally constructed for nuclear physics research, is housed inside a room-sized steel tank flooded with SF_6 (an insulating gas that maintains voltage holding capacity). The interior construction of the tank is a Van de Graaf design consisting of twin acceleration tubes and a belt of rotating Pelletron chain (alternating metal and plastic links) that conveys electropositive charge to the high voltage (10 MV) terminal at the heart of the accelerator. Inside the high voltage terminal is a canal fitted with an ultra-thin foil oriented in a plane perpendicular to the ion beam trajectory.

The tandem accelerator operates on electrostatic principles: as the negative ion beam (e.g. BeO^- or Al^-, including any molecular and/or atomic isobars) is directed through the first stage of the tandem accelerator toward the positive 8 MV terminal, components of the beam are accelerated from ground to MeV energies. The high kinetic energy achieved by particles in the beam line during the tandem acceleration process is the key event that permits separation of atomic ionic species from any molecular isobars in the ion beam line. Molecular species of almost any kind cannot withstand the high charge conditions at the high voltage terminal without immediately dissociating by Coulombic explosion; furthermore, the mean energy of dissociated molecular isobars ions is different from the energy of analyte ions.

The accelerated anions become so energetic upon reaching the high voltage terminal that, when they transverse the central canal that contains the narrow foil, a number of electrons is actually stripped from each dissociated ion. The stripping process is controlled by the properties of the foil and the operating voltages of the terminal selected for a particular application (e.g. for ^{10}Be analysis, the terminal is maintained at 8 MV). The preferred stripping state of analyte ions is also determined on the basis of the application. For example, for ^{10}Be analysis the preferred stripped ionic state of the analyte is ^{10}Be^{3+}, which is the most effective species for ultimate discrimination of boron. The stripping yield of the preferred charge state at the high voltage terminal is generally non-optimal and remains a major restriction in the goodness of net AMS detection efficiency. Thus, the stability of the terminal voltage and integrity of the stripper foil, both of which affect the charge distribution of ions at the terminal, are critical for reproducible transmission of analyte ions through the tandem accelerator.

Once the dissociated ion beam line components have been stripped to an appropriately high charged state, the newly electropositive ion beam is repelled by the high voltage terminal. The trajectory of the beam is through the second stage of the tandem accelerator toward the grounded far end of the accelerator tank. At this stage, the ion beam is still of relatively heterogeneous composition, populated by a variety of analytes and isobars, atoms and infrequent molecules (which escape Coulombic explosion at the terminal or reform in the beam line after stripping), and species with a distribution of kinetic energies and charge states. Thus, upon exiting the accelerator tank, the high energy stripped analyte ions still require separation from contaminating species.

This separation is achieved with a combination of mass analyzers, including magnetic sectors, an electrostatic sector, and Wein filters (velocity sectors consisting of perpendicular magnetic and electrostatic fields that provide net zero force on particles of pre-selected velocity). Only ions with equal M/q are passed identically by the magnetic sector; ions with equal E/q are passed identically by the electrostatic sector; and lastly, ions with equal E/q and M/q are passed identically by the Wein filter. In order to pass all post-accelerator sectors, the stripped ions must possess specific values M, E, and q as defined by the intersection of all analyzer loci (Figure 1-4).
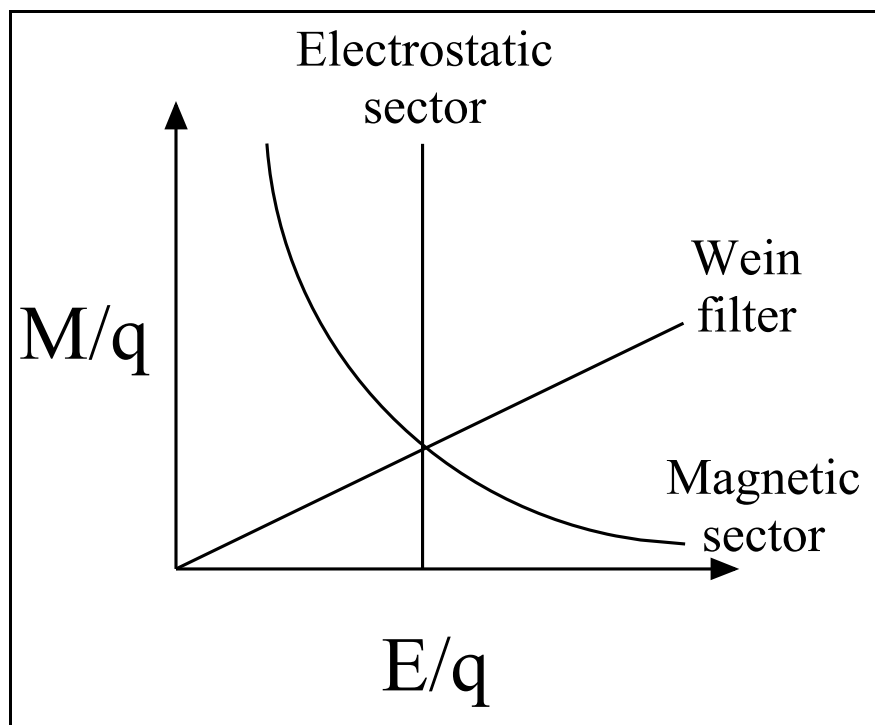
Figure 1-4: Mass and energy sector-based strategy for separating [10]Be and [26]Al from contaminations after acceleration.

The detection of abundant isotopes is performed by collecting the electropositive ion beam in a Faraday detector. In principle, the Faraday detector can be oriented at any site along the AMS beam line; however, it is common practice to position the cup after the tandem accelerator so that both abundant and rare nuclides are stripped to the same charge state. The detection of rare isotopes is accomplished with a gas ionization ΔE-E detector. Ions entering the ΔE-E detector are decelerated in a low pressure (10-200 torr) chamber containing ~90% Argon. Interaction of the ion beam and the gas results in production of discrete electron-ion pairs. The production rate of these pairs is proportional to energy lost as the ion beam penetrates the gas (i.e. as a function of how well the ion beam is slowed in the gas). The electron-ion pairs formed by the detector gas are separated in a homogeneous electrostatic field orthogonal to the ion beam trajectory. The electrostatically separated electrons are collected, according to their energy, along a detection train consisting of five anodes, each of which only detects electrons produced in its vicinity. The rate of energy loss (i.e. stopping power), measured by the response of each anode in the train, is characteristic of the atomic number of the ion. For AMS analysis of ^{10}Be, this is an important stage for isobaric separation of ^{10}B, which has more stopping power than ^{10}Be because of the difference in atomic number. The response of the detector is readily determined by a digitized a plot of E vs. ΔE.

1.7 AMS data reduction

The two principle data streams generated by the AMS system are (a) off-axis Faraday cup measurement of the abundant nuclide; and (b) gas ionization detector measurement of the cosmogenic nuclide. The first is measured as current, which provides an indirect count of the abundant species. The second is measured as a direct count of single atoms of the cosmogenic variety. The results of both data streams are digitized and returned as isotopic ratios (e.g. $^{10}Be/^{9}Be$ or $^{26}Al/^{27}Al$) indicative of the composition of chemically processed AMS cathode. In order to account for errors in the chemical pretreatment process itself, the isotopic ratio determined for a full chemical process blank is always subtracted from the experimental ratios of real samples.

The nuclide activity of the cosmogenic component is calculated by correcting the experimental isotope ratio for the mass of the original quartz substrate and any isotopic carrier added to the quartz digest during sample preparation. For example, for a measured $^{10}Be/^{9}Be$ abundance of 1×10^{-12}, obtained by AMS analysis of a BeO cathode prepared from 20 g quartz doped with 250 μg ^{9}Be isotope carrier, the corresponding activity is 8.36×10^{5} ^{10}Be atoms per gram of quartz. In accordance with conventions of the research community, the cosmogenic activity in quartz is normalized by the known activity at high latitude and sea level. This normalization permits inter-laboratory comparison of AMS data for quartz specimens sampled at any altitude, latitude, thickness, and exposure geometry.

1.8 AMS analytical figures of merit

The performance of AMS depends greatly on both the quality of the samples and optimization of instrumental analysis. Relevant analytical figures of merit that best define AMS performance for ^{10}Be and ^{26}Al analysis are (i) sensitivity, (ii) accuracy, (iii) precision, and (iv) throughput. Each of these figures of merit is described in brief below.

(i) Sensitivity: At present, the principle limitation in AMS sensitivity for ^{10}Be analysis is background due to boron contamination. If boron contaminations are not significant, typical ^{10}Be/^{9}Be abundances in quartz can be readily measured by AMS on the order of 1×10^{-13}. For perspective, samples that exhibit ^{10}Be/^{9}Be ratios as large as 1×10^{-12} are considered particularly active. For challenging analyses such as the measurement of samples with low ^{10}Be abundance, the AMS community use ^{10}Be blanks extracted from deeply mined beryl, which has no recent cosmic ray exposure history and is ancient enough for any contaminant ^{10}Be to have decayed.

The procedure for extracting pure beryllium from beryl is by (1) fusion of 1 g of pulverized mineral with 5 g KHF$_2$ and 1 g Na$_2$SO$_4$; (2) dissolution of the fusion cake in hot (90º C) water; (3) separation of the fluoro-beryllate complex by centrifugation; (4) separation of potassium by selective precipitation with a stoichiometric excess of concentrated HClO$_4$; and (5) storage as a Be(OH)$_2$ gel.[38] Using this procedure, we have generated a stock of beryllium standard with a ^{10}Be/^{9}Be abundance of approximately 1×10^{-16} (Figure 1-5). As the lowest level blank ever processed at CAMS, this stock of standard will permit the future design of otherwise sensitivity-limited experiments. In comparison, ^{26}Al can be measured by AMS with an abundance sensitivity of

approximately 1×10^{-15}. Typically, the measured abundances of ^{26}Al/^{27}Al in quartz are of the magnitude 1×10^{-11}.
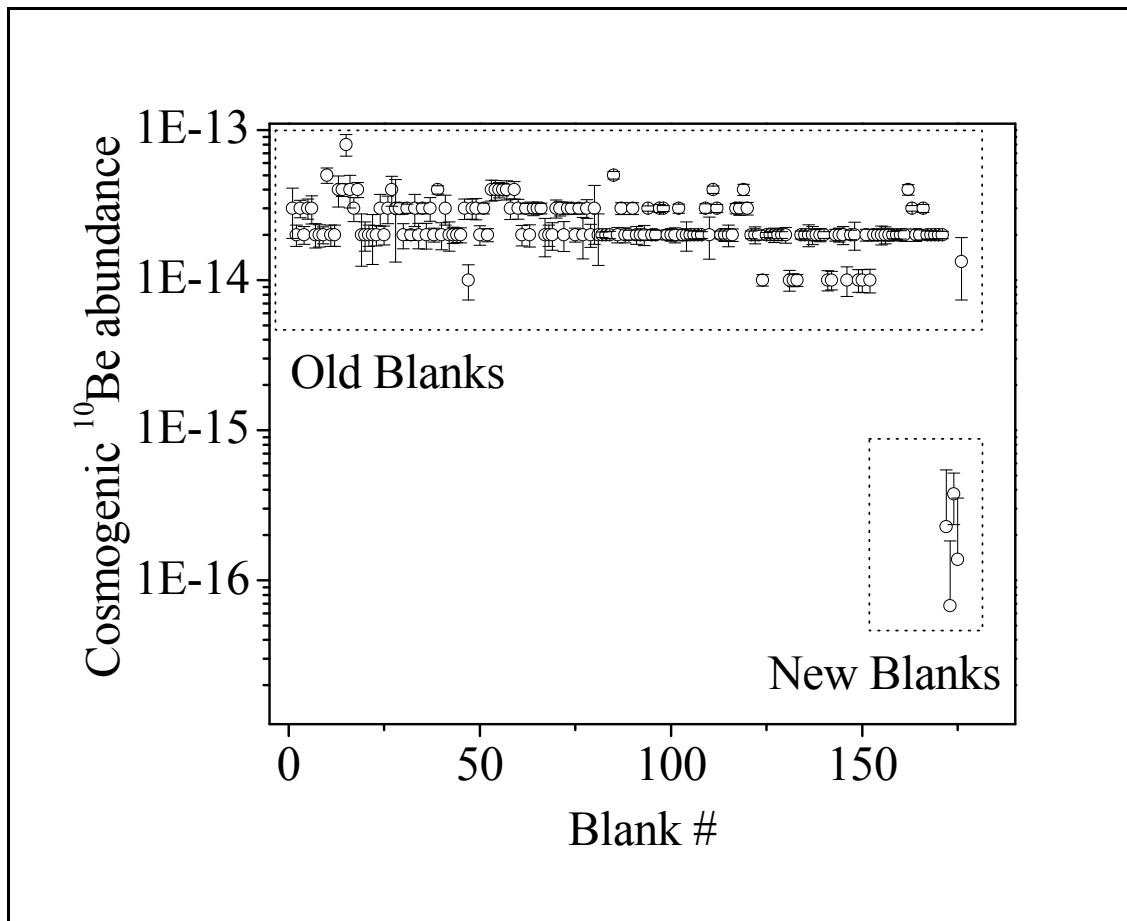
Figure 1-5: Recent improvements in the purity of low level blanks for cosmogenic ^{10}Be analysis. Blank #s indicated on the abscissa are representative of analyses preformed by the Bierman group between the years 1997 and 2007.

At present, the principle limitation in AMS sensitivity for ^{26}Al analysis is the generation of sufficient ion beam current. As a final point, memory effects in the ion source, which are a common source of background in the analysis of some other rare

isotopes, are not significant during ^{10}Be and ^{26}Al analysis, presumably due to the relatively low vapor pressure of the oxides of these species.

(ii) Accuracy: It is our protocol to run three analytical standards between every batch (eight samples including a blank) in order to monitor against instrumental drift. In most cases, ^{10}Be and ^{26}Al standards of known isotopic abundance are provided by the CAMS facility. The most common sources of instrumental drift are deviations in ion optic focusing (e.g. voltage drifts) and fluctuations in AMS ion source behavior (e.g. temperature, vacuum conditions, and primary ion beam current). In any case, standards are used to normalize actual samples, thereby reducing systematic errors.

(iii) Precision: The precision of AMS measurements for ^{10}Be and ^{26}Al is typically 2-5%. All samples are analyzed for a minimum of three replications. Statistical uncertainties are sometimes a function of external error, in which the standard deviation for replicate analyses of the same sample (or standard or blank) is larger than expected from statistics; however, in most cases, counting statistics are the most significant limitation on AMS precision. Such internal, or measurement errors, depend on the square root of the total number of detector counts for the rare nuclide. For example, 5.0% precision requires detection of 400 rare nuclides. In comparison, if 3.0% precision is desired, AMS analysis requires detection of 1100 rare nuclides. The constraints on precision that arise from counting statistics are of ongoing concern for AMS analysis, since the availability of rare nuclides counts is almost always restricted by a combination of (a) sample size, which limits the maximum yield of rare nuclides; and (b) analysis time, which is limited by operator endurance and financial expense.

(iv) Throughput: Sample wheels loaded to capacity with 64 samples typically require 10 hrs or 24 hrs for analysis of ^{10}Be or ^{26}Al respectively. Longer analysis times can be necessary for samples with naturally low rare nuclide abundances; however, a principle limitation in analytical throughput is almost always ion source efficiency. AMS ion source efficiency is inherently dictated by the qualitative and quantitative range of atomic and molecular ion yields attainable from a particular substrate. A comprehensive survey of ion yields for most elements is available in an unpublished, albeit widely circulated, authoritative treatise on this subject by R. Middleton who was a great innovator in the field AMS ion source design.[37] Compared to losses due to ion source efficiency, losses due to beam line transmission efficiencies are generally considered to be insignificant. Another major limitation in AMS efficiency is maintaining good stripping yields (i.e. charge distribution of the stripped analyte) in the accelerator.

The most reliable, albeit time-consuming, method to assess AMS throughput is to analyze a standard until it expires (i.e. no longer generates current in the ion source). For example, over an analysis time of ~16 hours, a BeO cathode (1.48 mg BeO prepared in an equimolar mixture of BeO powder with niobium matrix) registered a total of 2788 cosmogenic nuclide counts before it was interrogated to exhaustion (Figure 1-6). Based upon a maximum possible count number of 3.56×10^{-5} (assuming a natural isotopic abundance of 1×10^{-14} in commercial beryllium), the efficiency of ^{10}Be analysis at CAMS is calculated to be ~0.78%. This value is excellent compared to the maximum theoretical value of ~1%.[33]
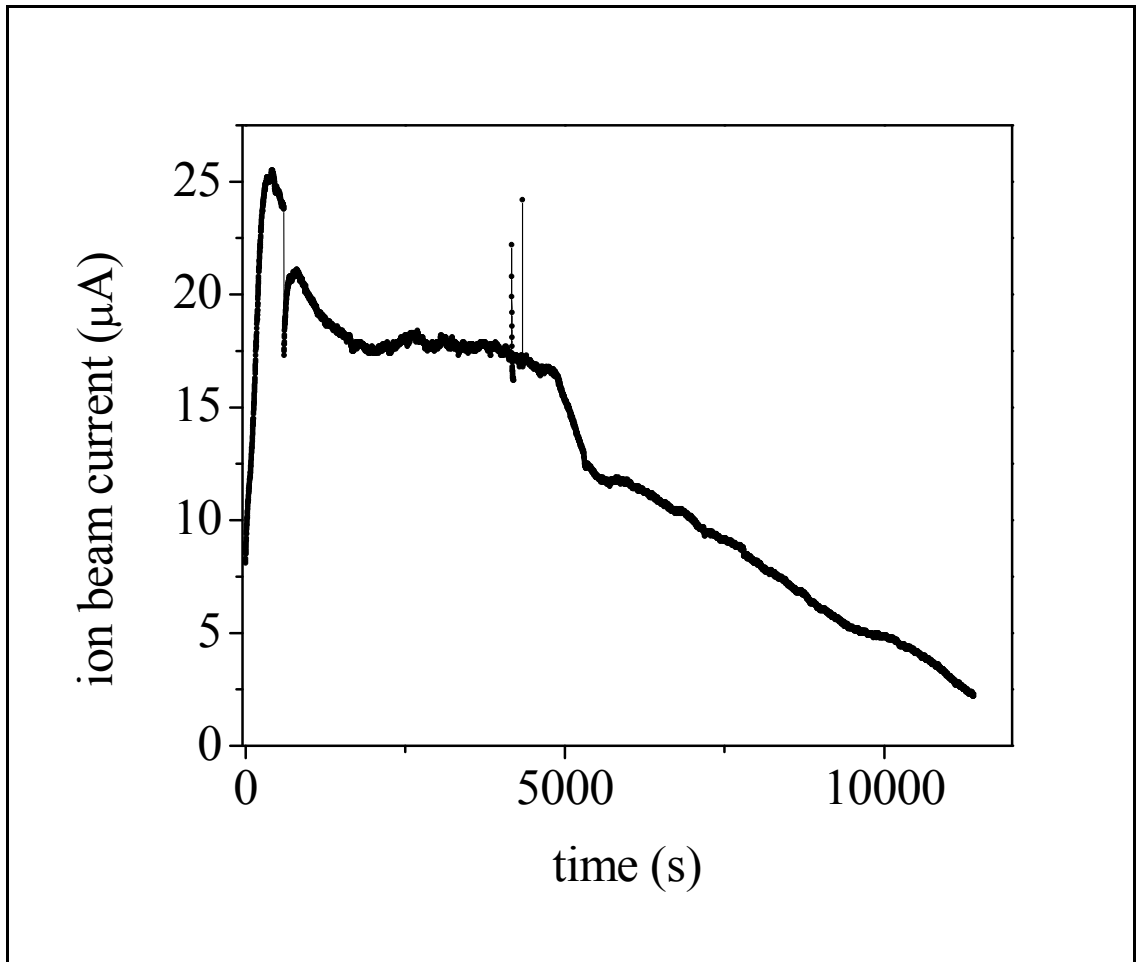
Figure 1-6: BeO⁻ ionization efficiency from BeO cathodes can be inferred from the integrated current of a standard target (datum acquisition rate is ~1 Hz)

1.9 AMS data interpretation

On account of their exceptionally long half lives, ^{10}Be (1.5 Ma) and ^{26}Al (0.7 Ma) are good chronometric tracers for geological phenomenon dating in the Pleistocene era. In terms of geological applications, the fundamental tenant of AMS data interpretation is that experimentally measured activities of rare nuclides are a direct function of cosmic ray exposure integrated over long timescales. Furthermore, in order for interpretation of

cosmogenic nuclide abundances to be meaningful, it is necessary to fully account for other possible mechanisms of rare nuclide production (e.g. other in situ nuclear reactions, meteoric production and deposition, and muon induced nuclear dissociations). In addition, it is necessary to account for isotopic production deviations that manifest as a function of latitude, altitude, geomagnetic activity, and solar flares.

In the most basic model for interpreting in situ cosmogenic nuclide data (Equation 1.2), the experimentally determined nuclide activity (e.g. ^{10}Be abundance in quartz) is dependant on two parameters: exposure time (t) and erosion rate (ε):

$$(1.2) \: N = \frac{P}{(\lambda + \varepsilon\rho/\Lambda) \: (1 - e^{-(\lambda + \varepsilon\rho/\Lambda)})}$$

where the production rate (P), quartz density (ρ), attenuation coefficient (Λ), and decay constant (λ) are well-defined values. Because of the dependence of nuclide activity on both exposure time and erosion rate, applications involving quantification of a single nuclide (i.e. analysis of ^{10}Be or ^{26}Al only) require confident approximation of one of these parameters. If such an approximation is impossible, the application requires quantification of dual nuclides (i.e. co-analysis of ^{10}Be and ^{26}Al).

Case #1: No erosion. The most straightforward application of cosmogenic nuclide activity to geochronology is the calculation of terrestrial surface exposure ages. The exposure age is defined as difference in time between a present age and a past age when a quartz surface was first irradiated by cosmic particles. For example, if there were some climactic terrestrial event that suddenly exposed quartz at Earth's surface (e.g. glacier

27

erosion, meteorite impact, volcanic activity, faulting, deep erosion, etc.), over time an inventory of cosmogenic ^{10}Be and ^{26}Al would accumulate in the surficial quartz lattice. Quantification of one of these rare nuclides (usually ^{10}Be on account of its longer half life and ease of measurement) accurately dates the climactic terrestrial event that initiated exposure.

The principle limitation of surface exposure dating is that the rock surface under investigation must be a closed system. In this case, a closed system is defined as a site with negligible erosion and zero topographic shielding over the duration of cosmic radiation. In general, episodic phenomena (such as burial by snow or oil) are the most significant uncertainty when considering the shielding history of a sample. When this criterion can be established (i.e. ε=0), the measured nuclide activity of ^{10}Be in quartz reflects the cosmogenic ^{10}Be production integrated over an exposure age minus losses due to radioactive natural decay (Equation 1.3)

$$(1.3)\ N= \frac{P}{\lambda(1-e^{-(\lambda+\varepsilon\rho/\Lambda)})}$$

The most extensively employed application of single cosmogenic nuclide analysis for exposure dating is the determination of glacial chronologies. In this context, AMS data have been used to determine the exposure ages of glacially polished bedrock and moraine boulders which, as products of glacial advance and retreat, provide an estimate of the history of these phenomena. Seminal examples of this application is the dating of North American moraines (in Wyoming)[39, 40] and Wisconsin,[41] and Antarctic moraines.[12]

Case #2: Steady state erosion. In most applications of cosmogenic [10]Be analysis, quartz

is acquired from non-glacial landscapes, which are generally prone to significant erosion

processed (e.g. $\varepsilon > 1$ mm/ka). In some ancient landscapes, steady state erosion occurs

whereby the cosmogenic nuclide activity in quartz is controlled by removal of mass from

the surface rather than the original exposure age. If it can be established that erosion is in

a steady state regime, occurring for a long time compared to the half life of the

cosmogenic nuclide (t=∞), the rate of erosion can be estimated on the basis of

cosmogenic nuclide activity (Equation 1.4).

$$(1.4)\ N = \frac{P}{(\lambda + \varepsilon\rho/\Lambda)}$$

The obvious constraint of this application is that the erosion rate must be constant;

whereas in reality local erosion rates are often discontinuous.[42] For example, large slabs

of rock can spall off of exposed surfaces due to freezing, thawing, or fires.

A classical example of this application is the determination of erosion rates of

Australian inselbergs (natural granitic domes). Using cosmogenic [10]Be activities and this

interpretive model, these inselbergs have a demonstrated history of erosion at a rate one

meter per 700,000 years (or ~1.5 mm ka[-1]), suggesting that the inselbergs among the most

stable geomorphic surfaces on Earth.[43]

In general, whereas applications described by Case 1 are generally restricted to

analysis of relatively ancient and unchanging landforms, Case 2 is more readily applied

to dynamic landscape processes such as sediment generation and transport.[44] For

example, this method has been used to determine an estimation of average sediment generation rates in dryland basins.[45, 46]

Case #3: Complex exposure and erosion. As described in Case 1 and Case 2, in applications involving landscape change, AMS data interpretation based upon single nuclide analysis always requires an assumption, without which it is impossible to determine the history of a sample. For instance, if the conditions of zero erosion ($\varepsilon=0$) and steady state erosion rate ($t=\infty$) can not be reasonably inferred for a quartz specimen with low experimental ^{10}Be activity relative to the known production rate, then the low activity may be either a consequence of (a) short exposure age or (b) long surface residence time. In order to determine the true history of such a sample, it is necessary to experimentally determine the activity of another cosmogenic nuclide (e.g. ^{26}Al). Therefore, in complex systems, the underdetermined relationship between nuclide activity, exposure, and erosion can only be determined by AMS analysis of a pair of rare nuclide activities (Equation 1.5).

$$(1.5) \, R_{\frac{^{10}Be}{^{26}Al}} = \frac{N_{^{10}Be}(t,\varepsilon)}{N_{^{26}Al}(t,\varepsilon)}$$

Thus, cosmogenic ^{10}Be and ^{26}Al activities are often measured together in the same sample in order to assess complex histories of quartz samples. The most common application of this model is burial dating, which is now emerging as a very active research field.[47, 48] This approach is essential for analysis of samples collected from locations which cannot be described as stable or steadily eroding. Note that the dual

isotope method can actually be applied to determine whether erosion can be considered to be steady state phenomenon over time.[49]

A two-nuclide diagram of ^{26}Al/^{10}Be versus ^{10}Be concentration (usually log/normal scale) demonstrates the manner whereby the ^{26}Al/^{10}Be value can be theoretically predicted to deviate from the nominal ^{26}Al/^{10}Be production ratio of 6.0 as a function of exposure times and erosion rates.[29, 50] The steady state erosion island (the enclosed sickle-shape region) is constrained by a lower envelope and upper envelope (for the case of irradiation upon a zero erosion, no prior exposure surface, i.e. ε=0). The saturation point, or secular equilibrium, is reached after four or five half-lives when the production and decay of cosmogenic nuclides are balanced. Experimental data points are typically plotted as overlays on the theoretical model.

There are four regimes in which experimental data can correlate to the theoretical production values: (1) data above the curves indicates anomalously high production values or analytical errors; (2) data along the production curve indicates that sample has undergone constant exposure and zero erosion, the relative contribution of which can be evaluated by proximity to the relevant boundary; (3) data inside the steady state erosion island indicates some combination of erosion and exposure; and (4) data below the steady state island indicate that the cosmic ray exposure of the sample was interrupted at some point in history. Note that the later response is generally of exceptional geomorphologic interest because it can be actually be used to identify the burial history of a sample. In practice, samples can move longitudinally and laterally on the two-nuclide diagram as they are repeatedly buried or eroded.[41]

By way of illustration, consider the two-nuclide diagram obtained for 61 exposed Australian bedrock samples[51] (Figure 1-7a). The goodness of the overlap between the theoretical steady state erosion island and experimental data indicates that the samples have simple exposure histories. In contrast, consider the two-nuclide diagram obtained for 12 quartz clasts from piedmont surfaces in an extremely arid region of Namibia[49] (Figure 1-7b). The dashed lines (which do not appear in Figure 1-7a) are a common feature in such plots that indicate burial isochrones. The position of the data relative to the lower boundary indicates that these samples have complex exposure histories, characterized by at least one a significant burial episode.
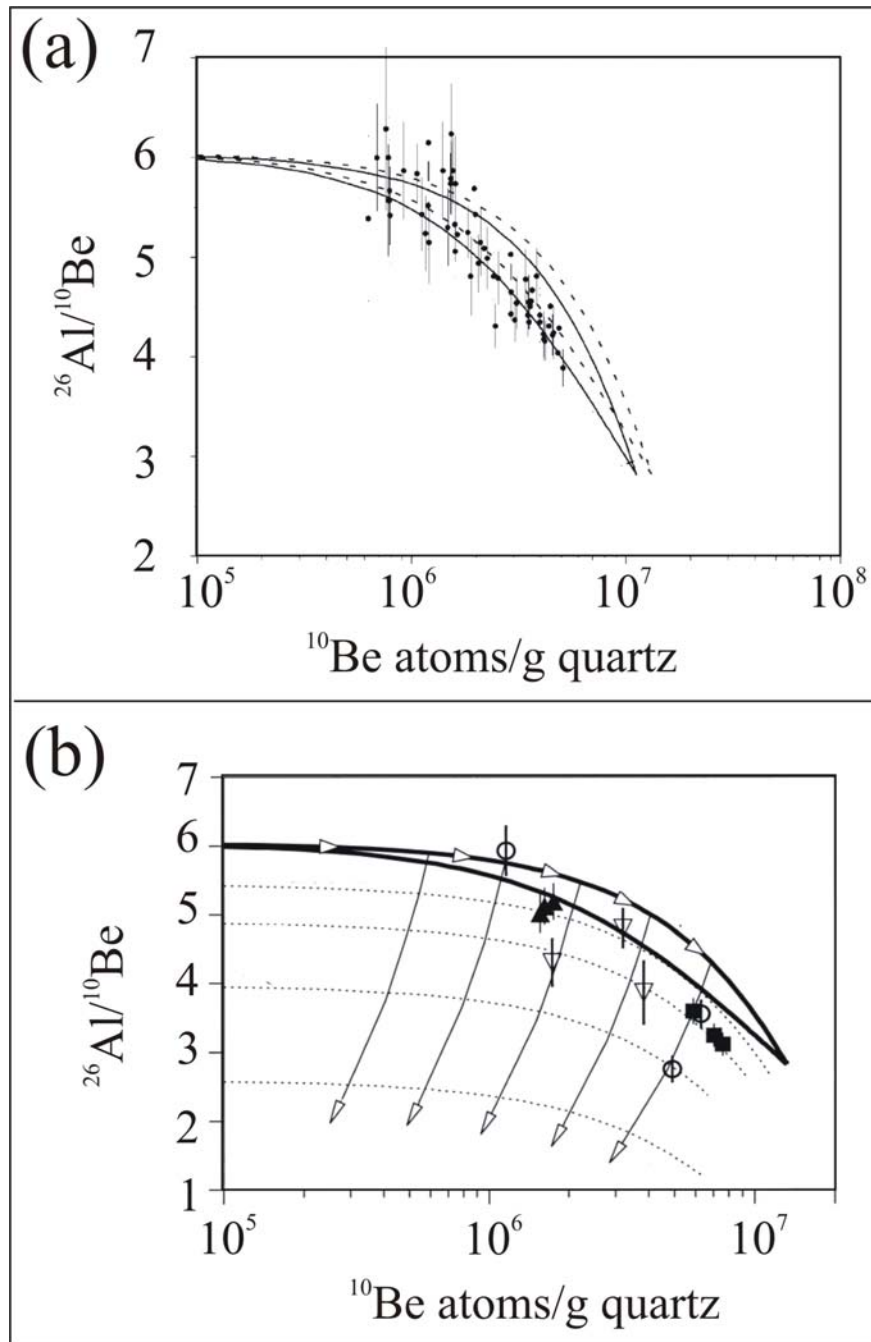
Figure 1-7: Classic two-nuclide "bananagram" for a sample population with (a) simple exposure history (modified from the work of Bierman[51]); and (b) complex exposure history (modified from the work of Bierman[49]). Symbols are experimental data.

1.10 Challenges to AMS analysis of ^{10}Be and ^{26}Al addressed in this work

Due to the complexity of cosmogenic ^{10}Be and ^{26}Al analysis, geomorphologic conclusions based upon AMS data should consider all possible sources of uncertainty.[52] As described previously, the analytical precision of the AMS method is usually 2-5%. Other (approximate) uncertainties are associated with long-term cosmogenic nuclide production rates including the contribution of non-cosmogenic sources and normalization for latitude, altitude, and geomagnetic field strength (<20%), isotope decay constants (<5%), assumed constants pertaining to mineral density (<5%) and the cosmic ray flux attenuation parameter (5%), and stable nuclide abundance (<5%). Moreover, if a dual nuclide analysis is employed, error is propagated through two respective equations that relate abundance, age, and erosion. Thus it can generally be assumed that the total propagated uncertainties in a typical geomorphologic application can easily approach ~20%.

One of the greatest challenges for AMS analysis is application to surfaces with exceptionally high erosion rates. In such cases, cosmogenic ^{10}Be and ^{26}Al abundances in the sample are always very low and difficult to measure with acceptable accuracy and precision. ^{10}Be/^{9}Be and ^{26}Al/^{27}Al ratios are generally limited by any combination of (a) successful isolation and purification of the analyte from quartz; (b) AMS sensitivity restrictions (due, for instance, to background ratios in blanks); and (c) production of AMS cathodes which generate sufficient ion beam current. Each of these challenges must be addressed in order to expand the timeline over which landscape changes can be accurately determined by AMS analysis of cosmogenic nuclides. The remainder of this

chapter of the dissertation outlines the manner in which these challenges will be experimentally addressed.

(a) Isolation and purification of BeO and Al$_2$O$_3$ from quartz. At present, the greatest challenge to ^{10}Be and ^{26}Al analysis by AMS is the extensive and time-consuming chemical pretreatment of sample necessary to isolate and purify beryllium and aluminum from rocks and soil. For the sole purpose of producing BeO and Al$_2$O$_3$ cathodes for AMS analysis, the Bierman group has a dedicated clean laboratory with fully exhausting laminar flow ventilation hoods and plastic (Teflon/HDPE/PP) labware to reduce contamination from boron (the pervasive isobar of ^{10}Be) due to trace-element leeching from borosilicate glass. The experimental methods for sample preparation employed in the laboratory are based largely upon an empirical and anecdotal knowledgebase pertaining to sample preparation. Furthermore, while most published geology reports contain brief experimental methods sections, there is a paucity of peer-reviewed literature that explicitly details AMS chemical processing methods or presents quantitative analysis of important steps. Chapter 2 of this dissertation summarizes a program to assess the efficiency of the chemical separation procedure from start to finish. This work has been submitted, in the same form presented herein, to the peer-reviewed journal *Analytical Chemistry*.

(b) AMS sensitivity. As described earlier in this chapter, a record-low isotopic blank for ^{10}Be analysis has been prepared from the fusion of a beryl specimen. Furthermore, the improved isotope carrier has been produced in quantities sufficient for many years of research. This is a technical achievement that will ultimately permit

measurement of low nuclide activities with much greater precision than has been previously possible. Of particular interest are the determination of sediment generation, delivery (i.e. removal), and accretion rates and mechanisms in rapidly eroding landscapes such as river networks[53] and drainage basins.[54]

(c) Optimization of AMS ion beam currents. The generation of high purity beryllium and aluminum samples is only half of the challenge in cosmogenic nuclide analysis. The other half is contingent upon the actual analysis at the AMS facility. The most prevalent symptom of samples which perform poorly is the generation of low ion beam currents of the abundant isotope. As a result, it is now common protocol at many AMS facilities that employ second generation, high intensity sputter ion sources to prepare cathodes in a matrix of conducting metal powder. Empirical evidence suggests that cathodes prepared with a matrix inclusion demonstrate improved ion beam current output and stability; however, the physicochemical mechanisms underlying this phenomenon are poorly understood. Thus, ion source matrix effects, although of great benefit to AMS (particularly for ^{10}Be analysis), provide yet another level of mystery to the general conundrum of "ion sourcery." Chapters 3 and 4 of this dissertation describe experiments to investigate matrix effects on AMS ion beam current for the analysis of ^{10}Be and ^{26}Al respectively. These works have been published, without modification herein, in the peer-reviewed journal *Nuclear & Instrument Methods Development*.

1.11 References

1.   Lal, D., In situ-produced cosmogenic isotopes in terrestrial rocks. *Annual Reviews of Earth and Planetary Science* **1988,** 16, 355-388.

2.   Lal, D., Cosmic ray labeling of erosion surfaces; in situ nuclide production rates and erosion models. *Earth and Planetary Science Letters* **1991,** 104, (2-4), 424-439.

3.   Nishiizumi, K.; Winterer, E. L.; Kohl, C. P.; Klein, J.; Middleton, R.; Lal, D.; Arnold, J. R., Cosmic ray production rates of ^{10}Be and ^{26}Al in quartz from glacially polished rocks. *Journal of Geophysical Research, B, Solid Earth and Planets* **1989,** 94, (12), 17,907-17,915.

4.   Kohl, C. P.; Nishiizumi, K., Chemical isolation of quartz for measurement of *in-situ* -produced cosmogenic nuclides. *Geochimica et Cosmochimica Acta* **1992,** 56, 3583-3587.

5.   Lal, D., Cosmogenic isotopes produced in situ in terrestrial solids. *Nuclear Instruments and Methods in Physics Research Section B: Beam Interactions with Materials and Atoms* **1987,** B29, 238-245.

6.   Lal, D.; Peters, B., Cosmic-ray produced isotopes and their application to problems in geophysics. In *Progress in elementary particle and cosmic ray physics*, ed.; Wilson, J. G.; Wouthysen, S. A., Eds. Wiley: New York, 1962; pp 1-74.

7.   Lal, D.; Peters, B., Cosmic ray produced radioactivity on the earth. In *Handbuch der Physik*, ed.; Sitte, K., Eds. Springer-Verlag: New York, 1967; pp 551-612.

8.   Brown, E. T.; Brook, E. J.; Raisbeck, G. M.; Yiou, F.; Kurz, M. D., Effective attenuation lengths of cosmic rays producing ^{10}Be and ^{26}Al in quartz; implications for exposure age dating. *Geophysical Research Letters* **1992,** 19, (4), 369-372.

9.   Brown, E. T.; Raisbeck, G. M.; Yiou, F.; Kurz, M.; Brook, E. J., Effective attenuation lengths of cosmic rays producing ^{10}Be and ^{26}Al in quartz: implications for exposure dating. *EOS* **1992,** 72, (44), 575.

10.   Sharma, P.; Middleton, R., Radiogenic production of ^{10}Be and ^{26}Al in uranium and thorium ores: Implications for studying terrestrial samples containing low levels of ^{10}Be and ^{26}Al. *Geochimica et Cosmochimica Acta* **1989,** 53, 709-716.

11.   Monaghan, M. C. K., S.; Turekian, K.K., The global-average production rate of ^{10}Be. *Earth and Planetary Science Letters* **1986,** 76 (1985/86), 279-287.

12.   Brown, E. T.; Edmond, J. M.; Raisbeck, G. M.; Yiou, F.; Kurz, M. D.; Brook, E. J., Examination of surface exposure ages of Antarctic moraines using in situ produced ^{10}Be and ^{26}Al. *Geochimica et Cosmochimica Acta* **1991,** 55, 2269-2283.

13.   Raisbeck, G. M.; Yiou, F.; Klein, J.; Middleton, R., Accelerator mass spectrometer measurement of cosmogenic ^{26}Al in terrestrial and extraterrestrial matter. *Nature* **1983,** 301, 690-692.

14.   Desilets, D.; Zreda, M., Scaling production rates of terrestrial cosmogenic nuclides for altitude and geomagnetic effects. *Geological Society of America Abstracts with Programs* **2000,** 31, (7), A-400.

15.   Desilets, D.; Zreda, M.; Lifton, N. A., Comment on 'Scaling factors for production rates of in situ produced cosmogenic nuclides: a critical reevaluation' by Tibor J. Dunai. *Earth and Planetary Science Letters* **2001,** 188, (1-2), 283-287.

16.   Dunai, T. J., Scaling factors for production rates of in situ produced cosmogenic nuclides: a critical reevaluation. *Earth and Planetary Science Letters* **2000,** 176, 157-169.

17.   Dunai, T. J., Reply to comment on `Scaling factors for production rates of in situ produced cosmogenic nuclides: a critical reevaluation'. *Earth and Planetary Science Letters* **2001,** 188, (1-2), 289-298.

18.   Masarik, J.; Frank, M.; Schafer, J.; Wieler, R., Correction of in-situ cosmogenic nuclide production rates for geomagnetic field intensity variations during the past 800,000 years. *Geochimica et Cosmochimica Acta* **2001,** 65, (17), 2995-3003.

19.   Masarik, J.; Reedy, R. C., Terrestrial cosmogenic-nuclide production systematics calculated from numerical simulations. *Earth and Planetary Science Letters* **1995,** 136, 381-396.

20.   Beer, J.; Blinov, A.; Bonani, G.; Finkel, R. C.; Hofmann, H. J.; Lehmann, B.; Oeschger, H.; Sigg, A.; Schwander, J.; Staffelbach, T.; Stauffer, B. R.; Suter, M.; Wolfli, W., Use of [10]Be in polar ice to trace the 11-year cycle of solar activity. *Nature* **1990,** 347, (6289), 164-166.

21.   Clark, D.; Bierman, P. R.; Larsen, P., Improving in situ cosmogenic chronometers. *Quaternary Research* **1995,** 44, (3), 366-376.

22.   Clark, D. H.; Bierman, P. R.; Gillespie, A. R., New cosmogenic [10]Be and [26]Al measurements of glaciated surfaces, Sierra Nevada, California; they're precise but are they accurate? *Geological Society of America, 1995 annual meeting Abstracts with Programs - Geological Society of America* **1995,** 27, (6), 170.

23.   Gosse, J. C.; Phillips, F. M., Terrestrial in situ cosmogenic nuclides: theory and application. *Quaternary Science Reviews* **2001,** 20, (14), 1475-1560.

24.   Dunne, A.; Elmore, D.; Muzikar, P., Scaling factors for the rates of production of cosmogenic nuclides for geometric shielding and attenuation at depth on sloped surfaces. *Geomorphology* **1999,** 27, (1-2), 3-11.

25.   Dunne, J. A. Calibration of the method of exposure dating of geomorphic surfaces on the Earth using in-situ-produced cosmogenic radionuclides, and applications in the Central Andes. Dissertation, Purdue University, West Lafayette, IN, 1999.

26.   Schildgen, T. F.; Purves, R. S.; Phillips, W. M., Modeling effects of snow burial on cosmogenic exposure age dating, Cairngorm Mountains, Scotland, and Wind River Range, WY. *Eos Transactions of AGU* **2002,** 83, (47), F550.

27.   Turekian, K. K.; Cochran, J. K.; Krishnaswami, S.; Langford, W. A.; Parker, P. D.; Bauer, K. A., The measurement of ^{10}Be in manganese nodules using a tandem Van De Graaff accelerator. *Geophysical Research Letters.* **1979,** 6, 417-420.

28.   Davis, R.; Schaeffer, O. A., Chlorine-36 in nature. *Annals of the New York Academy of Science* **1955,** 62, 105-122.

29.   Klein, J.; Giegengack, R.; Middleton, R.; Sharma, P.; Underwood, J. R.; Weeks, R. A., Revealing histories of exposure using in situ produced ^{26}Al and ^{10}Be in Libyan desert glass. *Radiocarbon* **1986,** 28, (2A), 547-555.

30.	Nishiizumi, K.; Lal, D.; Klein, J.; Middleton, R.; Arnold, J. R., Production of ^{10}Be and ^{26}Al by cosmic rays in terrestrial quartz in situ and implications for erosion rates. *Nature* **1986,** 319, (6049), 134-136.

31.	Elmore, D.; Phillips, F., Accelerator mass spectrometry for measurement of long-lived radioisotopes. *Science* **1987,** 236, 543-550.

32.	Middleton, R.; Klein, J., ^{26}Al: measurement and applications. *Philosophical Transactions of the Royal Society of London* **1987,** A 323, 121-143.

33.	Finkel, R.; Suter, M., AMS in the Earth Sciences: Technique and applications. *Advances in Analytical Geochemistry* **1993,** 1, 1-114.

34.	Roberts, M. L.; Bench, G. S.; Brown, T. A.; Caffee, M. W.; Finkel, R. C.; Freeman, S. P. H. T.; Hainsworth, L. J.; Kashgarian, M.; McAninch, J. E.; Proctor, I. D.; Southon, J. R.; Vogel, J. S., The LLNL AMS facility. *Nuclear Instruments and Methods in Physics Research Section B: Beam Interactions with Materials and Atoms* **1997,** 123, 57-61.

35.	Brown, T. A.; Roberts, M. L.; Southon, J. R., Ion-source modeling and improved performance of the CAMS high-intensity Cs-sputter ion source. *Nuclear Instruments and Methods in Physics Research Section B: Beam Interactions with Materials and Atoms* **2000**, (172), 344-349.

36.	Southon, J. R.; Roberts, M., Ten years of sourcery at CAMS/LLNL - Evolution of a Cs ion source. *Nuclear Instruments and Methods in Physics Research Section B: Beam Interactions with Materials and Atoms* **2000,** 172, 257-261.

37.   Middleton, R. *A Negative Ion Cookbook*; Department of Physics, University of Pennsylvania: Philadelphia, 1990.

38.   Stone, J., A rapid fusion method for separation of beryllium-10 from soils and silicates. *Geochimica et Cosmochimica Acta* **1998,** 62, (3), 555-561.

39.   Gosse, J. C.; Evenson, E. B.; Klein, J.; Lawn, B.; Middleton, R., Precise cosmogenic [10]Be measurements in western North America; support for a global Younger Dryas cooling event. *Geology* **1995,** 23, (10), 877-880.

40.   Gosse, J. C.; Klein, J.; Evenson, E. B.; Lawn, B.; Middleton, R., Beryllium-10 dating of the duration and retreat of the last Pinedale glacial sequence. *Science* **1995,** 268, 1329-1333.

41.   Bierman, P. R.; Marsella, K. A.; Patterson, C.; Davis, P. T.; Caffee, M., Mid-Pleistocene cosmogenic minimum-age limits for pre-Wisconsinan glacial surfaces in southwestern Minnesota and southern Baffin Island; a multiple nuclide approach. *Geomorphology* **1999,** 27, (1-2), 25-39.

42.   Bierman, P. R.; Gillespie, A. R., Range fires: A significant factor in exposure-age determination and geomorphic surface evolution. *Geology* **1991,** 19, 641-644.

43.   Bierman, P.; Turner, J., [10]Be and [26]Al evidence for exceptionally low rates of Australian bedrock erosion and the likely existence of pre-Pleistocene landscapes. *Quaternary Research* **1995,** 44, 378-382.

44.   Bierman, P.; Nichols, K., Rock to sediment - Slope to sea with [10]Be - Rates of landscape change. *Annual Review of Earth and Planetary Sciences* **2004,** 32, 215-255.

45.   Clapp, E. M.; Bierman, P. R.; Caffee, M. W., Using [10]Be and [26]Al to determine sediment generation rates and identify sediment source areas in an arid region drainage basin. *Geomorphology* **2002,** 45, 89-104.

46.   Clapp, E. M.; Bierman, P. R.; Nichols, K. K.; Pavich, M.; Caffee, M., Rates of sediment supply to arroyos from upland erosion determined using in situ produced cosmogenic [10]Be and [26]Al. *Quaternary Research (New York)* **2001,** 55, (2), 235-245.

47.   Granger, D. E.; Kirchner, J. W.; Finkel, R. C., Quaternary downcutting rate of the New River, Virginia, measured from differential decay of cosmogenic [26]Al and [10]Be in cave-deposited alluvium. *Geology* **1997,** 25, (2), 107-110.

48.   Granger, D. E.; Muzikar, P. F., Dating sediment burial with in situ-produced cosmogenic nuclides; theory, techniques, and limitations. *Earth and Planetary Science Letters* **2001,** 188, (1-2), 269-281.

49.   Bierman, P. R.; Caffee, M. W., Slow rates of rock surface erosion and sediment production across the Namib Desert and escarpment, Southern Africa. *American Journal of Science* **2001,** 301, (4-5), 326-358.

50.   Nishiizumi, K.; Kohl, C. P.; Arnold, J. R.; Klein, J.; Fink, D.; Middleton, R., Cosmic ray produced [10]Be and [26]Al in Antarctic rocks; exposure and erosion history. *Earth and Planetary Science Letters* **1991,** 104, (2-4), 440-454.

51.   Bierman, P. R.; Caffee, M., Cosmogenic exposure and erosion history of ancient Australian bedrock landforms. *Geological Society of America Bulletin* **2002,** 114, (7), 787-803.

52.   Gillespie, A. R.; Bierman, P. R., Precision of terrestrial exposure ages and erosion rates estimated from analysis of cosmogenic isotopes produced in situ. *Journal of Geophysical Research, B, Solid Earth and Planets* **1995,** 100, (12), 24,637-24,649.

53.   Reusser, L.; Bierman, P.; Pavich, M.; Zen, E.; Larsen, J.; Finkel, R., Rapid late Pleistocene incision of Atlantic passive-margin river gorges. *Science* **2004,** 305, (5683), 499-502.

54.   Clapp, E. M.; Bierman, P. R.; Schick, A. P.; Lekach, J.; Enzel, Y.; Caffee, M., Sediment yield exceeds sediment production in arid region drainage basins. *Geology* **2000,** 28, (11), 995-998.

CHAPTER 2: INVESTIGATION OF FACTORS WHICH AFFECT THE SENSITIVITY OF ACCELERATOR MASS SPECTROMETRY (AMS) FOR COSMOGENIC ^{10}Be AND ^{26}Al ISOTOPE ANALYSIS

2.1 Introduction

Cosmogenic nuclides are formed by nuclear reactions induced by cosmic rays, predominantly high-energy neutrons, which constantly bombard the Earth's surface penetrating with sufficient energy to spallate mineral phase atomic nuclei at depths up to several meters of rock.[1] For example, the rare terrestrial cosmogenic nuclides ^{10}Be and ^{26}Al accumulate in exposed quartz surfaces over a geological timescale (typically ka), primarily by spallation of O and Si, respectively. The abundance of these cosmogenic isotopes in quartz initially increases as a function of cosmic ray exposure; however, this natural enrichment is limited by eventual and on-going landscape erosion.[2] On account of their long half-lives (^{10}Be ~1.5 Ma; ^{26}Al ~0.7 Ma), these often-paired cosmogenic nuclides are useful chronologic tracers over timescales relevant to landscape changes at and near Earth's surface. For example, because background or radiogenic production rates of ^{10}Be are extremely low,[3] measured activities of ^{10}Be produced in quartz (i.e. the cosmogenic *in situ* component) are an indication of the residence time of quartz at and near Earth's surface, where most cosmogenic nuclide production occurs. Because production rates of ^{10}Be and ^{26}Al are very low (5.2 and 30.1 atoms g^{-1} a^{-1} respectively at sea level and high latitude),[4] even long-exposed quartz specimens have very low ^{10}Be and ^{26}Al concentrations; therefore, measurement of these isotopes is only feasible with the

highly sensitive analytical method of accelerator mass spectrometry (AMS).[5, 6] Nuclide abundances, as derived from AMS data, are interpreted using a variety of application-contingent models.[7] In most quartz specimens, ^{10}Be and ^{26}Al can be measured by AMS (in a practical working range and in respect to their stable isotopes) with ratio sensitivity of approximately 10^{-15} and 10^{-14} respectively.

The key terrestrial cosmogenic nuclides, ^{10}Be and ^{26}Al, are often analyzed in the same quartz aliquot because the chemical extraction procedures for Be and Al are similar and readily performed in concurrent fashion. In some geological applications, there is another benefit to co-analysis of both rare isotopes: simultaneous calculation of (a) exposure ages and long-term erosion rates of quartz samples in exposed landscapes;[8] and (b) burial dating of, for example, fluvial or fossil-containing sediments.[9] Unfortunately, the chemical methodology for concurrently extracting high-purity, μg quantities of Be and Al from quartz mineral separates is non-trivial. A typical batch of eight simultaneously processed samples (comprised of seven quartz specimens and a blank) typically requires an experimental work-up time of two weeks in order to process purified samples of BeO and Al_2O_3.

For ^{10}Be analysis by AMS, the typical sampling strategy is to accelerate BeO$^-$ from the AMS ion source rather than the metastable atomic ion (Be$^-$)[10]. Using this method, AMS ion beam currents (as a function of stripped ^{9}Be^{3+}) are generally < 20 μA, corresponding to total analysis times of ~10 min per sample. As a rule, AMS ion beam currents obtained during ^{26}Al analysis are significantly lower than for ^{10}Be analysis, predominantly because Al$^-$ is generated in relatively low yield from Al_2O_3 cathodes.[10]

Note that, molecular oxide anions of Al, despite higher ionization efficiencies that than Al$^-$, are not extracted because of the propensity for isobaric interferences due to Mg oxides, which are ubiquitous in the quartz phase. Al_2O_3 cathodes typically generate ion beam currents (as a function of stripped $^{27}Al^{7+}$) of less than 3 μA corresponding to AMS analysis times that routinely exceed 30 min.

The addition of a spike of stable isotope (^{9}Be and, as appropriate, ^{27}Al isotope carrier), to the quartz phase is important for the preparation of AMS cathodes that (a) generate high ion beam currents and (b) provide sufficient sputter lifetime in the AMS ion source. Always a balance is sought with respect to isotope carrier supplements so that, on the one hand, there is sufficient isotope carrier to ensure the necessary longevity of the cathode in the sputter source; and conversely, there is not excess of the stable isotope, which would reduce the cosmogenic/stable isotope ratio. For ^{10}Be analysis, ~250 μg Be isotope carrier is always necessary because ^{9}Be is not native to the quartz phase. For most geological applications, we use isotope carriers prepared from commercial standards, which have a native ^{10}Be abundance of 2×10^{-14}. Some researchers use Be carrier extracted from deeply mined beryl, which has a naturally low abundance of the cosmogenic nuclide.[11] Most beryl blanks have a native ^{10}Be abundance of 10^{-16} and are reserved for applications that demand exceptional analytical sensitivity. For ^{26}Al analysis, sufficient Al isotope carrier, typically up to 1 mg, may be added to ensure that the Al_2O_3 cathode contains in excess of 2 mg Al and thus can sustain the ~3 μA ion beam long enough for a precise isotope ratio measurement.

The geological timescale over which cosmogenic ^{10}Be and ^{26}Al isotope ratio analysis is applicable is inherently restricted by AMS detection limits for the rare isotopes, which in turn are contingent upon the net efficiency of AMS ion beam generation and transport. Thus, a principle challenge to improving AMS sensitivity for ^{10}Be and ^{26}Al analysis is the generation of sufficient negative ion beam current; without which, AMS analysis times must be extended in order to achieve the necessary precision (i.e. by acquisition of enough cosmogenic isotope counts). Extended analysis times are not only costly (AMS beam time is generally expensive) but also impossible for small volume samples, which expire in the AMS ion source prior to generating enough rare isotope counts for a statistically conclusive isotope ratio measurement.

In order to improve sample throughput and AMS sensitivity for geological applications, we seek to (1) determine the sensitivity of AMS ion beam current as a function of common impurities in BeO cathodes; (2) assess the effectiveness of various wet chemical procedures used in purification and isolation of Be and Al from the quartz phase; and (3) identify strategies to safeguard better against impurities that adversely affect AMS analytical sensitivity for ^{10}Be. Ultimately, improved AMS sensitivity permits application of cosmogenic isotope analysis to more challenging geological systems such as investigation of more ancient or rapidly occurring processes. Higher sensitivity capabilities also allow more precise measurement of multiple cosmogenic isotopes in the same sample, permitting determination of both exposure age and erosion history of the same sample.[12]

2.2 Experimental section

2.2.1 Sample preparation

Quartz is separated from rocks by a sequence of steps involving pulverization, size fractionation, acid etching and leaching, and liquid density separation. This protocol yields nominally a pure quartz mineral phase; however, trace–level contamination is inevitable: due, for example, to other mineral phases that resist etching or, more likely, multi-mineralic inclusions and lattice imperfections. As a consequence, quartz is almost always contaminated with some combination of native Al (an acceptable concentration for ^{26}Al analysis is <150 ppm in purified quartz), Fe, Ti, alkalis, and alkaline earth metals.

The separation of Be and Al from quartz, by common methods, is summarized in Figure 2-1. Typically, 20 to 40 g of quartz is dissolved with a multi-acid digestion adapted from standard US Geological Survey methods.[13] Most impurities native to the quartz phase, with the notable exception of Ti, are converted to fluoride forms under these conditions; meanwhile, B (the major isobar of cosmogenic ^{10}Be) is volatilized as BF_3. Upon complete dissolution, ~1 mL aliquots of the quartz digest are subsampled, evaporated to residue, and re-dissolved in 1.2 M HCl for quantitative elemental composition analysis by ICP-AES.
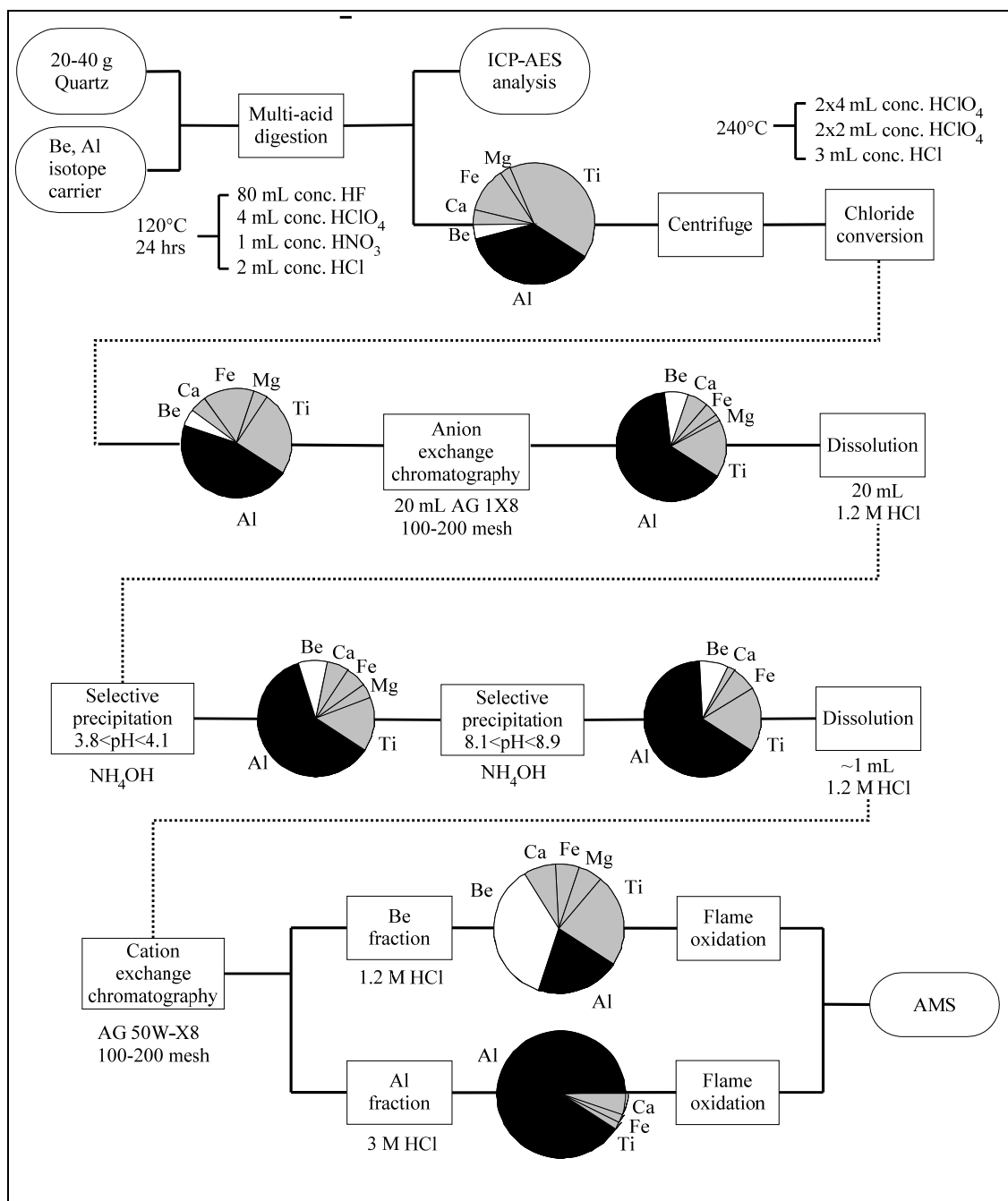
Figure 2-1: Overview of method used to separate Be and Al from quartz. Pie graphs at key process stages indicate a fractional abundance of the measured elements (i.e. mass of element per net mass of Al, Be, Ca, Fe, Mg, and Ti recovered for that stage). These are data for a typical process batch (n=8) of varying initial quartz composition.

The remaining digest is dried down leaving a bead of $HClO_4$ acid in which non-volatile elements are dissolved. Using repeated $HClO_4$ evaporations, fluorides are decomposed with concentrated $HClO_4$, yielding perchlorate salts that are re-dissolved in HCl. The resulting chloride solution is eluted from an anion exchange column (AG X18), evaporated to dryness, and re-dissolved in HCl. Two selective precipitations are performed from this solution to remove some metallic and alkaline earth impurities: (a) first at $3.8<pH<4.1$; and (b) second at $8.1<pH<8.9$.[14] The pH necessary for both precipitations is monitored with pH paper (pHydrion microfine), which is preferred because it does not provide opportunity for sample contamination. Be and Al are separated on a cation exchange column (AG 50W-X8).[15] The majority of remaining Ti is pre-eluted from the analyte mixture with dilute H_2SO_4 and a trace of H_2O_2;[16] the Be fraction is eluted with 1.2 M HCl; while the Al fraction is eluted with 3 M HCl. The Be fraction is evaporated to dryness and fumed with 1 mL concentrated $HClO_4$ to expel any trace B impurities remaining in the sample. $Be(OH)_2$ and $Al(OH)_3$ are precipitated from the respective Be and Al fractions by basification with NH_4OH to $8.1<pH<8.9$. The hydroxide gels are removed from the supernatant by centrifugation and transferred to acid-cleaned quartz vials, which are ignited in a gas flame to produce BeO and Al_2O_3 by thermal decomposition. BeO cathodes are prepared in a matrix of Nb powder to facilitate sample handling and enhance ion beam currents.

2.2.2 Yield tracing

The average yield of Be and Al, along with impurities of interest, was assessed for a batch of samples from the same geological specimen: quartz from Noosa, a beach in Queensland, Australia. This quartz is relatively clean, exhibiting 130 ppm Al, 15 ppm Ca, 31 ppm Fe, 11 ppm Mg, and 76 ppm Ti. Prior to multi-acid digestion of the quartz phase, a multi-element standard solution of common cationic impurities (Al, B, Ca, Fe, Mg, and Ti) was added to each sample along with standard Be isotope carrier, augmenting native levels of the Noosa quartz phase, ranging from conditions of low-to-high impurity concentration. The maximum impurity is a supplement of 8 mg Fe, Ti, and Al; 1 mg of Ca and Mg; and 0.1 mg of B. Other impurity levels were supplements of 50%, 25%, 10%, and 5% of the maximum level. In order to assess the efficiency of (a) anion exchange: aliquots were sampled post-column from the acid solutions used to prime the anion columns, the collected fraction, and waste washings; (b) selective precipitation: aliquots were sampled from the supernatants and re-dissolved solids obtained under the appropriate acidic and basic conditions; (c) cation exchange: aliquots were sampled post-column from primer solutions, Ti/B waste, Be and Al fractions, and subsequent rinses. All aliquots were diluted to 1.2 M HCl and analyzed by ICP-AES.

2.2.3 Instrumental Analysis

In order to identify elemental characteristics of BeO cathodes that affect AMS ion beam current, the composition of 8 complete quartz separation process batches (64 samples total; all extracted from quartz of diverse origins and lithologies) was assayed

prior to flame oxidation of extracted Be(OH)$_2$. The Be(OH)$_2$ extract was acidified with HCl to solubilize Be and any remaining contaminants. Aliquots of the acidic solution were analyzed by ICP-AES (JY-Ultima 2c); the remainder was re-basified and processed into BeO cathodes. Parameters of ICP-AES analysis include both monochromator and polychromator detection, four-point weighted $(1/[C]^2)$ calibration, matrix matched samples (typically 1.2 M HCl), and routine quality control analysis. Key spectral lines (all ionic state) include Al 309.271 nm, Be 313.042 nm, Ca 317.933 nm, Fe 238.207 nm, Mg 279.079 nm, and Ti 334.940 nm.

Measurement of the ^{10}Be/^{9}Be ratio was performed at the Center for Accelerator Mass Spectrometry at Lawrence Livermore National Laboratories (CAMS-LLNL). CAMS-LLNL is a high voltage (10 MV) tandem accelerator, employing a modified Middleton-type ion source design, that measures isotope ratios by rapidly switching between detection of the rare and stable isotopes at the injector magnet using an electrostatic acceleration gap.[17, 18] Reported ion beam currents represent the stable isotope as measured in a Faraday cup after the accelerator zone.

2.3 Results & Discussion

2.3.1 Trends in quartz purity

Depending upon the origin of geological specimens and the efficiency of quartz separation, the range of impurity concentrations in the quartz phase is widely variable. Using data from quartz samples purified at the University of Vermont over the past 10 years (1900 samples total) we determine that most cationic contaminants of concern are

present at levels ranging from 50 to 500 ppm (Figure 2-2a). The series of native concentration in purified quartz for metals of interest is Ti < Fe < Al; however, Fe exhibits the most significant variability in this group. Median concentrations of alkalis and alkaline earth metals are significantly lower, following the sequence Mg < Na < K < Ca. The wide distribution in the cationic contaminants of purified quartz demonstrates the necessity for a chemical methodology capable of extracting high purity Be and Al from quartz specimens of vastly disparate elemental composition. These data correlate with experiments by Kohl, who reports that common impurities in the quartz phase include 15-400 ppm Al, 0.1-50 ppm Mg, 0.5-50 ppm K, 0.5-30 ppm Ca, and 0.5-200 ppm Fe;[19] however, we do not find a correlation between increased Al levels and increases in other element levels, as described in that work. Ti impurities are not reported by Kohl; however, another study reports typical concentrations of <200 ppm Al, Ti, Mg, Ca, Fe in most quartz samples.[20]
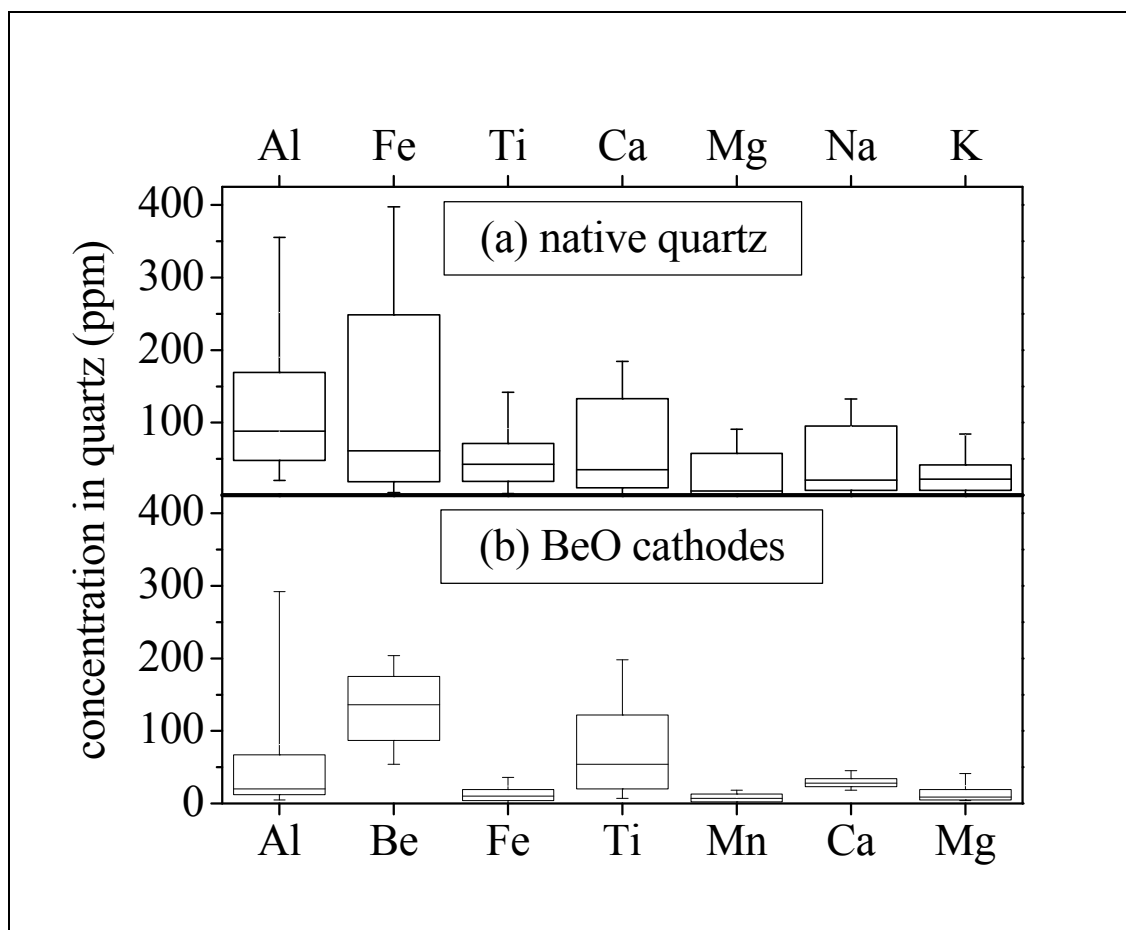
Figure 2-2: Elemental composition expressed as ppm (μg element per g quartz) determined by ICP-AES of (a) purified quartz; and (b) isolated Be fraction extracted from quartz and prior to BeO cathode ignition. Each box defines the 25th and 75th percentiles; the horizontal line inside the box is the median; the lower and upper error bars indicate 10th and 90th percentiles respectively.

2.3.2 Effects of elemental impurities on AMS ion beam currents for BeO cathodes

ICP-AES analysis of 64 samples of quartz-extracted Be samples (re-dissolved from $Be(OH)_2$ prior to flame oxidation) indicates that AMS BeO cathodes invariably contain levels of elemental impurities that are variable over a range of 0-400 ppm on a per sample basis (Figure 2-2b). These data are representative of typical cationic

contamination levels that exist in BeO cathodes prepared from quartz. The series of increasing median concentration in quartz for metals of interest is Mn (7 ppm) < Fe (10 ppm) < Al (20 ppm) < Ti (54 ppm). Ti and Al are present at the highest levels, although the extent between the median and 90th percentile concentrations is relatively high for Fe, indicating that occasionally significant levels of Fe can be anticipated along with Be in the AMS cathode. Among alkaline earth metals, Mg (8 ppm) exhibits a lower median than Ca (28 ppm). Na and K were not analyzed. Other elements measured include Cu appearing in 45 samples ([Cu]=0.024±0.0015 ppm); Si appearing in 23 samples ([Si]=0.028±0.021 ppm); Zn appearing in 28 samples ([Zn]=0.007±0.002 ppm). Elements analyzed which did not appear over the limit of quantification include As, Cd, Cr, Ga, Ni, P, Pb, Se, Sr, U, Y. Note that we do not observe a linear correlation between the concentration of native quartz impurities and the concentration of impurities in fully processed BeO cathodes, indicating that native quartz impurities are not a reliable indicator of contamination levels at the end of the process and thus the eventual magnitude of AMS ion beam current.

The AMS response for this same set of 64 samples is an example of the common range of ion beam currents obtained during ^{10}Be analysis (Figure 2-3). The mean ion beam current is 13.1±5.6 µA, with a range of 1.6 to 26.6 µA. Typically, each BeO cathode is interrogated by AMS a minimum of three times; however, in the case of considerable replication error, cathodes may need to be interrogated up to five or even six times. Note that external replication error (indicated here as standard deviation from the mean of replicate current measurements for the same cathode) is independent of the

magnitude of ion beam current itself. The most likely source of such deviations are fluctuations in AMS ion source behavior (e.g. as a consequence of sputtering mechanics or drift in the attenuation of ion beam optics).
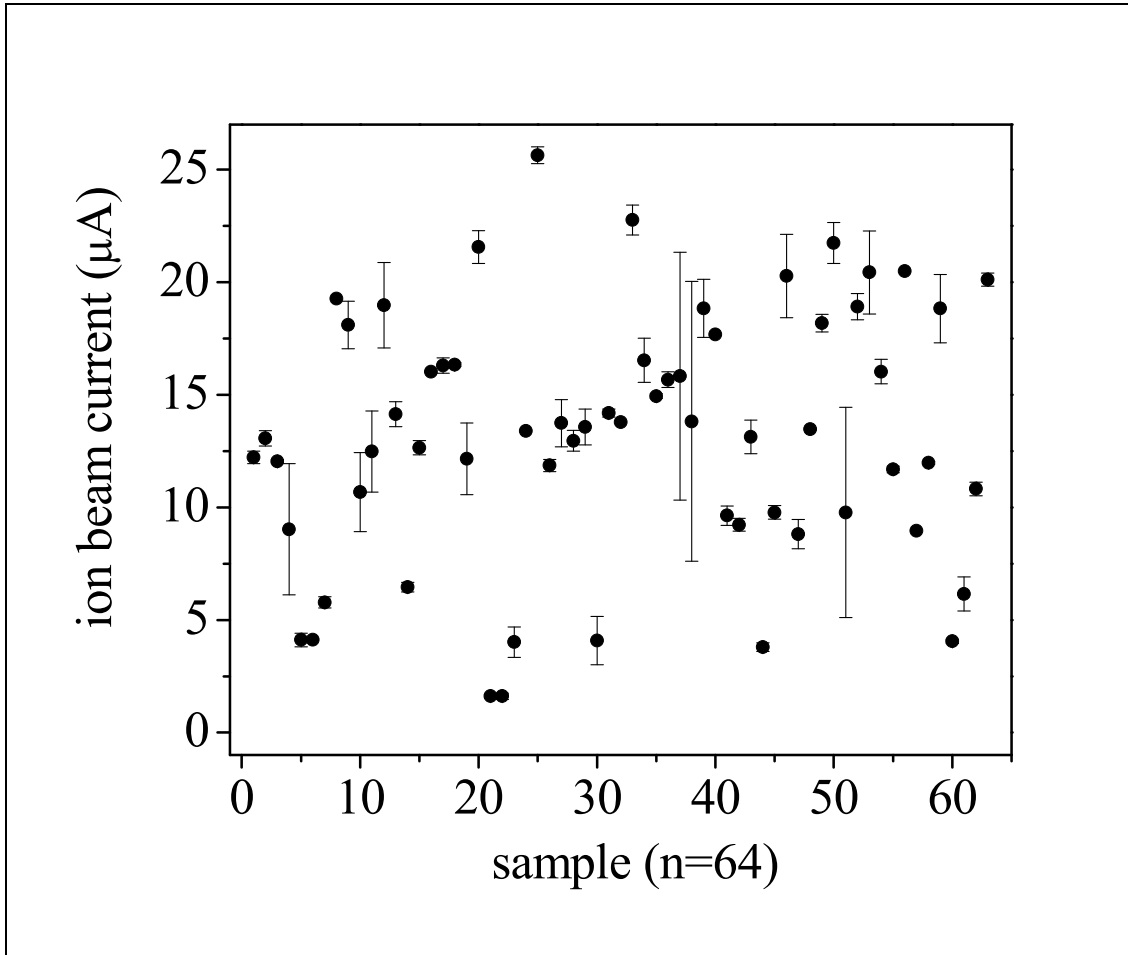
Figure 2-3: AMS ion beam current response for 8 process batches of BeO cathodes (n=64): data are mean AMS ion beam currents for BeO cathodes obtained over 3-6 replicate trials. Error bars are the standard deviation in current for each target.

By an analysis of variance (ANOVA) test on the same dataset, AMS ion beam current for BeO cathodes is fit by the variables of quantifiable elemental composition (Al,

Be, Fe, Mg, Mn, Ti) in a least squares model to identify how the AMS ion beam current responds to changes in these variables (Figure 2-4). This model specifies (a) AMS ion beam current of BeO cathodes as the response variable; and (b) cationic contaminations as effects that elicit the response. The goodness of the fit, comparing the actual response to a predicted response, indicates that the model is statistically meaningful ($R^2=0.70$). In this plot, points that fall along the regression line are perfectly predicted by the model; the curved lines are 95% confidence limits; and the horizontal reference line is the mean of the AMS ion beam current response (i.e. 13.1 µA). Based upon the calculated $F_{(63,54)}$ value of 15.65 and the sample size, there is a 99.99% probability that the model describes the dataset better than random chance alone. Thus, we conclude that AMS ion beam current for BeO cathodes can be predicted as a function of elemental contaminants in the cathode.
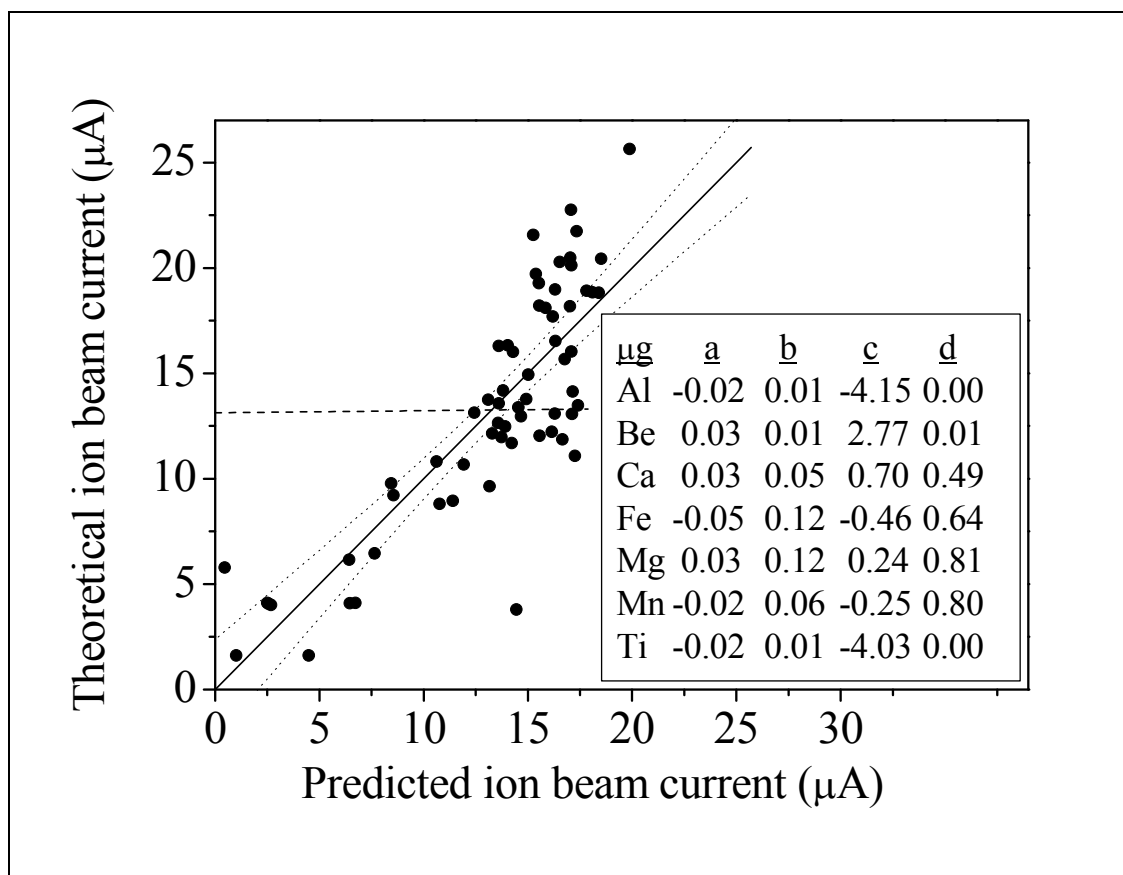
Figure 2-4: ANOVA model predicting AMS ion beam current for BeO cathodes as a function of common elemental impurities to the quartz phase. Inset: (a) parameter estimate; (b) standard error; (c) t ratio; (d) Prob>t.

The parameter estimates indicate the contribution of common impurities in BeO cathodes to the AMS ion beam current response (Figure 4 inset). A t-test was performed for each element in order to gauge its significance to the model. The estimate value (and associated standard error) for each element is a coefficient of the linear model found by least squares. The t-ratio is simply the estimate divided by the standard error. The Prob>t value indicates the probability that a t-value can be obtained by chance that is greater

than the indicated value; values of <0.05 are evidence that the parameter is not zero. Thus, these data indicate that impurities of Ca, Fe, Mg, and Mn do not significantly affect the AMS ion beam current obtained from BeO cathodes. Conversely, the compositional levels of Al, Be and Ti are all significant parameters in the model. Clearly, as the analyte under investigation, Be necessarily elicits a positive effect on AMS ion beam current; however, as evident from the negative sign of the corresponding estimates, Al and Ti elicit a significant suppressive effect on AMS ion beam currents. This may be a result in part of the relatively high electron affinity of these elements and their oxides during the sputter process.[21],[22] Consequently, quantitative separation of Al and Ti from Be is a paramount objective in the preparation of samples for cosmogenic [10]Be analysis.

2.3.3 Efficiency and purity of Be and Al extraction from quartz

One of the advantages of hot, multi-acid quartz digestion is that, while HF is evaporated relative to $HClO_4$, complex titanium fluoride ions (e.g. $[TiF_6]^{2-}$) can be oxidized and precipitated as the refractory compound TiO_2.[23] In this way, ~50% of Ti contamination, evident as a smoky white precipitate, can be removed by centrifugation early in the separation procedure. The dry mass of the refractory precipitate is a linear function (R^2=0.94) of initial mass of Ti in the quartz (native and supplement). An additional advantage of multi-acid digestion is that, because the mixture is never entirely evaporated in the presence of fluoride ions, losses of Al as insoluble alumino-fluoride complexes are minimized.

In general, Al and Be in quartz digest can be quantitatively separated from cationic Fe impurities on an anion exchange column in a solution of two column volumes of 8 M HCl at an elution rate of one drop/sec. Al and Be do not form chloride complexes of sufficient strength to adsorb on the resin. For a typical process batch, these elution conditions provide retention efficiencies of $99.7\pm0.1\%$ for Al, $99.2\pm0.5\%$ for Be, $6.3\pm5.9\%$ for Fe, and $95.9\pm1.9\%$ for Ti. A salient feature of the elution profile is the co-elution of Ti with the analyte fraction (Figure 2-5). Note that this profile was obtained from quartz digest with relatively high Fe levels. In any case, sequential rinses of one-half column volume of 1.2 M HCl strip the anion exchange resin of Fe in reasonable yield; with $77.8\pm6.3\%$ and $15.9\pm2.9\%$ draining in the first and second rinse respectively; the remaining Fe persists as a contaminant in the Be/Al fraction.
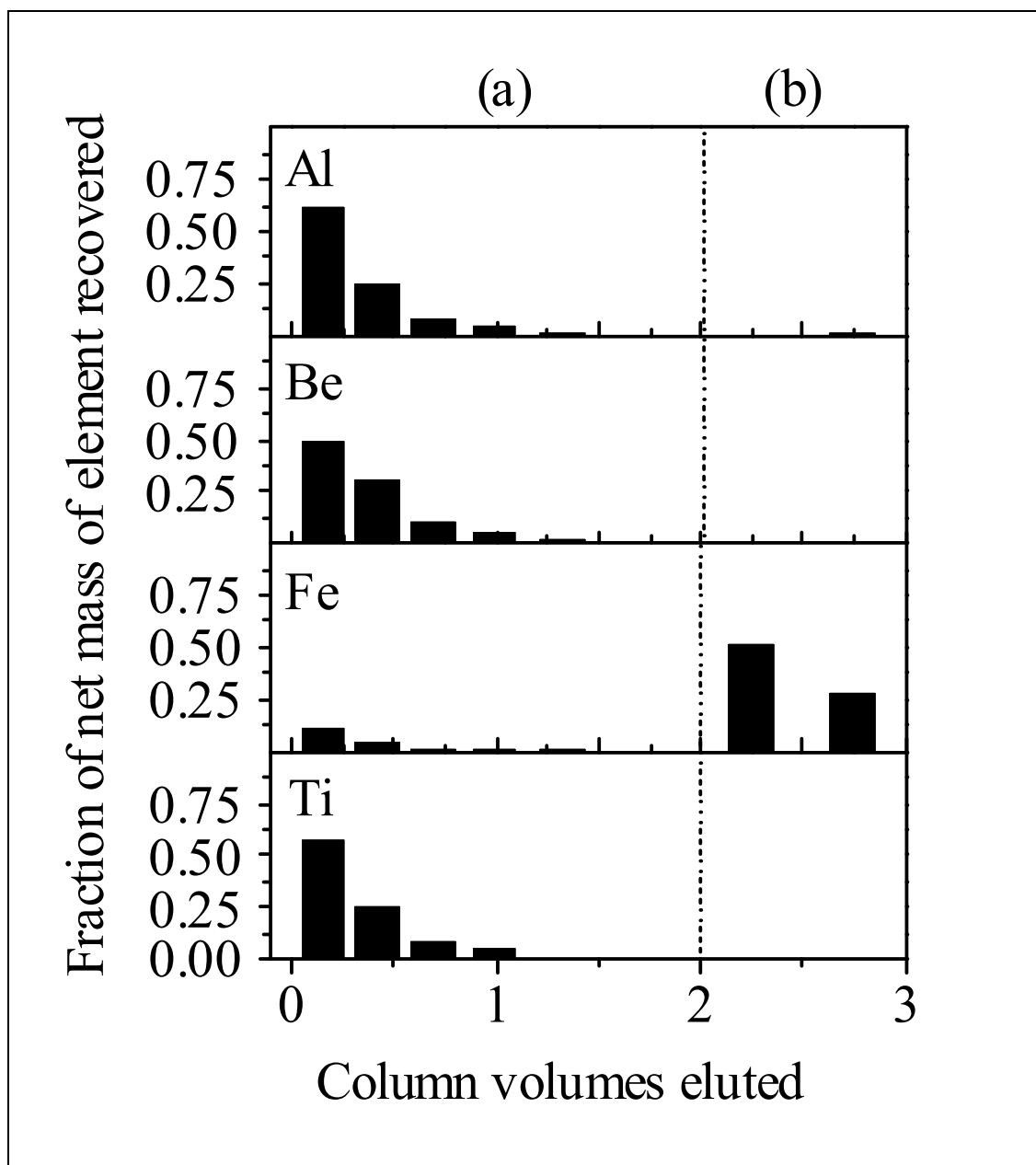
Figure 2-5: Elution profile of quartz digest (n=8, error bars not shown) through anion exchange column (20 mL AG X18 resin). Elution is in (a) 8 M HCl, (b) 1.2 M HCl.

The transmission of impurities along with the anion exchange eluent (μg vestigial impurity per g initial quartz) is a linear function of the original multi-element standard

mass for Al, Ca, Fe, and Mg (R^2=0.98, 0.98, 0.95, 0.98 respectively). The linearity indicates that the concentration of these cations in the anion exchange eluent is proportional to initial impurity levels of the quartz digest, at least over the experimental range of supplemental impurities in the multi-element standard (i.e. Al and Fe <8 mg, Ca and Mg <1 mg). In contrast, if the sample is not centrifuged prior to loading on the column, the vestigial transmission of Ti into the eluent is nonlinear with the supplementary impurity mass, amounting to a residual Ti baseline of 32±30 ppm. Most importantly, Be yield is not significantly affected by loading the column with impurity levels in the range of typical samples: the transmitted Be yields are relatively consistent at 98±3% (corresponding to 22±3 ppm, which is, in come cases, on par with Ti levels). In any case, Fe-free solutions of quartz digest can be qualitatively screened for high concentrations of residual Ti by oxidation with H_2O_2, which forms a distinct yellow complex.

After each separation, the anion exchange columns are loaded with 1.2 M HCl, so that the resin beds can be stored and recycled. In addition, prior to each separation, the anion exchange columns are always primed with 8 M HCl; furthermore, the primer waste contains negligible levels of Al and Be, and less than 1% of the total recovered Fe and Ti mass. This observation, in conjunction with consistently low [10]Be process blanks, is evidence of (a) relatively low sample cross-talk and (b) thorough column cleaning.

The effectiveness of Fe and Ti removal by selective precipitation at 3.8<pH<4.1 is strongly dependent on the accuracy of the experimental pH (Figure 2-6). A lower ratio (i.e. mass in supernatant per mass in precipitate) indicates more complete separation. A

prominent disadvantage of this method is that the 3.8<pH<4.1 criterion can be difficult to maintain, as the experimental acidity often drifts outside this range even hours after adjustment with strong base. Unless the pH is maintained at the maximum end of this range, a significant fraction of Fe and Ti can persist as contaminants in the analyte-containing supernatant; however, if the pH is raised too high, there exists a risk of initiating precipitation of Be and Al as hydroxides. Moreover, using a qualitative acidity measurement (i.e. pH paper), the efficiency of this precipitation has the potential for high variability on a sample-to-sample basis; for example, over this same pH range, precipitation efficiencies for Fe and Ti range from 39 to 99% and 62 to 96% respectively. The addition of multi-element standard to quartz digest does not appear to affect the efficiency of precipitation at 3.8<pH<4.1; however, due to the limitations of qualitative pH analysis, deviations in experimental acidity between samples are a potential bias masking any obvious trends in precipitation efficiencies. Note that digital pH meters are not preferred for this application because such direct probes introduce a high potential for sample contamination (especially B from borosilicate glass).
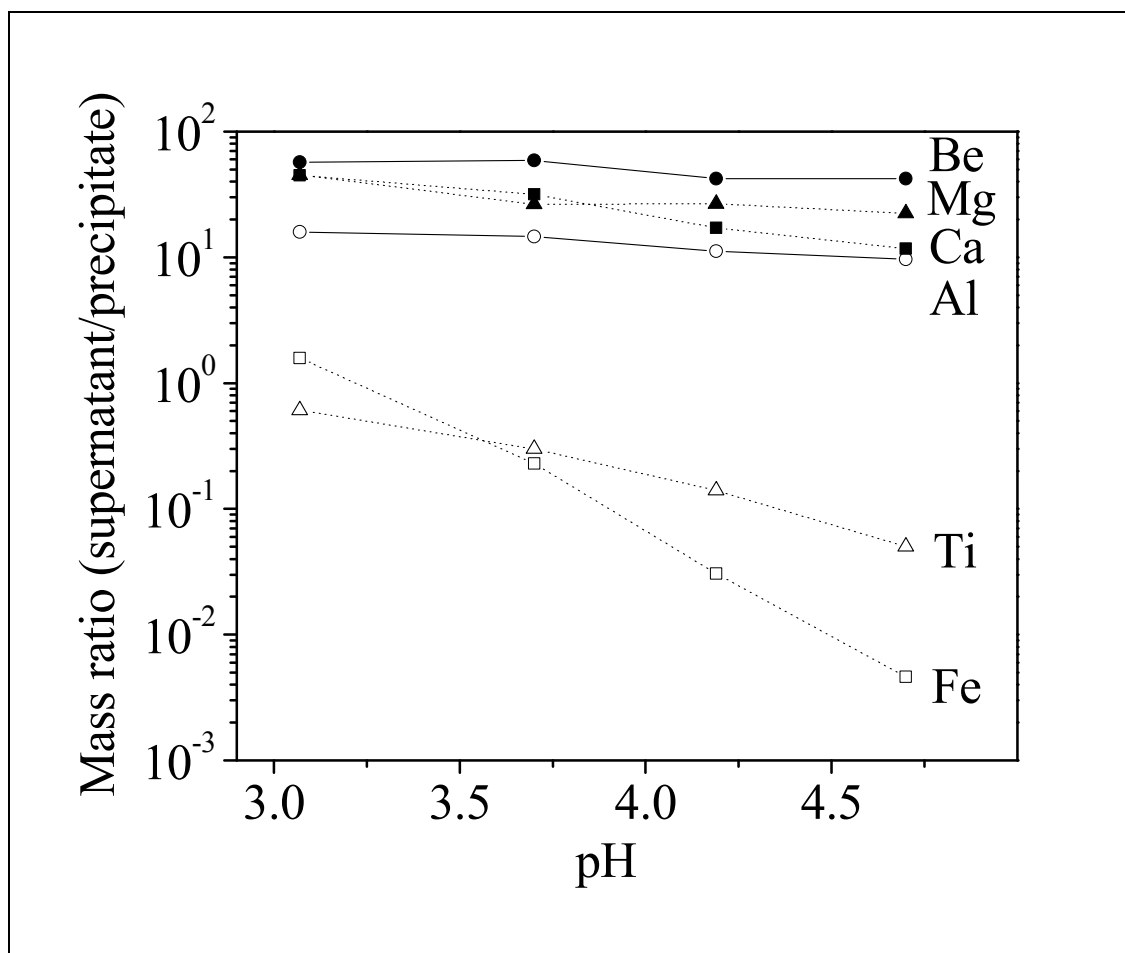
Figure 2-6: Selectivity of precipitation, defined as mass of element in supernatant per mass of element in precipitate, quartz digest as a function of pH. Symbols are experimental data points indicating Al (—●—), Be (—▲—), Ca (—■—), Fe (—o—), Mg (—△—), Ti (—□—).

Selective precipitation at 8.1<pH<8.9 is effective for removing common alkali earth metals from quartz digest; for example, in a typical batch of samples, Ca and Mg can be removed in the supernatant with 81±6% and 88±9% efficiency respectively. Most significantly, Al and Be (also any remaining Fe and Ti impurities) are retained in the floc with quantitative yield. The addition of multi-element standard does not affect selective

precipitation at 8.1<pH<8.9; however, once again, deviations due to qualitative analysis (i.e. pH measurement) are potentially significant compared to impurity-dependant deviations in the concentration of the re-dissolved precipitate.

Be and Al are isolated into discrete fractions by cation exchange chromatography, presuming that no Al fluorides remain. Any remaining Al fluorides will rapidly elute and either go to initial waste or tail into the Be fraction. Because Be is the first analyte eluted from the column, contamination due to co-elution of Al is a concern. As demonstrated, Al impurities in BeO cathode suppress AMS ion beam currents. Moreover, as Ti impurities are typically significant in the Be fraction, it is generally advantageous to pre-elute Ti with dilute H_2SO_4, improving the purity and chromatographic resolution of the Al and Be fractions. For a typical process batch, the net recovered Ti in the Be fraction can be reduced from 84±2% to 48±4%. The average cation exchange elution profile of a typical batch reveals a few other salient features (Figure 2-7). For example, Mg regularly co-elutes with both the Be and Al fractions; Ca co-elutes exclusively with Al; and B contamination (corresponding to a mean of 37±7 µg B per sample) can be isolated with the H_2SO_4 mobile phase with reproducible efficiency. In conjunction with volatilization of BF_3 during the initial acid digestion of quartz separate, the sequestering of B with the Ti-rich pre-elution waste provides additional safeguard against this nearly ubiquitous isobar of ^{10}Be. Finally, it is worth noting that oxalic acid, which forms a soluble complex with Be but no other divalent metals, has also been reported to be effective for the isolation of Be from quartz digests;[24] however, we have yet to yield trace this method.
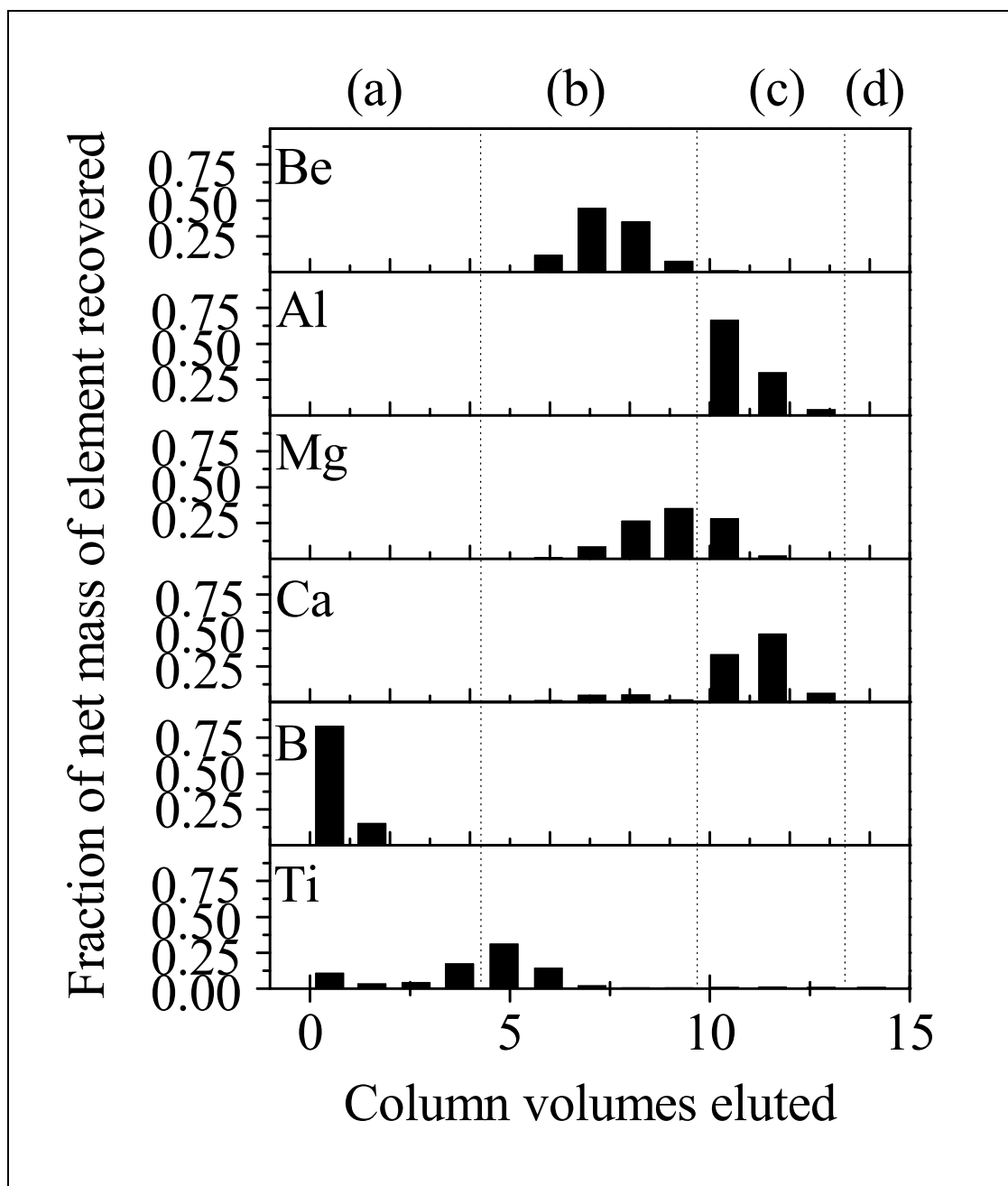
Figure 2-7: Elution profile of quartz digest (n=8, error bars not shown) through cation exchange column 10 mL AG 50W-X8 resin). Elution is in (a) 0.5 M H$_2$SO$_4$, (b) 1.2 M HCl, (c) 3.0 M HCl, (d) 6.0 M HCl.

At this point, the separation process is complete and the net yields (mass in cation exchange eluent per initial mass in quartz digest) of the key species, Al and Be, remain very high; meanwhile, the impurities of interest have been removed with varying degrees of efficiency. For example, in a typical batch, the net yield recovery of Be is 97.8±2.3%; while, yields of impurities (relative to initial amounts in the quartz digest) in the Be fraction are 0.1±0% for Al, 10.7±7.8% for Ca, 11.7±4.6% for Fe, and 28.6±27.8% for Ti. In the Al faction, the net yield of Al is 100±8.5%; while yields of impurities in the Al fraction are 0.8±1.1% for Be, 74.2±10.1% for Ca, 5.8±5.5 Fe, and 0.6±0.6% for Ti.

2.4 Conclusions

These data indicate that compositional impurities in BeO cathodes can have significant impact on AMS ion beam current, ultimately affecting the sensitivity of the AMS method itself. The most intense effect, a signal suppression of the ion beam, is observed for BeO targets containing relatively high levels of Ti and/or Al impurities. Yield tracing a common procedure for the extraction of Be and Al from quartz indicates that the former impurity is due to highly variable separation efficiencies during different stages of the extraction, while the later impurity is due to co-elution during cation exchange chromatography. Other impurities, which are of principle interest due to common presence in quartz, such as Fe and alkali earth metals, do not statistically affect AMS ion beam currents, at least under routine concentration regimes. Nevertheless, it is prudent to exercise care in the separation of these contaminants whenever mineral composition analysis indicates exceptionally high native levels in purified quartz.

In order to achieve high yield and purity of the analytes, Be and Al, from the digested quartz phase into AMS cathodes, key experimental steps include (1) multi-acid digestion of quartz; (2) anion exchange chromatography; (3) selective precipitations at $3.8<pH<4.1$ and $8.1<pH<8.9$, the efficiency of which is contingent upon highly accurate pH control; and (4) a three-step cation exchange chromatography elution protocol to separate the purified sample into discrete Ti/B (waste), Be, and Al fractions. Finally, Ca, which is evidently the most challenging species to separate with the experimental methods, appears most significantly in the Al fraction. Furthermore, based upon our model, Ca concentrations at typical levels are not statistically likely to suppress AMS ion beam currents for BeO cathodes. In any case, the experimental evidence of Ca closely following Al corroborates theoretical modeling of its behavior on cation exchange columns.[15] The effects of Ca impurities on AMS ion beam currents for Al_2O_3 cathodes remains the subject for future research.

2.5 Acknowledgment

2.6 References

1.   Lal, D.; Peters, B., Cosmic ray produced radioactivity on the earth. In *Handbuch der Physik*, ed.; Sitte, K., Eds. Springer-Verlag: New York, 1967; pp 551-612.

2.   Lal, D., In situ-produced cosmogenic isotopes in terrestrial rocks. *Annual Reviews of Earth and Planetary Science* **1988,** 16, 355-388.

3.   Sharma, P.; Middleton, R., Radiogenic production of ^{10}Be and ^{26}Al in uranium and thorium ores: Implications for studying terrestrial samples containing low levels of ^{10}Be and ^{26}Al. *Geochimica et Cosmochimica Acta* **1989,** 53, 709-716.

4.   Gosse, J. C.; Phillips, F. M., Terrestrial in situ cosmogenic nuclides: theory and application. *Quaternary Science Reviews* **2001,** 20, (14), 1475-1560.

5.   Elmore, D.; Phillips, F. M., Accelerator mass spectrometry for measurement of long-lived radioisotopes. *Science* **1987,** 236, 543-550.

6.   Finkel, R.; Suter, M., AMS in the Earth Sciences: Technique and applications. *Advances in Analytical Geochemistry* **1993,** 1, 1-114.

7.   Bierman, P. R., Using in situ produced cosmogenic isotopes to estimate rates of landscape evolution; a review from the geomorphic perspective. *Journal of Geophysical Research, B, Solid Earth and Planets* **1994,** 99, (7), 13885-13896.

8.   Bierman, P. R.; Marsella, K. A.; Patterson, C.; Davis, P. T.; Caffee, M., Mid-Pleistocene cosmogenic minimum-age limits for pre-Wisconsinan glacial surfaces in southwestern Minnesota and southern Baffin Island; a multiple nuclide approach. *Geomorphology* **1999,** 27, (1-2), 25-39.

9.   Granger, D. E.; Muzikar, P. F., Dating sediment burial with in situ-produced cosmogenic nuclides; theory, techniques, and limitations. *Earth and Planetary Science Letters* **2001,** 188, (1-2), 269-281.

10.   Middleton, R. *A Negative Ion Cookbook*; Department of Physics, University of Pennsylvania: Philadelphia, 1990.

11.   Stone, J., A rapid fusion method for separation of beryllium-10 from soils and silicates. *Geochimica et Cosmochimica Acta* **1998,** 62, (3), 555-561.

12.   Gillespie, A. R.; Bierman, P. R., Precision of terrestrial exposure ages and erosion rates estimated from analysis of cosmogenic isotopes produced in situ. *Journal of Geophysical Research, B, Solid Earth and Planets* **1995,** 100, (12), 24,637-24,649.

13.   Biggs, P. H.; Meier, A. L., The Determination of Forty-Two Elements in Geological Materials by Inductively Coupled Plasma-Mass Spectrometry. *U.S. Geological Survey Open File Report* **2002,** 02-223-I.

14.   Tera, F.; Brown, L.; Morris, J.; Sacks, I. S.; Klein, J.; Middleton, R., Sediment incorporation in island-arc magmas: inferences from ^{10}Be. *Geochimica et Cosmochimica Acta* **1986,** 50, 535-550.

15.   Ochs, M.; Ivy-Ochs, S., The chemical behavior of Be, Al, Fe,Ca, and Mg during AMS target preparations from terrestrial silicates modeled with chemical speciation calculations. *Nuclear Instruments and Methods in Physics Research Section B: Beam Interactions with Materials and Atoms* **1997,** 132, 235-240.

16.   Ditchburn, R. G.; Whitehead, N. E., The separation of ^{10}Be from silicates. *3d Workshop of the South Pacific Environmental Radioactivity Association* **1994**, 4-7.

17.   Middleton, R.; Klein, J.; Brown, L.; Tera, F., [10]Be in commercial beryllium. *Nuclear Instruments and Methods in Physics Research Section B: Beam Interactions with Materials and Atoms* **1984,** B5, 511-513.

18.   Southon, J. R.; Roberts, M., Ten years of sourcery at CAMS/LLNL - Evolution of a Cs ion source. *Nuclear Instruments and Methods in Physics Research Section B: Beam Interactions with Materials and Atoms* **2000,** 172, 257-261.

19.   Kohl, C. P.; Nishiizumi, K., Chemical isolation of quartz for measurement of *in-situ* -produced cosmogenic nuclides. *Geochimica et Cosmochimica Acta* **1992,** 56, 3583-3587.

20.   Child, D.; Elliott, G.; Mifsud, C.; Smith, A. M.; Fink, D., Sample processing for earth science studies at ANTARES. *Nuclear Instruments and Methods in Physics Research Section B: Beam Interactions with Materials and Atoms* **2000,** 172, 856-860.

21.   Hunt, A.; Petrucci, G.; Bierman, P.; Finkel, R., Metal matrices to optimize ion beam currents for accelerator mass spectrometry. *Nuclear Instruments and Methods in Physics Research Section B: Beam Interactions with Materials and Atoms* **2006,** 243, (1), 216-222.

22.   Hunt, A.; Petrucci, G.; Bierman, P.; Finkel, R., Investigation of metal matrix systems for cosmogenic [26]Al analysis by accelerator mass spectrometry. *Nuclear Instruments and Methods in Physics Research Section B: Beam Interactions with Materials and Atoms* **2007,** 260, (2), 633-636.

23.   Yokoyama, T.; Makishima, A.; Nakamura, E., Evaluation of the coprecipitation of incompatible trace elements with fluoride during silicate rock dissolution by acid digestion. *Chemical Geology* **1999,** 157, (3-4), 175-187.

24.   von Blanckenburg, F.; Belshaw, N. S.; O'Nions, R. K., Separation of ^{9}Be and cosmogenic ^{10}Be from environmental materials and SIMS isotope dilution analysis. *Chemical Geology* **1996,** 129, 93-99.

CHAPTER 3: METAL MATRICES TO OPTIMIZE ION BEAM CURRENTS FOR ACCELERATOR MASS SPECTROMETRY

3.1 Introduction

Long-lived cosmogenic nuclides are produced in rock and soil samples at or near the Earth's surface predominantly by spallation reactions.[1] Surface exposure dating employing the measurement of cosmogenic ^{10}Be in geological samples with accelerator mass spectrometry (AMS) has been used since the late 1980s to study geomorphologic phenomena, e.g..[2-4] This ultra-sensitive analytical method requires the rapid and accurate determination of as little as 10^6 atoms of ^{10}Be typically distributed in tens of grams of rock sample. Since the isotope counting statistics are Poisson distributed, precision of the isotope ratio measurement scales inversely with the square root of the total number of collected ion counts. Furthermore, the rate of ion counting is, in part, a function of ion source behavior. For samples with small cosmogenic isotope content, AMS precision is inherently low, even with long counting times, limiting applicability for a variety of challenging dating and tracing methods.[5] Optimization of AMS ion beam currents improves the statistical certainty of geomorphic models based upon isotope ratios and reduces the amount of sample required, especially for samples with low cosmogenic nuclide abundance.

For geological applications, the most commonly measured nuclide is ^{10}Be, which is extracted from quartz and measured by AMS with a ^{10}Be/^{9}Be abundance sensitivity of about 10^{-15}.[6] The tandem van de Graaff accelerator, used in nearly all AMS systems

today, requires an ion source that can produce negative ions. The ion source used at Lawrence Livermore National Laboratory (LLNL) Center for Accelerator Mass Spectrometry (CAMS) has evolved from a design originated by Middleton[7] and uses a Cs sputter source to produce negative ions.[8] The principal challenge to the analysis of ^{10}Be is that atomic Be only forms metastable anions due to its negligible electron affinity. Therefore, Be cathodes are prepared as BeO so that BeO$^-$ is extracted from the AMS source instead of the low-yield atomic anion, Be$^-$.

BeO is routinely dispersed in a matrix of metal powder to facilitate the ion sputter process in the AMS source.[9] In most cases, the dispersion of analyte in a matrix is the final step of sample preparation, performed immediately prior to pressing a sample into its target cathode. Metal matrices were originally used to facilitate sample handling and extend sample lifetime in the AMS ion source.[10, 7] In addition, a conductive metal matrix minimizes charging of the cathode surface, which affects the energy, focusing and extraction of secondary ions. At present we are assessing the effect of matrices on additional aspects of cathode behavior, including the rise time taken for a cathode to deliver a useable beam current and/or the magnitude of the matrix-induced signal enhancement.

During the 1980s and 1990s, Ag, and to a lesser extent Cu, powders were the prevalent metal matrices for geological applications involving cosmogenic ^{10}Be analysis at most AMS facilities.[11,6,12,13] The principal advantage of Ag and Cu matrices with respect to ionization is that the ion beam current rapidly stabilizes, resulting in a significant reduction in AMS analysis time. For example, at the University of

75

Pennsylvania ion source, pure BeO produced anion beam currents of 3 µA after 5 min (increasing to 11 µA after 40 min); by comparison, BeO dispersed in Ag matrix produced 10.5 µA after 5 min (decreasing to 7.5 µA after 40 min).[7]

At present, Nb powder is the preferred metal matrix for BeO at many AMS facilities, including CAMS at LLNL, because of the high attainable beam currents.[14,15] The implementation of a protocol using Nb as the matrix for ^{10}Be analysis at CAMS has extended the sensitivity of the isotope ratio method for more challenging research areas, such as measuring erosion rates in rapidly eroding terrain,[16] or applying burial dating to shielded samples.[17] Conventional mixing ratios are typically 1:1 Nb:BeO by volume, providing 3 to 7 fold enhancement in anion beam currents over Ag matrix at the same mixing ratio; however, different AMS facilities throughout the world, employing ion sources of different design, use a range of matrices and mixtures. Despite evidence that matrices affect ion beam currents in many AMS ion sources, experimental matrix:oxide mixing ratios are rarely reported in the literature. Moreover, in spite of the widespread use of AMS to measure ^{10}Be for geochronology, a thorough investigation identifying how different metal matrices affect ion beam currents, and ultimately AMS sensitivity, has been lacking.

Herein we describe experiments that measure the abundance of stripped ions, $^9Be^{+3}$, after the accelerator, under the assumption that ion loss in the accelerator is relatively invariant. Therefore, in the following discussion, the $^9Be^{3+}$ current will serve as a proxy for BeO$^-$ that is directly formed in, and subsequently extracted from, the ion source. Total $^9Be^{3+}$ currents in the post accelerator Faraday cup correlate to the BeO$^-$

current measured just after the 90° injection magnet between the ion source and the accelerator.[18]

We have evaluated AMS beam currents for BeO as a function of matrix composition and of sample packing depth in the AMS cathode. In addition to conventional matrices (Ag and Nb), we selected four other metals (Mo, Ta, V, and W) for study. The new matrices span a range of fundamental elemental properties (e.g. electron affinity, metal work function, thermal conductivity, electrical resistivity, vaporization enthalpy) in order to help identify specific physicochemical phenomena that influence the matrix enhancement effect on AMS ion beam currents.

3.2 Methods

All powders were of particle diameter < 45 μm and purity > 99.5% (Sigma-Aldrich Co.). For each matrix, ten samples were prepared over a range of matrix mole fractions (χ_{matrix}) so that χ_{matrix} ranged from 0.50 to 0.95 in 0.05 increments. Samples with Ag and Nb matrices were prepared in triplicate; samples with Mo, Ta, V, and W were prepared singly. Ta and W powders are pyrophoric so samples incorporating these matrices were prepared in a glove bag flushed with N_2, but were exposed to air after packing into the cathode. The powders were volumetrically sampled with either a 1.0 mm or 2.5 mm stainless steel Meyhoefer Chalazion curette (Robbins Instruments). The molar capacity of the curette for each powder was calibrated with a microbalance. BeO and matrix powders were thoroughly mixed in a quartz tube using a stainless steel rod. After BeO was evenly dispersed in matrix, a known volume of the mixed sample was removed

for packing into standard CAMS stainless steel cathode targets. The cathode consists of a stainless steel cylinder with a 0.25-inch diameter, 0.25-inch deep cylindrical hole bored into a funnel-shaped cavity in one end. The oxide-metal mixture is packed into this cavity with a stainless steel rod (*cf.* Fig 2 of reference[8]). Subsequent samples were prepared by serial dilution of the remaining mixture with the relevant matrix powder. Sample packing depths in the cathodes were measured with a micrometer to a resolution of 10 μm. Instrumental analysis was performed at the LLNL CAMS facility. For each sample, the ion source was permitted a warm-up interval of 30 s. The beam current due to $^9Be^{3+}$ was monitored with a 1 s time resolution in an off-axis Faraday cup positioned after the first 90° magnet following the accelerator. The beam currents were integrated over 300 s for each measurement. Standards with $\chi_{Nb} = 0.50$ were interspersed among the samples to test for beam current drift over time. A 2.8% relative standard deviation in integrated $^9Be^{3+}$ beam current of the Nb:BeO samples over the ~24 hr measurement period verifies the stability of the CAMS ion source after exposure to unconventional matrices and indicates that changes in the current measured in the off-axis Faraday cup for different BeO:matrix mixtures were dominated by changes in source output.

3.3 Results & Discussion

Depending on the selection of matrix, the depth to which a sample is tamped in the AMS cathode cavity has a significant effect on ion beam current (Figure 3-1). For example, as the cathode is loaded nearer to capacity, the integrated ion beam current for BeO dispersed in Ag matrix increases exponentially. No such depth effect is observed for

analyte dispersed in Nb matrix. This effect was not investigated for BeO dispersed in other metals. At present, the depth-dependent enhancement in ion beam current afforded by Ag is of limited practical merit since the absolute currents are still not on par with currents afforded by Nb.
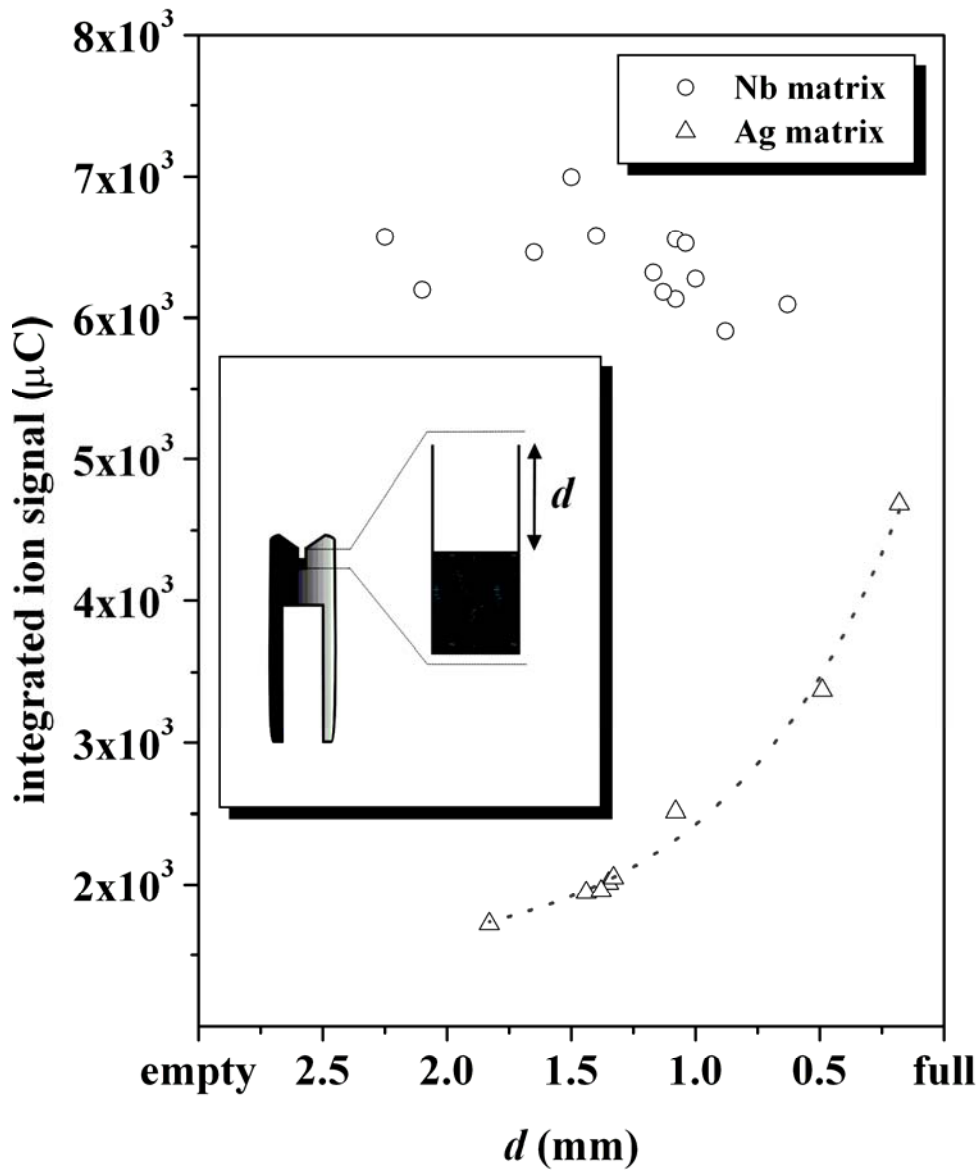
Figure 3-1: Effect on integrated ion beam current of sample packing depth (*d*) in the CAMS cathode cavity for equimolar Ag:BeO and Nb:BeO samples. Integrated beam current was measured between 30th and 330th second of data acquisition. Symbols represent experimental data points. Dashed line is to aid the eye. Inset: cross-section of CAMS cathode showing how *d* is defined.

The temporal evolution of the ion beam currents (Figure 3-2) provides a clear illustration of the advantages of using Nb instead of Ag as a matrix when measuring cosmogenic ^{10}Be by AMS. For example, for an equimolar sample, the mean beam current for BeO in Ag matrix is 6.7 µA whereas for Nb it is 18.8 µA. However, one advantage of Ag matrix at any dilution is that there is no apparent delay in current generation. In contrast, the rise time for samples dispersed in Nb matrix is longer, especially when the analyte concentration is high, so that an equimolar mixture of BeO and Nb requires 260 s to reach 90% of maximum value. For most applications in geochronology, this delay does not compromise the advantage of having ~20 µA beam currents.

Figure 3-2: Temporal evolution of instantaneous ion beam currents for analyte dispersed in different mole ratios of Ag, Nb, Ta, V, W, and Mo. Panels show representative data for each metal at matrix mole fractions of 0.5 (——), 0.6 (------), 0.7 (••••••), 0.85 (–•–•–•), and 0.95 (–••–••).
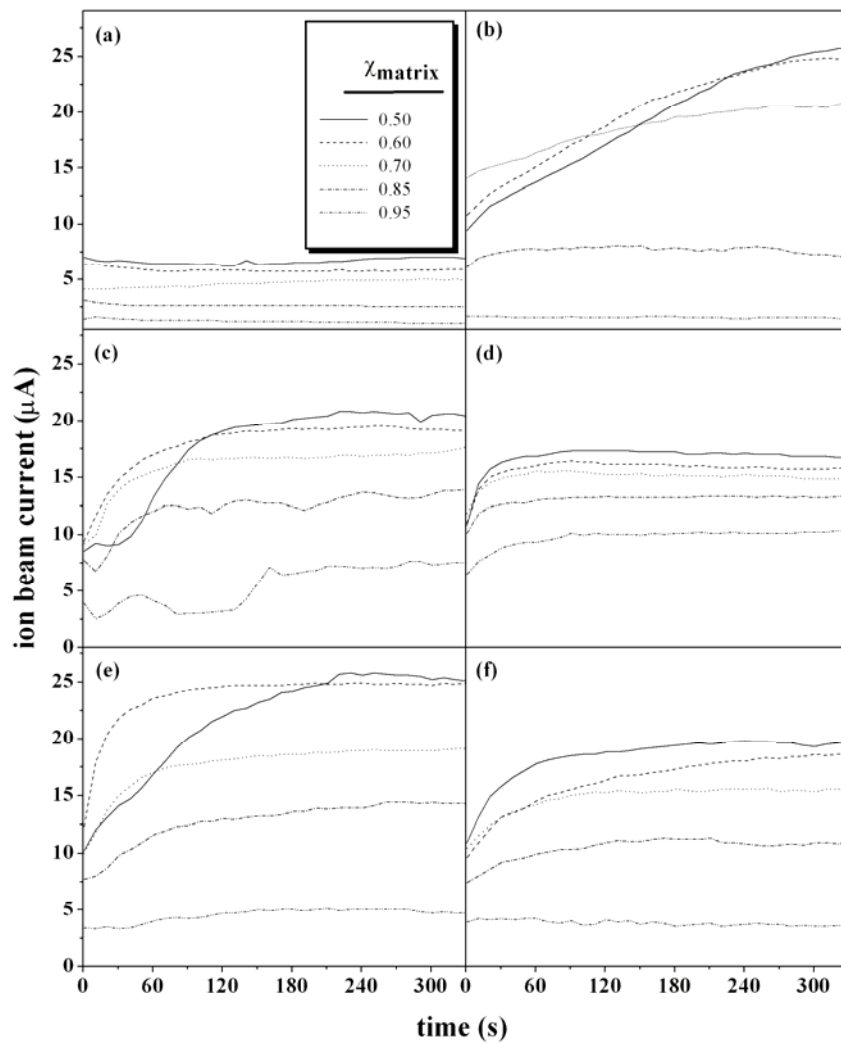
In general, beam currents for samples prepared with Mo, Ta, V, and W exhibit time dependence comparable to beam currents for samples prepared with Nb. The rise times and magnitudes of the beam current are consistently greater for these matrices than observed for Ag. For equimolar mixtures, the times required to reach 90% maximum beam current are 130 s for V (max at 23.2 μA), 110 s for Mo (max at 18.8 μA), 50s for W (max at 17.8 μA), and 20 s for Ta (max at 15.7 μA). None of these metal matrices offer the pragmatic attribute of zero beam current rise time; but all offer the more important advantage of higher average and integrated beam currents than Ag.

As an indicator of AMS response to different matrix elements, we normalize the integrated beam current to the mass of BeO in each sample, then convert to a counting efficiency of ions detected per atom Be loaded (Figure 3-3). This value indicates the total integrated $^9Be^{3+}$ beam that might be derived from a given amount of BeO dispersed in any of the experimental matrices during a 300 s measurement time. This number is quite small. Even during a relatively long 10- or 15-minute measurement time, most of the sample is unused. Note that this response is not a direct measure of AMS ionization efficiency since ion beam currents are also anticipated to be a function of space-charge effects, sputtering rates, ion focusing behavior, and charge state distribution in the stripper. Larger values indicate greater beam currents and correspondingly improved isotope ratio statistical certainty. By this criterion, Ag matrix demonstrates the poorest AMS response, providing a counting efficiency of between 1.6×10^{-4} to 3.3×10^{-4} ions per atom depending on the mixing ratio. Clearly Nb is a more effective matrix than Ag, providing a maximum counting efficiency of 5.5×10^{-4}. Yet, while the widespread

application of Nb in AMS protocols for the analysis of cosmogenic ^{10}Be is certainly warranted, the effectiveness of this matrix diminishes at higher matrix:oxide mole ratios. Thus, the experimental mixing ratio needs to be carefully controlled between with $0.50 <$ $\chi_{Nb} < 0.75$ (or 4:1 to 11:1 Nb:BeO by mass) for optimal AMS response. For BeO samples prepared in this dilution range, we observe a relatively constant integrated beam current of 5.7 mC with 10% relative standard deviation. This result indicates that as the matrix mole fraction increases over this range, less BeO can be incorporated into a sample while sustaining the same integrated ion beam currents. Thus, for cosmogenic ^{10}Be analysis, if Nb:BeO ratios are systematically controlled, quartz samples can be spiked with less ^{9}Be carrier, effectively improving the precision of isotope ratio measurement without compromising counting statistics.
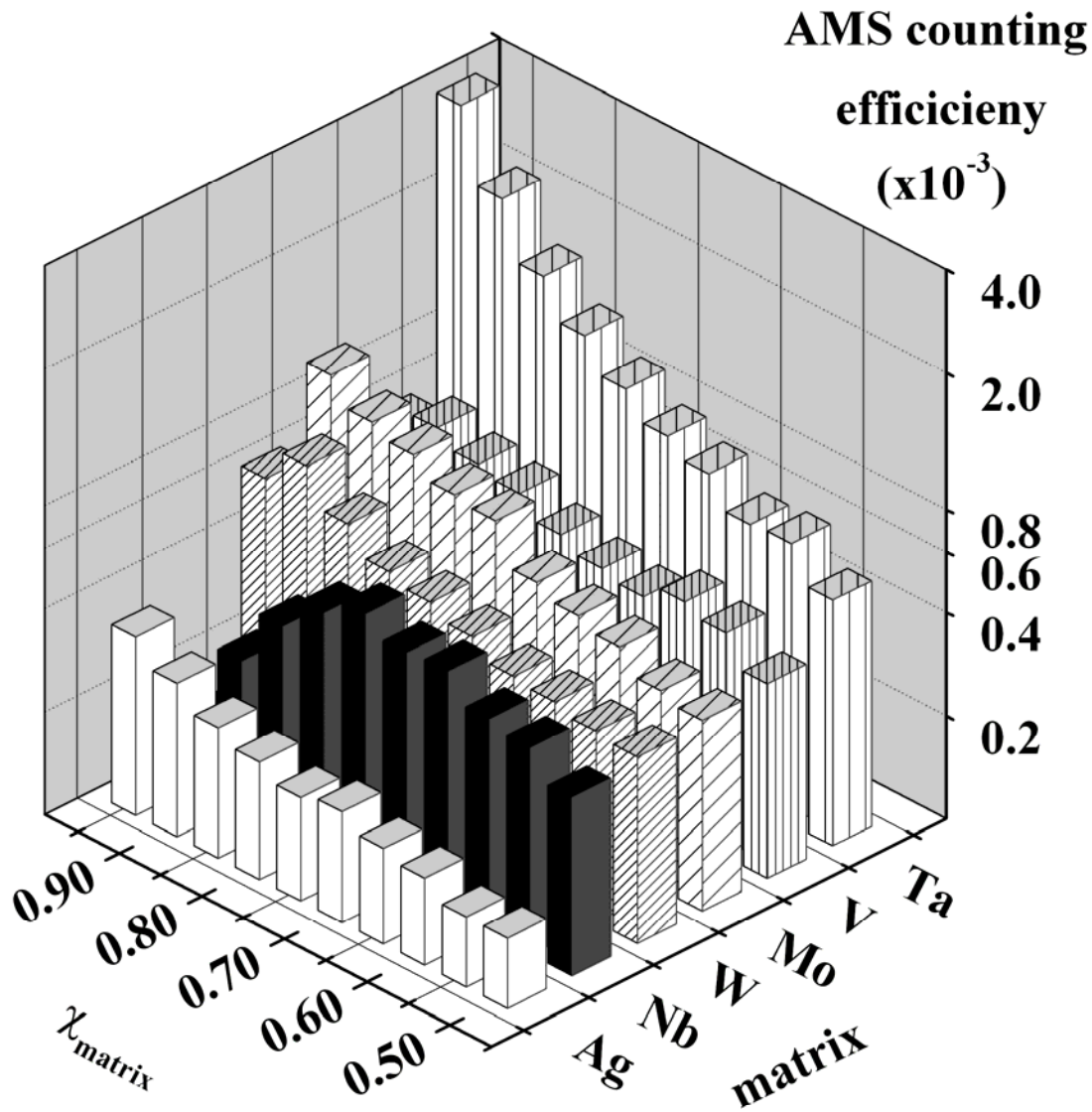
Figure 3-3: AMS counting efficiencies for analyzed matrices and dilutions (note that *z*-axis is logarithmic) expressed as ions detected per atom Be loaded.

Our data indicate that V can be substituted for Nb to provide a slightly improved response for $0.50 < \chi_V < 0.60$ samples, or a V:BeO ratio between 2:1 and 3:1 by mass. Over this range, V matrix provides a counting efficiency of 3.7×10^{-4} to 4.7×10^{-4} compared to the counting efficiency of 3.3×10^{-4} to 4.6×10^{-4} provided by Nb at identical matrix concentrations. Among the remaining matrices, at conventional mixing ratios, Mo and W do not appear to offer any significant advantage or disadvantage over Nb; however, our results indicate that these matrices actually perform better than Nb in very dilute samples. Ta remains the most intriguing matrix for use with small (low carrier) samples as it is the only matrix to induce high integrated ion beam currents with only small amounts of BeO, providing a counting efficiency of 4.0×10^{-3} in the most dilute samples. This order of magnitude advantage over other matrices may be of practical use in challenging applications, such as are encountered when the geological sample is small and/or the cosmogenic nuclide activity is suspected to be very low, necessitating very small stable isotope spikes.

From our systematic studies of χ_{matrix} effects on ion beam current, we observe that the presence of the matrix enhances ion beam currents above levels that would be anticipated simply on the basis of BeO concentration, which decreases with increasing addition of metal matrix (Figure 3-4). In order to quantify this, we calculate an anticipated ion beam current assuming that there is linear dependence of current on BeO concentration. In this case, we use the integrated beam current of an equimolar mixture of BeO and matrix as a reference to which subsequent serial dilutions are compared. The

difference between the experimental beam currents and the calculated responses is a measure of the magnitude of matrix enhancement. This matrix enhancement effect is clearly more pronounced for Nb than Ag.

In order to evaluate the enhancing performance of each matrix in its ability to surpass the theoretical response, we define in Eq. 1, the relative enhancement (ξ_χ) of a matrix normalized to the response of an equimolar sample:

$$\xi_\chi = \frac{\int_{30}^{330} i_\chi \, d(t) - \frac{m_\chi}{m_o} \int_{30}^{330} i_o \, d(t)}{\int_{30}^{330} i_o \, d(t)} \qquad (1)$$

The relative enhancement is a function of the beam current (i_χ) for a sample with a given matrix mole fraction (χ), the mass of BeO in the sample (m_χ), and the current (i_o) and mass of BeO (m_o) for a standard (i.e. equimolar) mixture of analyte in the same matrix. The factor m_χ/m_o corrects for anticipated reduced beam current due to mass dilution introduced as a function of increasing χ; therefore, any difference between i_χ and i_o is attributed entirely to an enhancing effect of the matrix.

The relative enhancement is a simplification that assumes a linear response of ion beam current with BeO mass in the sample. While this assumption appears reasonable at the higher dilutions ($\chi \geq 0.7$), it is not as appropriate at the lower mole fractions of matrix ($\chi \leq 0.7$) studied (Figure 2), where we measure little dependence of ion beam current on BeO concentration in the target. The relative enhancement ξ_χ varies considerably from matrix to matrix (Figure 4). For Ag, ξ_χ increases approximately linearly as the matrix mole fraction increases. For Nb, there is a local maximum at $\chi_{Nb} = 0.80$, suggesting that

87

matrix enhancement does not offset dilution effects on the ion beam current beyond this mole fraction of Nb matrix. In general, the trend in ξ_χ for Mo, Ta, and V resembles the general response for Ag. Only W is analogous to Nb with respect to the incidence of a local maximum in relative enhancement at higher matrix mole fractions. Ta is of particular note because, among all the experimental matrices, it exhibits the most significant ξ_χ values for very dilute samples.

Figure 3-4: Experimental integrated ion beam⁻ currents (—o—) compared to theoretical linear response (-------, considering BeO dilution by matrix) as a function of analyzed matrices and dilutions. Also shown is the relative enhancement (ξ) in ion beam current (---●---) due to metal matrix (see Eq.1). Each panel shows the response of a different metal matrix.
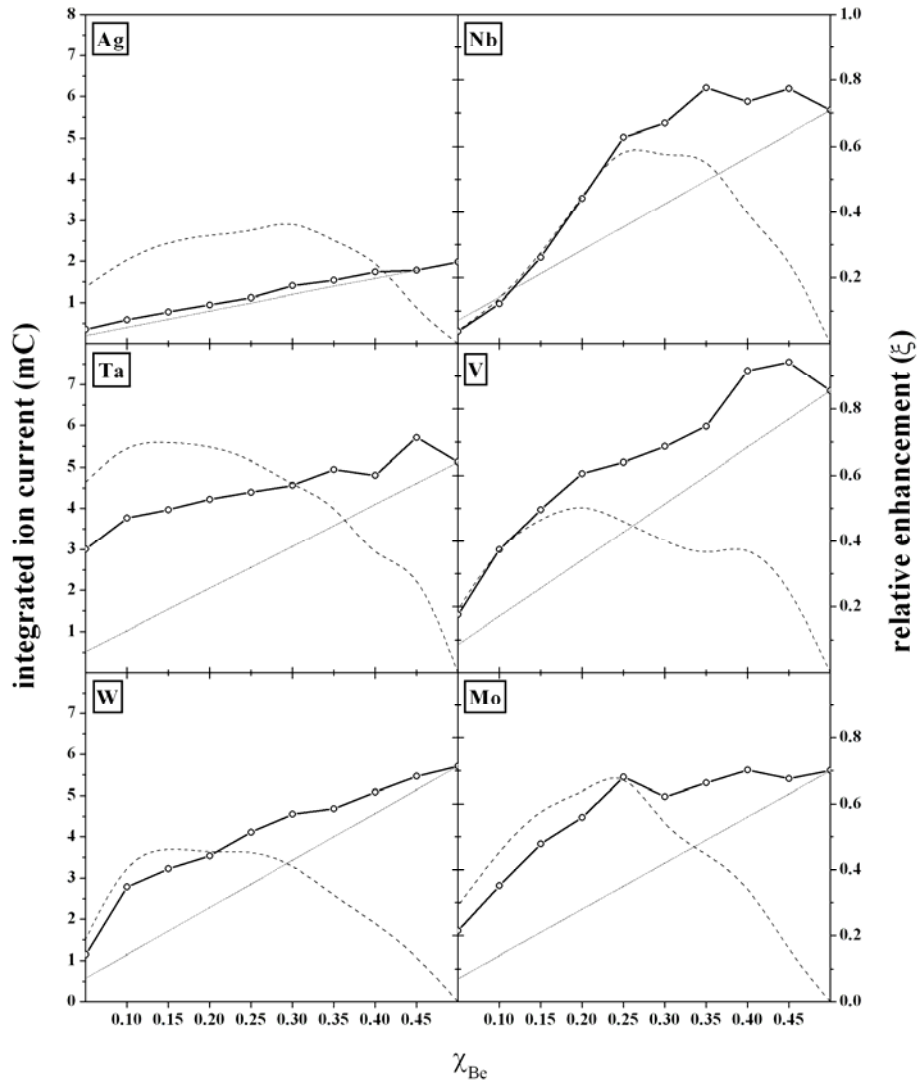
Although ξ_χ is a useful means of comparing the relative enhancement between matrices, high ξ_χ values may not necessarily correspond to experimental conditions that provide the highest possible integrated ion beam currents or the most efficient AMS analyses. The implied advantage of systems that exhibit high relative enhancement may be neutralized in circumstances in which high ionization efficiency (rate of BeO^- production relative to amount of BeO in the sample) is compromised by low sputtering efficiency (rate of BeO vaporization) or vice versa. This discrepancy is a consequence of interpreting the ion beam current as an absolute indicator of matrix performance, whereas the current is more accurately represented as a composite function of many concurrent interdependent processes that may or may not depend on the matrix (e.g. space-charge effects, sputtering, ionization, ion focusing/extraction). For example, on first inspection of the Ta panel in Figure 4 one might conclude that the highest matrix mole fraction (i.e. 0.95) should be used to obtain the greatest enhancement in ion beam current; however, it is possible that, at these high dilutions, the absolute current levels measured are so low as to impractically prolong the collection time necessary to achieve acceptable counting statistics on the ^{10}Be. In any case, the possibility of such large enhancements is intriguing and warrants further investigation. Experiments are underway to evaluate the experimental practicability of using such large dilutions with reduced masses of ^{9}Be to improve ion currents while simultaneously increasing the ^{10}Be/^{9}Be isotope ratio, thereby significantly improving the capabilities of cosmogenic isotope dating.

Considering the fundamental properties of the metal matrices, we find that electron affinity of the matrix exhibits the strongest correlation with the integrated ion

90

beam current normalized to the mass of BeO dispersed in that matrix (Figure 3-5). The correlation with matrix electron affinity is highest when the oxide and matrix are mixed in equimolar ratios (linear $R^2 = 0.93$). The correlation is less significant when the analyte is more dilute; however, this trend may reflect experimental error rather than fundamental effects. Of the fundamental physical properties studied (electron affinity, metal work function, thermal conductivity, electrical resistivity, vaporization enthalpy), no other single property provides as good a correlation for equimolar samples as does electron affinity.
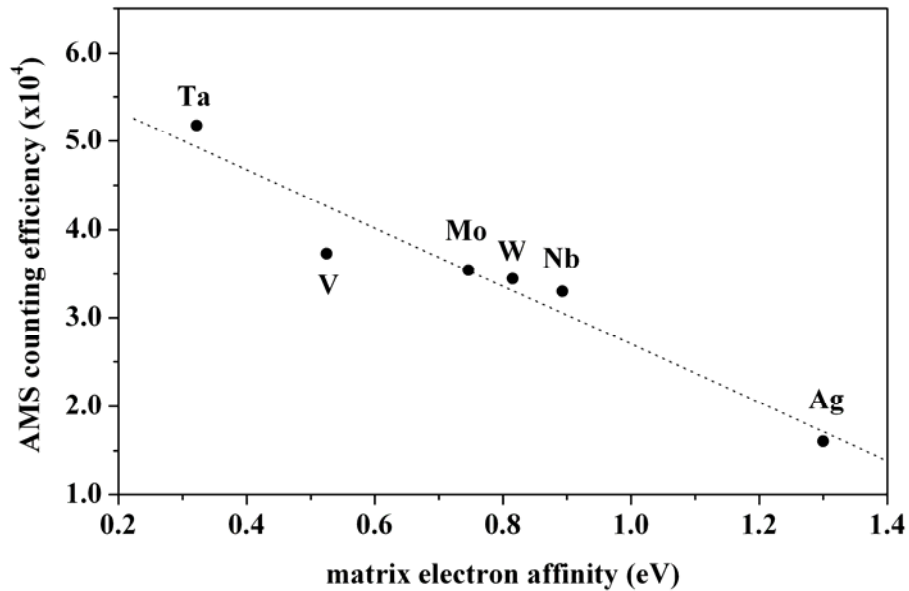

Figure 3-5: Dependence of AMS counting efficiencies on electron affinity of metal matrix for equimolar mixtures of matrix:BeO. The line is a linear fit to the experimental data ($R^2 = 0.93$).

Metal work function also exhibited a reasonable correlation to the mass normalized integrated current (linear $R^2 = 0.74$); however, this result is based upon the

nominal work function of the matrix, not the modified work function describing the composite mixture of condensed Cs from the ion source, BeO, and matrix that is continuously changing during the sputter event. The only other property that significantly correlates to matrix performance is thermal conductivity (linear R^2=0.67); however, this association is unexpected, especially considering evidence that water-cooled ion sources have no apparent advantage for high ion beam currents.[8]

3.4 Conclusion

The results of our experiments confirm the empirical advantages of using Nb instead of Ag as a matrix for AMS [10]Be analysis. In an effort to understand the enhancement mechanism and optimize the metal matrix for [10]Be analysis, we have demonstrated that other metal matrices can provide ion beam current enhancements comparable, and in some instances superior, to Nb. Our results suggest an inverse correlation between the electron affinity of the metal matrix and the ion beam current. We propose therefore that one ionization mechanism operative in the AMS source involves a competition between the matrix and BeO for available electrons. Hence, a metal matrix that is present in great excess compared to the analyte and that also possesses a stronger affinity for electrons (for example Ag *vs.* V) may sequester a greater number of electrons, leaving fewer available for attachment to BeO thereby decreasing the measured ion beam current. At this time, it is not possible to rule out other mechanisms that might affect ion beam currents as a function of metal matrix. For example, the BeO sputter yields may also be altered as a function of other

physicochemical characteristics of the metal matrix, such as thermal conductivity and heat of vaporization. Such possibilities are reinforced by the observed packing depth dependence of ion beam current for some but not all metals (Figure 1). Nonetheless, we have found the correlation of ion beam current with matrix electron affinity to be significantly stronger than with any other physical characteristic of the matrix.

The systematic investigation of metal matrix effects on BeO ion beam currents that we present here provides insight into AMS ion sputter source behavior and also a practical means to guide sample preparation in order to optimize the analysis of cosmogenic [10]Be. While the observed matrix effects are directly applicable to the CAMS ion source, the methodologies we use could be employed to determine optimal experimental conditions at other AMS facilities and for other cosmogenic isotopes. The identification of improved matrices and optimal mixing ratios improves the precision AMS and extends its applicability to more demanding geo-chronological applications.

3.6 References

1.   Lal, D.; Peters, B., Cosmic ray produced radioactivity on the earth. In *Handbuch der Physik*, ed.; Sitte, K., 'Ed.'^'Eds.' Springer-Verlag: New York, 1967; 'Vol.' p^pp 551-612.

2.   Bierman, P.; Nichols, K., Rock to sediment - Slope to sea with ^{10}Be - Rates of landscape change. *Annual Review of Earth and Planetary Sciences* **2004,** 32, 215-255.

3.   Gosse, J. C.; Phillips, F. M., Terrestrial in situ cosmogenic nuclides: theory and application. *Quaternary Science Reviews* **2001,** 20, (14), 1475-1560.

4.   Nishiizumi, K.; Lal, D.; Klein, J.; Middleton, R.; Arnold, J. R., Production of ^{10}Be and ^{26}Al by cosmic rays in terrestrial quartz in situ and implications for erosion rates. *Nature* **1986,** 319, (6049), 134-136.

5.   Gillespie, A. R.; Bierman, P. R., Precision of terrestrial exposure ages and erosion rates estimated from analysis of cosmogenic isotopes produced in situ. *Journal of Geophysical Research, B, Solid Earth and Planets* **1995,** 100, (12), 24,637-24,649.

6.   Finkel, R.; Suter, M., AMS in the Earth Sciences: Technique and applications. *Advances in Analytical Geochemistry* **1993,** 1, 1-114.

7.   Middleton, R.; Klein, J.; Brown, L.; Tera, F., ^{10}Be in commercial beryllium. *Nuclear Instruments and Methods in Physics Research Section B: Beam Interactions with Materials and Atoms* **1984,** B5, 511-513.

8.   Southon, J. R.; Roberts, M., Ten years of sourcery at CAMS/LLNL - Evolution of a Cs ion source. *Nuclear Instruments and Methods in Physics Research Section B: Beam Interactions with Materials and Atoms* **2000,** 172, 257-261.

9.   Stone, J.; Fifield, K.; Beer, J.; Obrist, c.; Grajcar, M.; Kubik, P.; Muscheler, R.; Finkel, R.; Caffee, M., Co-precipitated silver-metal oxide aggregates for accelerator mass spectrometry of ^{10}Be. *Nuclear Instruments and Methods in Physics Research Section B: Beam Interactions with Materials and Atoms* **2004,** 223-224, 272-277.

10.   Middleton, R. *A negative ion cookbook*; Department of Physics, University of Pennsylvania: Philidephia, 1990; p^pp.

11.   Bierman, P. R.; Caffee, M. W., Slow rates of rock surface erosion and sediment production across the Namib Desert and escarpment, Southern Africa. *American Journal of Science* **2001,** 301, (4-5), 326-358.

12.   Granger, D. E.; Riebe, C. S.; Kirchner, J. W.; Finkel, R. C., Modulation of erosion on steep granitic slopes by boulder armoring, as revealed by cosmogenic ^{26}Al and ^{10}Be. *Earth and Planetary Science Letters* **2001,** 186, (2), 269-281.

13.   Raisbeck, G. M.; Yiou, F.; Bourles, D.; Lorius, C.; Jouzel, J.; Barkov, N. I., Evidence for two intervals of enhanced ^{10}Be deposition in Antarctic ice during the last glacial period. *Nature* **1987,** 326, (6110), 273-277.

14.   Fink, D.; McKelvey, B.; Hannan, D.; Newsome, D., Cold rocks, hot sands: In-situ cosmogenic applications in Australia at ANTARES. *Nuclear Instruments and Methods in Physics Research Section B: Beam Interactions with Materials and Atoms* **2000,** 172, 838-846.

15.   Smith, A. M.; Fink, D.; Child, D.; Levchenko, V. A.; Morgan, V. I.; Curran, M.; Etheridge, D. M.; Elliot, G., ^{7}Be and ^{10}Be concentrations in recent firn and ice at Law

Dome, Antarctica. *Nuclear Instruments and Methods in Physics Research Section B: Beam Interactions with Materials and Atoms* **2000,** 172, 847-855.

16.   Duncan, C.; Masek, J.; Bierman, P.; Larsen, J.; Caffee, M., Extraordinarily high denudation rates suggested by ^{10}Be and ^{26}Al analysis of river sediments, Bhutan Himalayas. *Geological Society of America Abstracts with Programs* **2001,** 33.

17.   Granger, D. E.; Kirchner, J. W.; Finkel, R. C., Quaternary downcutting rate of the New River, Virginia, measured from differential decay of cosmogenic ^{26}Al and ^{10}Be in cave-deposited alluvium. *Geology* **1997,** 25, (2), 107-110.

18.   Roberts, M. L.; Bench, G. S.; Brown, T. A.; Caffee, M. W.; Finkel, R. C.; Freeman, S. P. H. T.; Hainsworth, L. J.; Kashgarian, M.; McAninch, J. E.; Proctor, I. D.; Southon, J. R.; Vogel, J. S., The LLNL AMS facility. *Nuclear Instruments and Methods in Physics Research Section B: Beam Interactions with Materials and Atoms* **1997,** 123, 57-61.

CHAPTER 4: INVESTIGATION OF METAL MATRIX SYSTEMS FOR COSMOGENIC ^{26}Al ANALYSIS BY ACCELERATOR MASS SPECTROMETRY

4.1 Introduction

The long-term accumulation of the terrestrial cosmogenic nuclide (TCN) ^{26}Al can be determined with accelerator mass spectrometry (AMS)[1] and provide information indicating the exposure history of a landscape[2] or, with complementary ^{10}Be data, the burial history of a sample.[3] The double dating method is readily applied to quartz, from which Al and Be can be extracted and isolated with established chemistry. Despite the elevated natural production rate of ^{26}Al relative to ^{10}Be by a factor of six, the determination of ^{26}Al continues to challenge most AMS facilities because Al generally generates low stable ion beam currents, necessitating long analysis times for reproducible isotope ratio statistics. At the Center for Accelerator Mass Spectrometry (CAMS) at Lawrence Livermore National Laboratories (LLNL), where the ion source is a modification of the Middleton design,[4,5] low Al ion beam currents (0.1-3.0 μA) result in ^{26}Al/^{27}Al analysis times as long as 30 minutes per sample.

It is protocol at many AMS facilities to prepare TCN samples in a metal powder matrix in order to facilitate handling of low volume samples which might otherwise prematurely expire in the ion source. In addition, some matrices exhibit auxiliary benefits in specific applications; for example, in ^{10}Be analysis, Nb has been demonstrated to dramatically enhance Be ion beam currents,[6] providing sufficient sensitivity to measure erosion rates in rapidly eroding landscapes.[7] We seek to identify matrix systems with

potential to enhance ion beam currents for ^{26}Al analysis in a manner analogous to that whereby Nb improves Be ion beam currents.[7, 8] Related work involving ^{10}Be analysis has demonstrated that Be ion beam currents can be optimized as a function of matrix mixing ratios and physical properties;[8] however, a direct extension of these results to the Al system is not feasible because of inherent differences in the mechanism of ionization; i.e., Be ion beam currents are affected predominantly by yields of an abundant molecular ion (BeO$^-$), while Al ion beam currents are affected by the formation of a non-abundant atomic ion (Al$^-$). The utility of relatively high yield molecular oxides (e.g. AlO$^-$) is limited by the cost and availability of an auxiliary isobaric suppression method, such as a gas-filled magnet.[9]

4.2 Methods

All target materials (Al, Al$_2$O$_3$, Ag, Mo, Nb, Re, and V) were >99.5% pure powders of particle diameter <45 μm (Sigma-Aldrich Co). The metals were sampled with a stainless steel Meyhoefer Chalazion curette, whose capacity (by mass) for each powder was predetermined with a microbalance. For each matrix, five samples were prepared over a range of matrix mole fractions (χ_{matrix}) so that χ_{matrix} ranged from 0.5 to 0.9 in 0.1 increments. The powders were mixed in a quartz crucible with a stainless steel rod; the resulting mixture was tamped into stainless steel targets. AMS analysis was performed at LLNL CAMS, where the ^{27}Al^{7+} beam current was monitored with a 1 s resolution in an off-axis Faraday cup positioned after the first post-accelerator 90° magnet. The stripped ions are used as a proxy for Al$^-$ that is formed in the ion source, under the assumption that

net losses of Al ions in the accelerator are relatively invariant. Standards (χ_{Ag} = 0.50) required 15 min to stabilize at a mean ion beam current of 1.54 µA ± 5.0% over the subsequent 15 min. All reported data were collected using a 15 minute stabilization time followed by 15 minute acquisition window.

4.3 Results and Discussion

For Al_2O_3 in Ag matrix, the depth to which the mixed powder is tamped in the cathode cavity has a significant bearing on ion beam current (Figure 1). The integrated ion beam is highest when the cathode load is near capacity and lowest when the cathode is nearly empty. The depth effect on ion beam current has been observed previously in Be samples prepared in Ag (although not in Be samples prepared in Nb). It remains uncertain whether the effect of packing depths on ion beam current is a function of the physicochemical interaction between Al_2O_3 and the matrix or of ion source geometry (e.g. a change in proximity of the sample surface relative to the focal point of the primary ion (Cs^+) beam), either of which might affect the formation or collimation of negative ions.
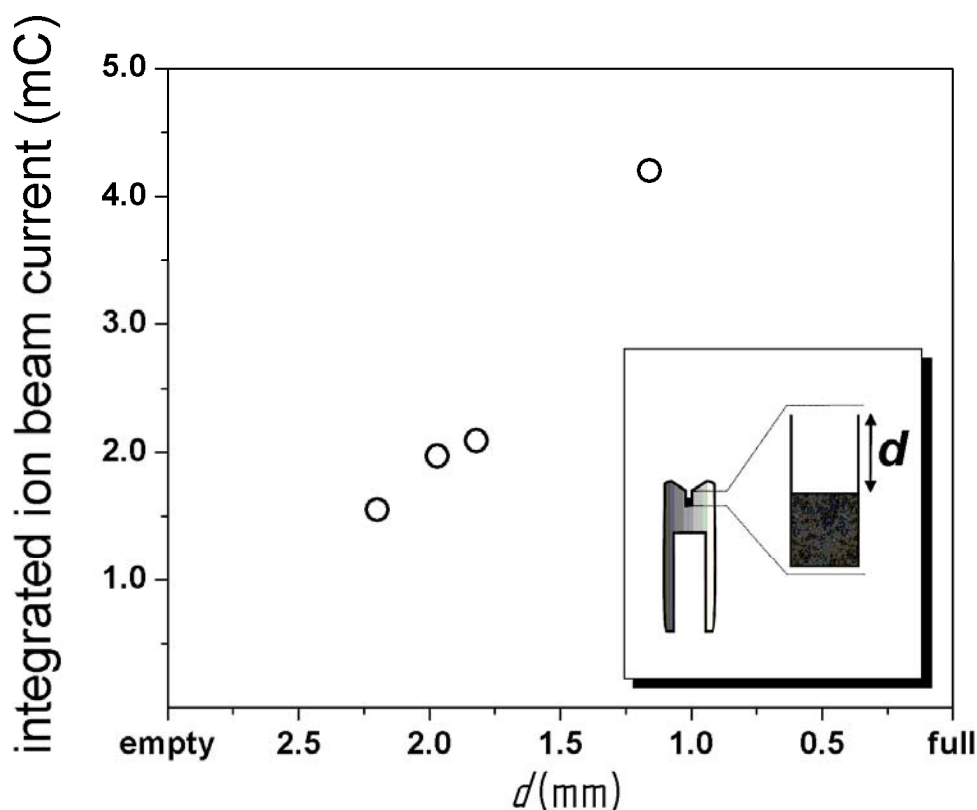
Figure 4-1: Effect on integrated ion beam current of sample packing depth (*d*) in the CAMS cathode cavity for equimolar Ag:Al$_2$O$_3$ samples. Symbols are experimental data points. Inset: cross-section of CAMS cathode showing how *d* is defined.

A comparison of the temporal evolution of ion beam currents for pure Al$_2$O$_3$ and Al$_2$O$_3$ in Ag matrix indicates that the principle utility of Ag matrix is a stabilization effect rather than enhancement of the ion beam current (Figure 2). In general, the Ag matrix improves the stability over the measurement window and suppresses otherwise extensive noise in the signal. A salient feature of the beam current profiles is a significant rise time to the maximum current for samples with no matrix or low χ_{matrix}. In general, ~4 min are

required for an equimolar mixture to achieve 90% of the maximum ion beam current. These results are consistent with typical warm up times observed during routine [26]Al analysis samples at CAMS. We have observed that Ag can significantly reduce, and in some instances eliminate, ion beam current rise times for BeO samples;[8] however, this advantage is not as significant for Al_2O_3.
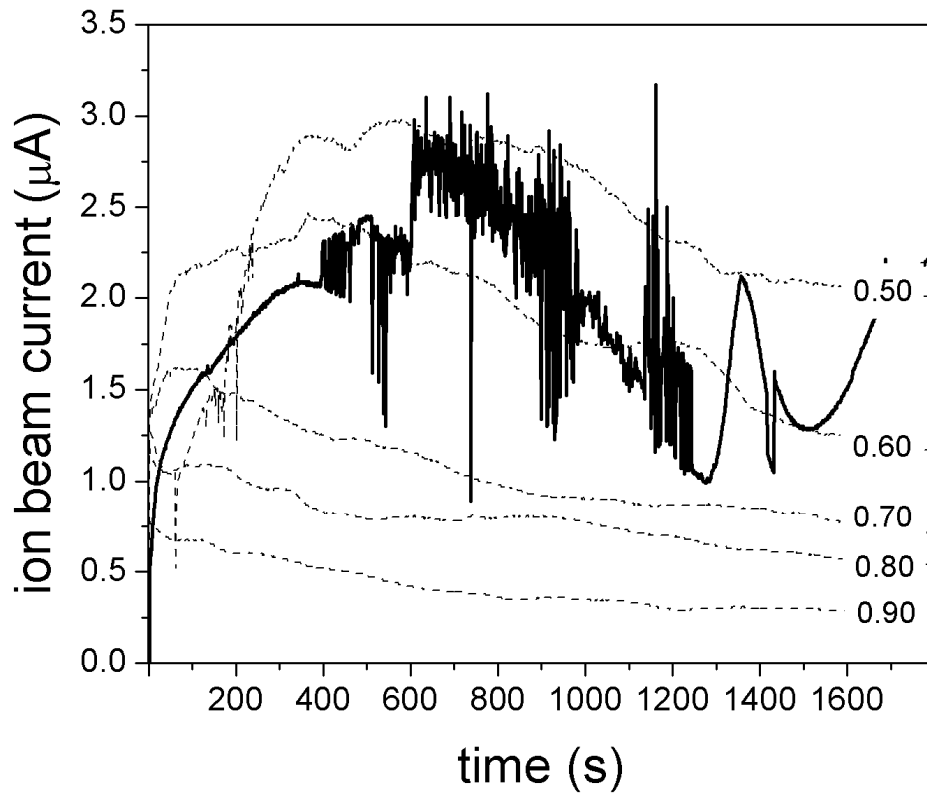
Figure 4-2: Temporal evolution of ion beam current for pure Al_2O_3 (1.69 μA ± 23%) and Al_2O_3 with different matrix mixing ratios (χ_{Ag} = 0.5 (2.26 μA ± 11%), 0.6 (1.50 μA ± 16%), 0.7 (0.84 μA ± 7%), 0.8 (0.65 μA ± 13%), 0.9 (0.31 μA ± 8%)).

No improvement in Al ion beam currents was measured for matrices other than Ag (2.26 µA ± 11%). Of the alternative matrices, the one that provided the second best absolute current response was Re (2.17 µA ± 13%), followed by Nb (1.73 µA ± 1%), V (1.92 µA ± 20%), and finally Mo (1.73 µA ± 6%) (Figure 3). For all of these matrices, the ion beam current decreases with increasing χ_{matrix} (data not shown). Note that Nb is singular in providing a relatively stable response. Al_2O_3 prepared in Mo and Re exhibits erratic behavior during the warm-up interval: the early ion beam current evolution demonstrates a local maximum for the former and a local minimum for the latter. V is notable for providing ion beam currents with significant noise and deviation; moreover, very high cathode currents were observed in V-doped samples, indicating erratic behavior in the ion source.
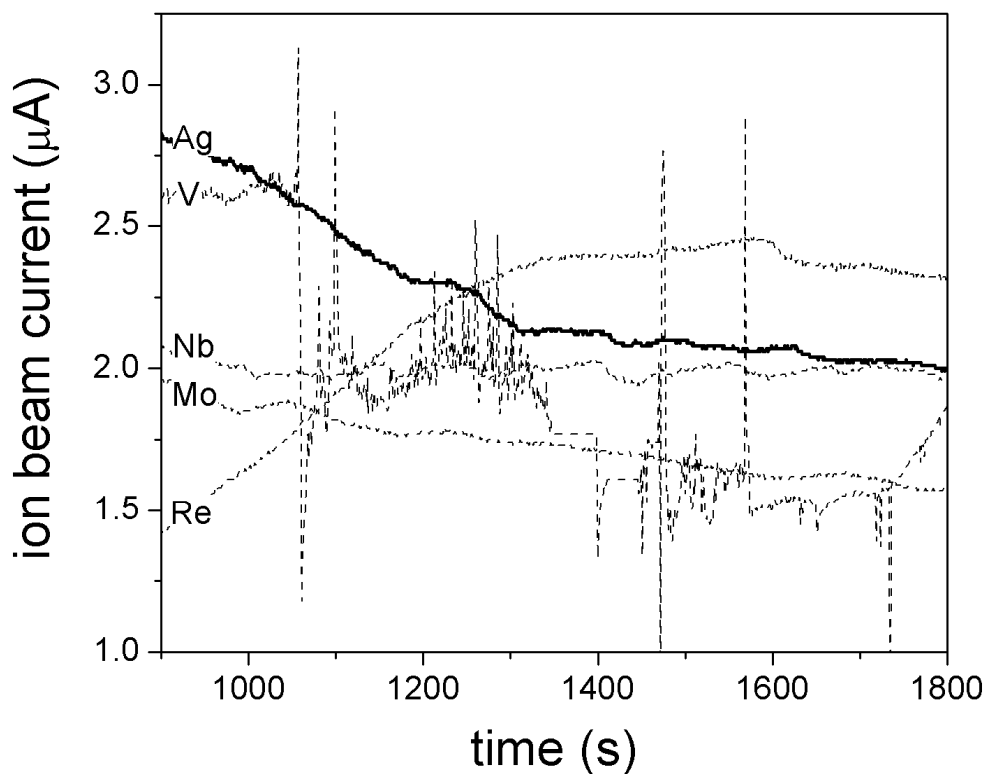
Figure 4-3: Temporal evolution of ion beam currents for Al$_2$O$_3$ with χ_{matrix} = 0.5 for Ag, Mo, Nb, Re, and V.

All AMS targets were prepared with a constant volume of tamped powder, irrespective of Al$_2$O$_3$: matrix mole ratio, in order to expose a reproducible sample surface depth to the primary ion (Cs$^+$) beam. Therefore, the Al$_2$O$_3$ mass in each target varies slightly on a sample-to-sample basis depending upon the density of packed powder for any given Al$_2$O$_3$: matrix combination. In order to account for this discrepancy, the integrated ion beam current is normalized with Al$_2$O$_3$ mass loaded in each sample, then converted to a counting efficiency of ions detected per net atom Al loaded (Figure 4). Al

counting efficiency is a proxy for comparing the AMS ionization efficiency for samples with different matrix composition. In principle, matrices that provide higher Al counting efficiencies are capable of providing conditions for the generation of higher ion beam currents; therefore, these matrices have the most potential for improving isotope ratio statistical certainty in TCN analyses.
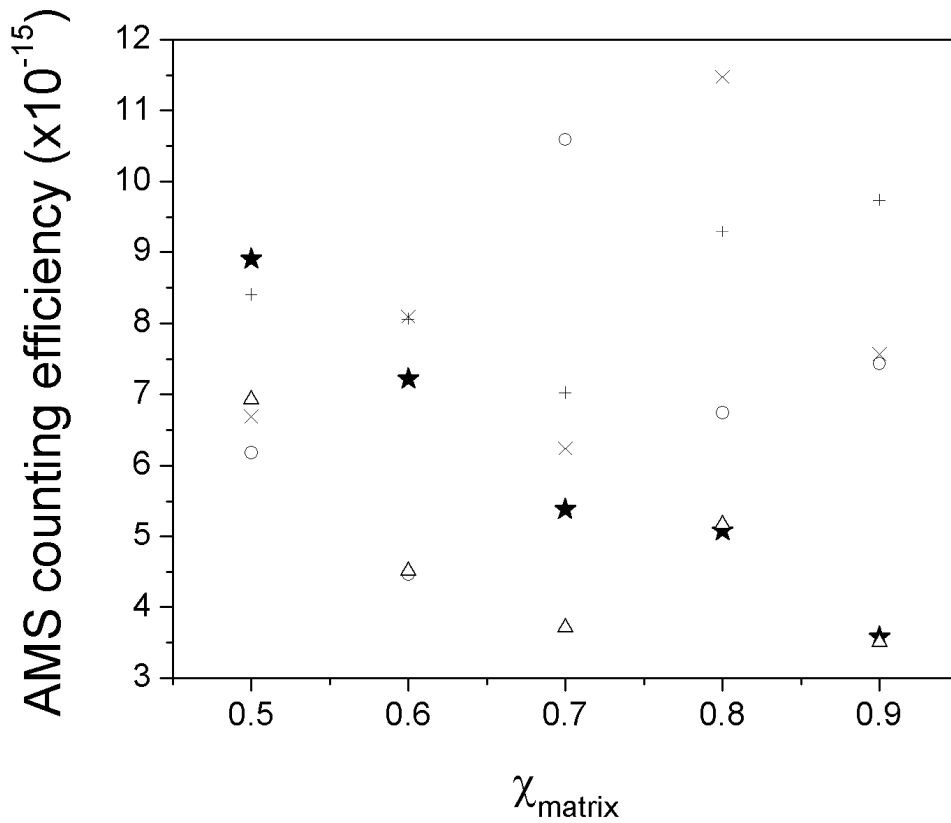
Figure 4-4: Al AMS counting efficiency for Al$_2$O$_3$ in Ag ($\bigstar$), Mo (0), Nb ($\triangle$), Re (+), V (x) for different χ_{matrix} expressed as ions detected per atom of Al loaded in the target.

For an equimolar Al$_2$O$_3$: matrix sample, the Al counting efficiency (x10^{-5}) is 8.9 for Ag, 8.4 for Re, 6.9 for Nb, 6.7 for V, and 6.2 for Mo; all of these values are

104

approximately two orders of magnitude less than AMS counting efficiencies for Be. Therefore, of all these matrices, Ag appears to be the best for routine [26]Al analysis. The Al counting efficiency correlates with matrix metal work function (R^2=0.78) and inverse vaporization enthalpy (R^2=0.72). Al_2O_3 samples in Ag and Nb matrix exhibit a decrease in Al counting efficiency in high χ_{matrix}. Al_2O_3 samples prepared in Mo, Re, and V exhibit higher Al counting efficiencies than Ag or Nb at high χ_{matrix}, indicating a potential utility in geochronology applications where the [26]Al content is anticipated to be very low (or small sample size limits the availability of Al in general).
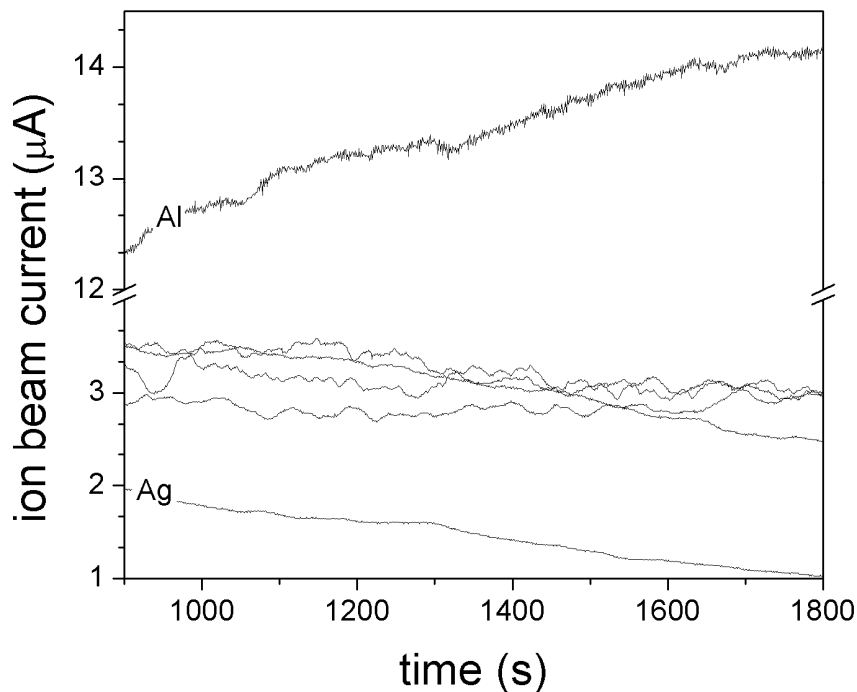
Figure 4-5: Temporal evolution of instantaneous ion beam currents for metal Al and Al in equimolar mixtures of V, Re, Nb, Mo, and Ag. Al (bold) yields the highest current; Ag yields the lowest; V, Re, Nb, and Mo are all ~3 µA.

The ion beam current for Al metal (no matrix addition) increases as time in the source increases to a mean of 13.3 μA (Figure 5). Mixing pure Al with metal matrices lowers beam currents by a factor of more than 4. Beam currents for Al mixed with Nb (3.14 μA ± 4.4%) are followed in sequence by Re (3.07 μA ± 10.6%), Mo (2.85 μA ± 2.7%), V (3.23 μA ± 5.82%), and Ag (1.46 μA ± 18%). The Al counting efficiency for elemental Al correlates inversely with matrix electron affinity (R^2=0.95) and to a lesser extent matrix thermal conductivity (R^2=0.70).

4.4 Conclusion

The major conclusion of the study is that no large increases in ion current output or efficiency were obtained with novel matrix systems relative to those available with equimolar mixtures of Al_2O_3 and Ag. The correlation of Al counting efficiency for Al_2O_3 with fundamental elemental properties of the matrix indicate that an ideal matrix for [26]Al analysis is a metal that must neither readily enter the gas-phase nor contribute to thermionic emission of electrons in the ion source. Although Ag has high thermal conductivity compared to other tested matrices, there is no significant evidence of correlation between Al counting efficiency and matrix thermal conductivity. Yet it has been widely purported that the effectiveness of Ag for TCN analysis is a function of metallic conductivity, presumably via a mechanism whereby the matrix facilitates heat removal by conduction and/or prevention of charge accumulation at the sample surface. Thus, Cu is a common matrix for [26]Al analysis in other AMS laboratories; however, no advantage has been demonstrated using Cu at CAMS. Nonetheless, it is plausible that a

particular permutation of analyte/matrix physical properties is vital for providing a characteristic ion beam current response. Note, for example, that matrices with low work functions (Mo, Nb, V) also have high vaporization enthalpies.

Ion beam currents for elemental Al are significantly higher than for Al_2O_3 in any matrix; however, this effect is not at present exploitable due to the experimental difficulty of isolating reduced Al from the mineral phase. The correlation of Al counting efficiency for elemental Al mixed with various matrices with physical properties of those matricies supports the hypothesis that, in a simple two-component mixture, a matrix operates by fielding a competitive (high electron affinity) or non-competitive (low electron affinity) environment for atomic ionization. For elemental Al, matrix systems with high electron affinity compete directly with Al for free electrons during the Cs sputter event, sequestering electrons from the analyte and depressing ion beam current.

Because the stripped atomic ion yield is only a fraction of the diverse net ion population formed from Al_2O_3 in the ion source, it remains unclear whether the matrix affects ion beam current by changing the distribution of atomic and molecular species ejected from the Al_2O_3 target in the ion source (i.e. a sputter effect), or by changing the propensity of the sputtered atomic population to react with free electrons in the ion source (i.e. an atomic ionization effect). In order to assess the mechanism of matrix effects on the Al_2O_3 system, it would be necessary to investigate the population distributions of molecular and atomic species sputtered in the ion source. For example, changes in ion source response to AMS target composition could be investigated with laser excited

atomic and ionic fluorescence in order to measure ion densities at or above the target surface.

4.5 Acknowledgments

4.6 References

1.   Middleton, R.; Klein, J., Accelerator mass spectrometry with ^{26}Al. *Nuclear Instruments and Methods in Physics Research Section B: Beam Interactions with Materials and Atoms* **1983,** 218, 430-439.

2.   Nishiizumi, K.; Winterer, E. L.; Kohl, C. P.; Klein, J.; Middleton, R.; Lal, D.; Arnold, J. R., Cosmic ray production rates of ^{10}Be and ^{26}Al in quartz from glacially polished rocks. *Journal of Geophysical Research, B, Solid Earth and Planets* **1989,** 94, (12), 17,907-17,915.

3.   Granger, D. E.; Fabel, D.; Palmer, A. N., Pliocene-Pleistocene incision of the Green River, Kentucky, determined from radioactive decay of cosmogenic ^{26}Al and ^{10}Be in Mammoth Cave sediments. *Geological Society of America Bulletin* **2001,** 113, (7), 825-836.

4.   Middleton, R.; Klein, J.; Brown, L.; Tera, F., ^{10}Be in commercial beryllium. *Nuclear Instruments and Methods in Physics Research Section B: Beam Interactions with Materials and Atoms* **1984,** B5, 511-513.

5.   Southon, J. R.; Roberts, M., Ten years of sourcery at CAMS/LLNL - Evolution of a Cs ion source. *Nuclear Instruments and Methods in Physics Research Section B: Beam Interactions with Materials and Atoms* **2000,** 172, 257-261.

6.   Fink, D.; McKelvey, B.; Hannan, D.; Newsome, D., Cold rocks, hot sands: In-situ cosmogenic applications in Australia at ANTARES. *Nuclear Instruments and Methods in Physics Research Section B: Beam Interactions with Materials and Atoms* **2000,** 172, 838-846.

7.   Duncan, C.; Masek, J.; Bierman, P.; Larsen, J.; Caffee, M., Extraordinarily high denudation rates suggested by ^{10}Be and ^{26}Al analysis of river sediments, Bhutan Himalayas. *Geological Society of America Abstracts with Programs* **2001,** 33.

8.   Hunt, A.; Petrucci, G.; Bierman, P.; Finkel, R., Metal matrices to optimize ion beam currents for accelerator mass spectrometry. *Nuclear Instruments and Methods in Physics Research Section B: Beam Interactions with Materials and Atoms* **2006,** 243, (1), 216-222.

9.   Paul, M., Separation of isobars with a gas-filled magnet. *Nuclear Instruments and Methods in Physics Research Section B: Beam Interactions with Materials and Atoms* **1990,** 52, 315-321.

CHAPTER 5: CLOSING REMARKS

5.1 Prospects for future research

Research involving the rare terrestrial cosmogenic nuclides ^{10}Be and ^{26}Al has gained considerable momentum since 1986 when these isotopes were demonstrated by Klein to be present in Libyan glass and also by Nishiizumi in terrestrial quartz.[1,2] Since then, this analytical methodology has been applied with global success to provide dates for a variety of geomorphic surfaces with many applications. According to Gosse, there so far have been four distinct phases in the history of the terrestrial cosmogenic nuclide method,[3] namely: (1) demonstration of the utility of terrestrial cosmogenic nuclides for determining surface exposure ages; (2) estimation the production of such isotopes as a function of elevation and altitude; (3) adoption of AMS for the sensitive analysis of ultra-rare isotopes; and (4) the continuing refinement of terrestrial cosmogenic nuclide techniques. At present, the 4th stage is well underway and progress along these lines continues to provide momentum for the next generation of geological applications.

In general, analysis of ^{10}Be by AMS is considered by the research community to be an accurate and precise method. At present, the main obstacles in ^{10}Be analysis are suppression of boron and achieving adequate sensitivity in measurement of low isotope ratio samples. The latter is of concern for the pursuit of vanguard geomorphologic applications, for instance studies of rapidly eroding landscapes, where the ^{10}Be content is anticipated to be exceptionally low. The judicial use of a suitable matrix (e.g. Nb) in the optimal quantitative proportions for Be samples can improve ion beam currents

(presumably due to a low electron affinity of the matrix) and greatly facilitate analysis. Furthermore, particularly through a multi-acid digestion procedure and a triple acid cation exchange chromatography elution scheme, Be samples can be prepared with low levels Al and Ti impurities, which are demonstrated suppressors of ion beam current.

In contrast to the ^{10}Be system, analysis for ^{26}Al is not as advanced. The definitive challenge to ^{26}Al measurements remains the sensitivity for detection that is limited by ion beam currents. Samples with low ^{26}Al content require long analysis times to achieve sufficient counts of the rare isotope and to provide precision comparable to that obtainable via ^{10}Be analysis. The challenges afforded by ^{26}Al analysis can be limiting in applications where a single nuclide cannot provide adequate information (e.g. when there is evidence of erosion). Complex applications, such as those involving phenomena as erosion, sedimentation and burial, require (a) both ^{10}Be and ^{26}Al measurements; and (b) many samples, which are expensive and time-consuming to process. Unfortunately, ion beam current enhancements due to action of the sample matrix observed during ^{10}Be analysis do not translate to the same effect in the ^{26}Al system. Due to the preference for accelerating the anionic atomic ion (which is generated in relatively low yield in a high intensity Cs sputter ion source) rather than a molecular oxide anion, it is perhaps inappropriate to expect that the role of the matrix in the ionization process for ^{26}Al is the same as for ^{10}Be analysis.

One possibility for improving ion beam currents during ^{26}Al analysis is the use of a gas-filled magnet for isobar separation. [4] The theoretical advantage of this approach is the capability to accelerate a high yield molecular oxide aluminum anion (e.g. AlO$^-$) with

good discrimination from magnesium isobars (i.e. $^{26}MgO^-$). In the gas-filled magnet, the average charge states of isobars are different due to atomic collisions with the gas medium. Moreover, the mean charge state determines the mean trajectory of ions in the magnetic field. The practical implication of this phenomenon is that isobars can be coalesced into mean trajectories and therefore separated into discrete beams (then directed on- or off-axis toward the detector). There is already precedence for integration of gas-filled magnet technology with working AMS systems.[5, 6]. This method has been useful for improving the sensitivity of AMS measurements of heavy isotopes (e.g. ^{53}Mn, ^{59}Ni, ^{60}Fe), which is commonly limited by high backgrounds of their isobars. The disadvantages of the gas-filled magnet are a combination of expense and the engineering challenge of implementation.

Another possible approach to improving ion beam currents for ^{26}Al analysis is to analyze the atomic ion directly from a fully reduced aluminum cathode. The electrochemical preparation of elemental Al cathodes from the extracted oxide is a technical challenge and would add another potentially time-consuming step to the sample preparation. In any case, if elemental cathodes could be constructed in a cost- and time-effective manner, magnesium isobars would not be limiting because Mg^- is unstable.

Finally, it has been observed that after AMS analysis, the sputter ionization process can leave a topographic fingerprint on the remaining sample volume in the spent cathode. In general, spent cathodes exhibit differences in cratering patterns, visible indications of cesiation (blackening due to Cs deposition), and sputtered sample volume that vary widely on a sample-to-sample basis. These differences are likely related to any

112

combination of physical inhomogeneities of the tamped targets, chemical impurities, and/or ion source memory effects. Post-AMS analysis of the physical and chemical composition of spent targets (by for instance microscopy and/or spectroscopy) may provide information that can be correlated to the performance of cathodes in the ion source (i.e. the magnitude of ion beam current).

Although the focus of the discussion herein has been restrained to the cosmogenic isotopes of paramount geomorphologic interest, namely ^{10}Be and ^{26}Al, the methodology described for optimization of ion beam currents is readily applicable to other nuclides typically measured by AMS. Moreover, as ^{10}Be and ^{26}Al comprise only a fraction of routinely measured nuclides at most AMS facilities, general strategies for improving ion beam currents may be useful in any number of applications. In fact, there have been reports of employing analogous methods in entirely unrelated applications. For example, it has been reported that Nb is a good matrix for the AMS analysis of ^{99}Tc, which is a byproduct of nuclear testing that has been widely distributed through the environment.[7] Improving the sensitivity of the present generation of AMS applications will undoubtedly empower the origination and evolution of the next generation of applications and the future of the AMS method itself.

In any case, in order for inter-laboratory comparisons of data to be more meaningful, it would be useful for researches to report experimental details which have generally been undocumented in scientific literature, including measurements of sample purity and matrix composition. As demonstrated in this work, ion beam currents (and by

extension: the utility of the AMS methodology) can be improved by a combination of improved wet chemistry and analytical chemistry.

5.2 References

1.   Klein, J.; Giegengack, R.; Middleton, R.; Sharma, P.; Underwood, J. R.; Weeks, R. A., Revealing histories of exposure using in situ produced ^{26}Al and ^{10}Be in Libyan desert glass. *Radiocarbon* **1986,** 28, (2A), 547-555.

2.   Nishiizumi, K.; Lal, D.; Klein, J.; Middleton, R.; Arnold, J. R., Production of ^{10}Be and ^{26}Al by cosmic rays in terrestrial quartz in situ and implications for erosion rates. *Nature* **1986,** 319, (6049), 134-136.

3.   Gosse, J. C.; Phillips, F. M., Terrestrial in situ cosmogenic nuclides: theory and application. *Quaternary Science Reviews* **2001,** 20, (14), 1475-1560.

4.   Paul, M., Separation of isobars with a gas-filled magnet. *Nuclear Instruments and Methods in Physics Research Section B: Beam Interactions with Materials and Atoms* **1990,** 52, 315-321.

5.   Alfimov, V.; Possnert, G.; Aldahan, A., Measurements of ^{36}Cl with a gas-filled magnet at the Uppsala tandem laboratory. *Nuclear Instruments and Methods in Physics Research Section B: Beam Interactions with Materials and Atoms* **2007,** 259, (1), 199-203.

6.   Knie, K.; Faestermann, T.; Korschinek, G., AMS at the Munich gas-filled analyzing magnet system GAMS. *Nuclear Instruments and Methods in Physics Research Section B: Beam Interactions with Materials and Atoms* **1997,** 123, (1-4), 128-131.

7.   Berquist, B. A.; Marchetti, A. A.; Martinelli, R. E.; McAninch, J. E.; Nimz, G. J.; Proctor, I., D; Southon, J. R.; Vogel, J. S., Technetium measurements by accelerator

mass spectrometry at LLNL. *Nuclear Instruments & Methods in Physics Research B* **2000,** 172, 328-332.

COMPREHENSIVE REFERENCE LIST

Alfimov, V.; Possnert, G.; Aldahan, A. "Measurements of ^{36}Cl with a gas-filled magnet at the Uppsala tandem laboratory" *Nuclear Instruments and Methods in Physics Research Section B: Beam Interactions with Materials and Atoms* 2007, 259, (1), 199-203.

Beer, J.; Blinov, A.; Bonani, G.; Finkel, R. C.; Hofmann, H. J.; Lehmann, B.; Oeschger, H.; Sigg, A.; Schwander, J.; Staffelbach, T.; Stauffer, B. R.; Suter, M.; Wolfli, W. "Use of ^{10}Be in polar ice to trace the 11-year cycle of solar activity" *Nature* 1990, 347, (6289), 164-166.

Berquist, B. A.; Marchetti, A. A.; Martinelli, R. E.; McAninch, J. E.; Nimz, G. J.; Proctor, I., D; Southon, J. R.; Vogel, J. S. "Technetium measurements by accelerator mass spectrometry at LLNL" *Nuclear Instruments & Methods in Physics Research B* 2000, 172, 328-332.

Bierman, P.; Nichols, K. "Rock to sediment - Slope to sea with ^{10}Be - Rates of landscape change" *Annual Review of Earth and Planetary Sciences* 2004, 32, 215-255.

Bierman, P.; Turner, J. "^{10}Be and ^{26}Al evidence for exceptionally low rates of Australian bedrock erosion and the likely existence of pre-Pleistocene landscapes" *Quaternary Research* 1995, 44, 378-382.

Bierman, P. R. "Using in situ produced cosmogenic isotopes to estimate rates of landscape evolution; a review from the geomorphic perspective" *Journal of Geophysical Research, B, Solid Earth and Planets* 1994, 99, (7), 13885-13896.

Bierman, P. R.; Caffee, M. "Cosmogenic exposure and erosion history of ancient Australian bedrock landforms" *Geological Society of America Bulletin* 2002, 114, (7), 787-803.

Bierman, P. R.; Caffee, M. W. "Slow rates of rock surface erosion and sediment production across the Namib Desert and escarpment, Southern Africa" *American Journal of Science* 2001, 301, (4-5), 326-358.

Bierman, P. R.; Gillespie, A. R. "Range fires: A significant factor in exposure-age determination and geomorphic surface evolution" *Geology* 1991, 19, 641-644.

Bierman, P. R.; Marsella, K. A.; Patterson, C.; Davis, P. T.; Caffee, M. "Mid-Pleistocene cosmogenic minimum-age limits for pre-Wisconsinan glacial surfaces in southwestern Minnesota and southern Baffin Island; a multiple nuclide approach" *Geomorphology* 1999, 27, (1-2), 25-39.

Biggs, P. H.; Meier, A. L. "The Determination of Forty-Two Elements in Geological Materials by Inductively Coupled Plasma-Mass Spectrometry" *U.S. Geological Survey Open File Report* 2002, 02-223-I.

Brown, E. T.; Brook, E. J.; Raisbeck, G. M.; Yiou, F.; Kurz, M. D. "Effective attenuation lengths of cosmic rays producing ^{10}Be and ^{26}Al in quartz; implications for exposure age dating" *Geophysical Research Letters* 1992, 19, (4), 369-372.

Brown, E. T.; Edmond, J. M.; Raisbeck, G. M.; Yiou, F.; Kurz, M. D.; Brook, E. J. "Examination of surface exposure ages of Antarctic moraines using in situ produced ^{10}Be and ^{26}Al" *Geochimica et Cosmochimica Acta* 1991, 55, 2269-2283.

Brown, E. T.; Raisbeck, G. M.; Yiou, F.; Kurz, M.; Brook, E. J. "Effective attenuation lengths of cosmic rays producing ^{10}Be and ^{26}Al in quartz: implications for exposure dating" *EOS* 1992, 72, (44), 575.

Brown, T. A.; Roberts, M. L.; Southon, J. R. "Ion-source modeling and improved performance of the CAMS high-intensity Cs-sputter ion source" *Nuclear Instruments and Methods in Physics Research Section B: Beam Interactions with Materials and Atoms* 2000, (172), 344-349.

Child, D.; Elliott, G.; Mifsud, C.; Smith, A. M.; Fink, D. "Sample processing for earth science studies at ANTARES" *Nuclear Instruments and Methods in Physics Research Section B: Beam Interactions with Materials and Atoms* 2000, 172, 856-860.

Clapp, E. M.; Bierman, P. R.; Caffee, M. W. "Using ^{10}Be and ^{26}Al to determine sediment generation rates and identify sediment source areas in an arid region drainage basin" *Geomorphology* 2002, 45, 89-104.

Clapp, E. M.; Bierman, P. R.; Nichols, K. K.; Pavich, M.; Caffee, M. "Rates of sediment supply to arroyos from upland erosion determined using in situ produced cosmogenic ^{10}Be and ^{26}Al" *Quaternary Research (New York)* 2001, 55, (2), 235-245.

Clapp, E. M.; Bierman, P. R.; Schick, A. P.; Lekach, J.; Enzel, Y.; Caffee, M. "Sediment yield exceeds sediment production in arid region drainage basins" *Geology* 2000, 28, (11), 995-998.

Clark, D.; Bierman, P. R.; Larsen, P. "Improving in situ cosmogenic chronometers" *Quaternary Research* 1995, 44, (3), 366-376.

Clark, D. H.; Bierman, P. R.; Gillespie, A. R. "New cosmogenic ^{10}Be and ^{26}Al measurements of glaciated surfaces, Sierra Nevada, California; they're precise but are they accurate?" *Geological Society of America, 1995 annual meeting Abstracts with Programs - Geological Society of America* 1995, 27, (6), 170.

Davis, R.; Schaeffer, O. A. "Chlorine-36 in nature" *Annals of the New York Academy of Science* 1955, 62, 105-122.

Desilets, D.; Zreda, M. "Scaling production rates of terrestrial cosmogenic nuclides for altitude and geomagnetic effects" *Geological Society of America Abstracts with Programs* 2000, 31, (7), A-400.

Desilets, D.; Zreda, M.; Lifton, N. A. "Comment on 'Scaling factors for production rates of in situ produced cosmogenic nuclides: a critical reevaluation' by Tibor J. Dunai" *Earth and Planetary Science Letters* 2001, 188, (1-2), 283-287.

Ditchburn, R. G.; Whitehead, N. E. "The separation of ^{10}Be from silicates" *3d Workshop of the South Pacific Environmental Radioactivity Association* 1994, 4-7.

Dunai, T. J. "Reply to comment on `Scaling factors for production rates of in situ produced cosmogenic nuclides: a critical reevaluation'" *Earth and Planetary Science Letters* 2001, 188, (1-2), 289-298.

Dunai, T. J. "Scaling factors for production rates of in situ produced cosmogenic nuclides: a critical reevaluation" *Earth and Planetary Science Letters* 2000, 176, 157-169.

Duncan, C.; Masek, J.; Bierman, P.; Larsen, J.; Caffee, M. "Extraordinarily high denudation rates suggested by ^{10}Be and ^{26}Al analysis of river sediments, Bhutan Himalayas" *Geological Society of America Abstracts with Programs* 2001, 33.

Dunne, A.; Elmore, D.; Muzikar, P. "Scaling factors for the rates of production of cosmogenic nuclides for geometric shielding and attenuation at depth on sloped surfaces" *Geomorphology* 1999, 27, (1-2), 3-11.

Dunne, J. A. Calibration of the method of exposure dating of geomorphic surfaces on the Earth using in-situ-produced cosmogenic radionuclides, and applications in the Central Andes. Dissertation, Purdue University, West Lafayette, IN, 1999.

Elmore, D.; Phillips, F. "Accelerator mass spectrometry for measurement of long-lived radioisotopes" *Science* 1987, 236, 543-550.

Elmore, D.; Phillips, F. M. "Accelerator mass spectrometry for measurement of long-lived radioisotopes" *Science* 1987, 236, 543-550.

Fink, D.; McKelvey, B.; Hannan, D.; Newsome, D. "Cold rocks, hot sands: In-situ cosmogenic applications in Australia at ANTARES" *Nuclear Instruments and Methods in Physics Research Section B: Beam Interactions with Materials and Atoms* 2000, 172, 838-846.

Finkel, R.; Suter, M. "AMS in the Earth Sciences: Technique and applications" *Advances in Analytical Geochemistry* 1993, 1, 1-114.

Gillespie, A. R.; Bierman, P. R. "Precision of terrestrial exposure ages and erosion rates estimated from analysis of cosmogenic isotopes produced in situ" *Journal of Geophysical Research, B, Solid Earth and Planets* 1995, 100, (12), 24,637-24,649.

Gosse, J. C.; Evenson, E. B.; Klein, J.; Lawn, B.; Middleton, R. "Precise cosmogenic [10]Be measurements in western North America; support for a global Younger Dryas cooling event" *Geology* 1995, 23, (10), 877-880.

Gosse, J. C.; Klein, J.; Evenson, E. B.; Lawn, B.; Middleton, R. "Beryllium-10 dating of the duration and retreat of the last Pinedale glacial sequence" *Science* 1995, 268, 1329-1333.

Gosse, J. C.; Phillips, F. M. "Terrestrial in situ cosmogenic nuclides: theory and application" *Quaternary Science Reviews* 2001, 20, (14), 1475-1560.

Granger, D. E.; Fabel, D.; Palmer, A. N. "Pliocene-Pleistocene incision of the Green River, Kentucky, determined from radioactive decay of cosmogenic ^{26}Al and ^{10}Be in Mammoth Cave sediments" *Geological Society of America Bulletin* 2001, 113, (7), 825-836.

Granger, D. E.; Kirchner, J. W.; Finkel, R. C. "Quaternary downcutting rate of the New River, Virginia, measured from differential decay of cosmogenic ^{26}Al and ^{10}Be in cave-deposited alluvium" *Geology* 1997, 25, (2), 107-110.

Granger, D. E.; Muzikar, P. F. "Dating sediment burial with in situ-produced cosmogenic nuclides; theory, techniques, and limitations" *Earth and Planetary Science Letters* 2001, 188, (1-2), 269-281.

Granger, D. E.; Riebe, C. S.; Kirchner, J. W.; Finkel, R. C. "Modulation of erosion on steep granitic slopes by boulder armoring, as revealed by cosmogenic ^{26}Al and ^{10}Be" *Earth and Planetary Science Letters* 2001, 186, (2), 269-281.

Hunt, A.; Petrucci, G.; Bierman, P.; Finkel, R. "Investigation of metal matrix systems for cosmogenic ^{26}Al analysis by accelerator mass spectrometry" *Nuclear Instruments and Methods in Physics Research Section B: Beam Interactions with Materials and Atoms* 2007, 260, (2), 633-636.

Hunt, A.; Petrucci, G.; Bierman, P.; Finkel, R. "Metal matrices to optimize ion beam currents for accelerator mass spectrometry" *Nuclear Instruments and Methods in Physics Research Section B: Beam Interactions with Materials and Atoms* 2006, 243, (1), 216-222.

Klein, J.; Giegengack, R.; Middleton, R.; Sharma, P.; Underwood, J. R.; Weeks, R. A. "Revealing histories of exposure using in situ produced ^{26}Al and ^{10}Be in Libyan desert glass" *Radiocarbon* 1986, 28, (2A), 547-555.

Knie, K.; Faestermann, T.; Korschinek, G. "AMS at the Munich gas-filled analyzing magnet system GAMS" *Nuclear Instruments and Methods in Physics Research Section B: Beam Interactions with Materials and Atoms* 1997, 123, (1-4), 128-131.

Kohl, C. P.; Nishiizumi, K. "Chemical isolation of quartz for measurement of *in-situ* - produced cosmogenic nuclides" *Geochimica et Cosmochimica Acta* 1992, 56, 3583- 3587.

Lal, D. "Cosmic ray labeling of erosion surfaces; in situ nuclide production rates and erosion models" *Earth and Planetary Science Letters* 1991, 104, (2-4), 424-439.

Lal, D. "Cosmogenic isotopes produced in situ in terrestrial solids" *Nuclear Instruments and Methods in Physics Research Section B: Beam Interactions with Materials and Atoms* 1987, B29, 238-245.

Lal, D. "In situ-produced cosmogenic isotopes in terrestrial rocks" *Annual Reviews of Earth and Planetary Science* 1988, 16, 355-388.

Lal, D.; Peters, B., Cosmic-ray produced isotopes and their application to problems in geophysics. In *Progress in elementary particle and cosmic ray physics*, ed.; Wilson, J. G.; Wouthysen, S. A., 'Ed.'^'Eds.' Wiley: New York, 1962; 'Vol.' p^pp 1-74.

Lal, D.; Peters, B., Cosmic ray produced radioactivity on the earth. In *Handbuch der Physik*, ed.; Sitte, K., 'Ed.'^'Eds.' Springer-Verlag: New York, 1967; 'Vol.' p^pp 551-612.

Masarik, J.; Frank, M.; Schafer, J.; Wieler, R. "Correction of in-situ cosmogenic nuclide production rates for geomagnetic field intensity variations during the past 800,000 years" *Geochimica et Cosmochimica Acta* 2001, 65, (17), 2995-3003.

Masarik, J.; Reedy, R. C. "Terrestrial cosmogenic-nuclide production systematics calculated from numerical simulations" *Earth and Planetary Science Letters* 1995, 136, 381-396.

Middleton, R. *A negative ion cookbook*; Department of Physics, University of Pennsylvania: Philidephia, 1990; p^pp.

Middleton, R.; Klein, J. "[26]Al: measurement and applications" *Philosophical Transactions of the Royal Society of London* 1987, A 323, 121-143.

Middleton, R.; Klein, J. "Accelerator mass spectrometry with [26]Al" *Nuclear Instruments and Methods in Physics Research Section B: Beam Interactions with Materials and Atoms* 1983, 218, 430-439.

Middleton, R.; Klein, J.; Brown, L.; Tera, F. "[10]Be in commercial beryllium" *Nuclear Instruments and Methods in Physics Research Section B: Beam Interactions with Materials and Atoms* 1984, B5, 511-513.

Monaghan, M. C. K., S.; Turekian, K.K. "The global-average production rate of [10]Be" *Earth and Planetary Science Letters* 1986, 76 (1985/86), 279-287.

Nishiizumi, K.; Kohl, C. P.; Arnold, J. R.; Klein, J.; Fink, D.; Middleton, R. "Cosmic ray produced [10]Be and [26]Al in Antarctic rocks; exposure and erosion history" *Earth and Planetary Science Letters* 1991, 104, (2-4), 440-454.

Nishiizumi, K.; Lal, D.; Klein, J.; Middleton, R.; Arnold, J. R. "Production of [10]Be and [26]Al by cosmic rays in terrestrial quartz in situ and implications for erosion rates" *Nature* 1986, 319, (6049), 134-136.

Nishiizumi, K.; Winterer, E. L.; Kohl, C. P.; Klein, J.; Middleton, R.; Lal, D.; Arnold, J. R. "Cosmic ray production rates of [10]Be and [26]Al in quartz from glacially polished rocks" *Journal of Geophysical Research, B, Solid Earth and Planets* 1989, 94, (12), 17,907-17,915.

Ochs, M.; Ivy-Ochs, S. "The chemical behavior of Be, Al, Fe,Ca, and Mg during AMS target preparations from terrestrial silicates modeled with chemical speciation

calculations" *Nuclear Instruments and Methods in Physics Research Section B: Beam Interactions with Materials and Atoms* 1997, 132, 235-240.

Paul, M. "Separation of isobars with a gas-filled magnet" *Nuclear Instruments and Methods in Physics Research Section B: Beam Interactions with Materials and Atoms* 1990, 52, 315-321.

Raisbeck, G. M.; Yiou, F.; Bourles, D.; Lorius, C.; Jouzel, J.; Barkov, N. I. "Evidence for two intervals of enhanced [10]Be deposition in Antarctic ice during the last glacial period" *Nature* 1987, 326, (6110), 273-277.

Raisbeck, G. M.; Yiou, F.; Klein, J.; Middleton, R. "Accelerator mass spectrometer measurement of cosmogenic [26]Al in terrestrial and extraterrestrial matter" *Nature* 1983, 301, 690-692.

Reusser, L.; Bierman, P.; Pavich, M.; Zen, E.; Larsen, J.; Finkel, R. "Rapid late Pleistocene incision of Atlantic passive-margin river gorges" *Science* 2004, 305, (5683), 499-502.

Roberts, M. L.; Bench, G. S.; Brown, T. A.; Caffee, M. W.; Finkel, R. C.; Freeman, S. P. H. T.; Hainsworth, L. J.; Kashgarian, M.; McAninch, J. E.; Proctor, I. D.; Southon, J. R.; Vogel, J. S. "The LLNL AMS facility" *Nuclear Instruments and Methods in*

Physics Research Section B: Beam Interactions with Materials and Atoms 1997, 123, 57-61.

Schildgen, T. F.; Purves, R. S.; Phillips, W. M. "Modeling effects of snow burial on cosmogenic exposure age dating, Cairngorm Mountains, Scotland, and Wind River Range, WY" *Eos Transactions of AGU* 2002, 83, (47), F550.

Sharma, P.; Middleton, R. "Radiogenic production of ^{10}Be and ^{26}Al in uranium and thorium ores: Implications for studying terrestrial samples containing low levels of ^{10}Be and ^{26}Al" *Geochimica et Cosmochimica Acta* 1989, 53, 709-716.

Smith, A. M.; Fink, D.; Child, D.; Levchenko, V. A.; Morgan, V. I.; Curran, M.; Etheridge, D. M.; Elliot, G. "^{7}Be and ^{10}Be concentrations in recent firn and ice at Law Dome, Antarctica" *Nuclear Instruments and Methods in Physics Research Section B: Beam Interactions with Materials and Atoms* 2000, 172, 847-855.

Southon, J. R.; Roberts, M. "Ten years of sourcery at CAMS/LLNL - Evolution of a Cs ion source" *Nuclear Instruments and Methods in Physics Research Section B: Beam Interactions with Materials and Atoms* 2000, 172, 257-261.

Stone, J. "A rapid fusion method for separation of beryllium-10 from soils and silicates" *Geochimica et Cosmochimica Acta* 1998, 62, (3), 555-561.

Stone, J.; Fifield, K.; Beer, J.; Obrist, c.; Grajcar, M.; Kubik, P.; Muscheler, R.; Finkel, R.; Caffee, M. "Co-precipitated silver-metal oxide aggregates for accelerator mass spectrometry of ^{10}Be" *Nuclear Instruments and Methods in Physics Research Section B: Beam Interactions with Materials and Atoms* 2004, 223-224, 272-277.

Tera, F.; Brown, L.; Morris, J.; Sacks, I. S.; Klein, J.; Middleton, R. "Sediment incorporation in island-arc magmas: inferences from ^{10}Be" *Geochimica et Cosmochimica Acta* 1986, 50, 535-550.

Turekian, K. K.; Cochran, J. K.; Krishnaswami, S.; Langford, W. A.; Parker, P. D.; Bauer, K. A. "The measurement of ^{10}Be in manganese nodules using a tandem Van De Graaff accelerator" *Geophysical Research Letters.* 1979, 6, 417-420.

von Blanckenburg, F.; Belshaw, N. S.; O'Nions, R. K. "Separation of ^{9}Be and cosmogenic ^{10}Be from environmental materials and SIMS isotope dilution analysis" *Chemical Geology* 1996, 129, 93-99.

Yokoyama, T.; Makishima, A.; Nakamura, E. "Evaluation of the coprecipitation of incompatible trace elements with fluoride during silicate rock dissolution by acid digestion" *Chemical Geology* 1999, 157, (3-4), 175-187.